Journal of Pharmaceutical and Biomedical Analysis 222 (2023) 115089

Contents lists available at ScienceDirect

Journal of Pharmaceutical and Biomedical Analysis

journal homepage: www.journals.elsevier.com/journal-of-pharmaceutical-and-biomedical-analysis

Advances and applications of capillary electromigration methods in the analysis of therapeutic and diagnostic recombinant proteins – A Review

Hanno Stutz

Department of Biosciences and Medical Biology, University of Salzburg, Hellbrunnerstrasse 34, 5020 Salzburg, Austria

ARTICLE INFO

Keywords:
Recombinant proteins
Proteoforms and conformations
Capillary electrophoresis techniques
Biotechnological production
Cell cultures
Review

ABSTRACT

This review provides a comprehensive overview of methodological advances and applications of CE in the analysis and characterization of recombinant therapeutic and diagnostic proteins over the past two decades. The first part of the review discusses various aspects of biotechnological protein production and the related effects on the final product. This covers upstream processes, e.g., selection and transfection of host cells, up-scaling of cell cultures and cultivation conditions, as well as downstream processing and a discussion of future trends in biotechnological manufacturing. This part is essential for relating biotechnological production to analytical challenges and requirements in order to provide a holistic insight. In this context, the influence of manufacturing steps on the quality of the final drug substance/product is discussed in terms of related post-translational modifications of the target molecule with a major focus on glycosylation pattern and conformational effects. Particular attention is given to host cell specific and non-human modifications affecting the efficacy and safety of recombinant products. Endowed with this propaedeutic knowledge, the major part of the review discusses the manifold contributions of different CE techniques to the development and optimization of the manufacturing process, to the evaluation and characterization of the final drug product and their role in quality control. Different CE techniques, such as CZE, capillary gel electrophoresis (CGE), (imaged) capillary isoelectric focusing ((i)CIEF), μChipCE, CE-Western blot, affinity CE (ACE), and CE-MS are discussed including a brief introduction in the respective separation and hyphenation principle as well as their applications in the analysis of different recombinant biologics together with recent strategies. The addressed analyte portfolio comprises a vast variety of recombinant proteins with molecular masses from 4.1 kDa up to 20.3 MDa (for recombinant virus-like particles), and a pI range from 2.0 to 11.2. Antibodies are not explicitly covered in the survey. The review is complemented by compiling validation aspects and proposed suitability tests in order to assure the feasibility of methods to industrial and pharmaceutical needs.

Abbreviations: AAV, adeno-associated virus; Ab, antibody; ACE, affinity capillary electrophoresis; ACN, acetonitrile; α-Gal, Gal-α(1,3)-Gal; BACE1, beta-site amyloid precursor protein cleavage enzyme; bfs, bare fused-silica; BGE, background electrolyte; BHK, Baby Hamster Kidney cells; BRP, biological reference product; BRS, biological reference substance; β2-M, β2-microglobulin; CA, carrier ampholyte; CHO, Chinese Hamster Ovary cells; CIEF, capillary isoelectric focusing; CQA, critical quality attribute; CRS, chemical reference substance; CSD, charge state distribution; DAB, diaminobutane; dl, double layered; DRA, dialysis-related amyloidosis; DHFR, dihydrofolate reductase; DS, dextran sulfate; *E. coli*, *Escherichia coli*; EMA, European Medicines Agency; EDQM, European Directorate for the Quality of Medicines and Health Care; EMMA, electrophoretically mediated microanalysis; EOF, electroosmotic flow; EPO, erythropoietin; FBS, fetal bovine serum; FGF 21, fibroblast growth factor 21; Gal, galactose; G-CSF, granulocyte colony stimulating factor; GH, growth hormone; GS, glutamine synthetase; hCG, human chorionic gonadotropin; HCP, host cell protein; HEK 293, human embryonic kidney cells; HPV, human papillomavirus; HRP, horseradish peroxidase; HT-1080, human fibrosarcoma cells; iCIEF, imaged capillary isoelectric focusing; IDE, insulin degrading enzyme; IgG, immune globulin G; IL, interleukin; IFN, interferon; ISTD, internal standard; LIF, laser induced fluorescence; LPA, linear polyacrylamide; Man, mannose; MSX, methionine sulfoximine; MTX, methotrexate; Neu5Ac, N-acetylneuraminic acid; Neu5Gc, N-glycolneuraminic acid; PAA, polyacrylamide; PB, polybrene; PEG, polyethylene glycol; PEI, polyethylene imine; pI, isoelectric point; PEO, polyethylene oxide; PHEA, poly-N-hydroxyethylacrylamide; PSA, prostate-specific antigen; PTH, parathyroid hormone; PTM, post-translational modification; PVA, polyvinyl alcohol; PVS, polyvinyl sulfonic acid; qPCR, quantitative polymerase chain reaction; RLP, rotavirus-like particle; SL, sheath liquid; TDLFP, transverse diffusion of laminar flow profiles; tl, triple layered; VLP, virus-like particle; VP, viral protein; WT, wild type.

E-mail address: Ernst-Hanno.Stutz@plus.ac.at.

https://doi.org/10.1016/j.jpba.2022.115089
Received 27 July 2022; Received in revised form 28 September 2022; Accepted 29 September 2022
Available online 1 October 2022

1. Introduction

With the approval of the first recombinant therapeutic biologic, i.e., insulin, in 1982 [1], recombinant proteins have gained progressive importance in the biopharmaceutical industry and have advanced diagnosis and treatment of diseases. Since then, a plethora of recombinant proteins, differing in physicochemical and biological properties was developed and has entered the market [2]. The development of a successful manufacturing process of recombinant proteins requires their characterization both upstream and downstream. This ensures the selection of appropriate host cells [3,4], of cell culture media and cultivation conditions [4,5], the effective scale-up of the fermentation process [6,7], as well as tailored downstream purification and polishing steps after recombinant proteins have been harvested [8,9]. Once the final manufacturing process is built, the drug substance and the final drug product have to be characterized. Both, the established production process as well as the final drug substance/drug product are subjected to quality control in order to assure that acceptance criteria are within defined specifications and recombinant proteins are produced in consistent quality [10,11]. Changes in the biotechnological manufacturing either during the product development or after the final settlement of the production require an evaluation of possible differences in (relevant) protein properties, so-called quality attributes, with a subsequent assessment of their impact. This targets the comparability of the pre-change and the post-change product as outlined by the ICH guideline 5QE [12].

With the advent of biosimilars, analysis methods are also required to compare these follow-on products with their related reference products, i.e., originators, in order to confirm their similarity [13,14]. Unlike small therapeutic molecules, the expression of recombinant proteins in host cells together with the multiple factors in upstream and downstream processes may prevent the production of a single-species product. Instead, a population of slightly differing but related protein variants is mostly produced. Moreover, the product composition might vary within defined specifications even between batches of the same manufacturer including also the risk of intended drifts caused by modifications in the manufacturing [13–15]. This variability of the originator must also be reflected by the biosimilar [13]. Minute deviations of the biosimilar from its originator are acceptable if they are clinically not relevant in terms of safety, purity and potency [14]. Contrary to the concept of the European Medicines Agency (EMA), which leaves the decision about the option for a general originator-to-biosimilar switch to the EU member states, according to the US FDA “interchangeability” of products on the individual patient level has to be proven in order to allow for a substitution directly in pharmacies [13].

The biopharmaceutical industry employs a portfolio of complementary analysis methods to address numerous properties (i.e., quality attributes) for novel products as well as for biosimilars with a special focus on so-called critical quality attributes (CQAs), which affect product safety and drug efficacy [15,16]. These methods include for instance CD, fluorescence, DSC, analytical ultracentrifugation, asymmetric flow field flow fractionation, dynamic light scattering (DLS), Fourier-transform infrared (FTIR)-spectroscopy, NMR, x-ray crystallography, MALDI-TOF-MS and ESI-MS [14,15,17]. The rationale behind this comparison is actually based on the ICH guideline Q5E as outlined above [12,13]. Besides established separation techniques, such as SEC, RP-HPLC, IEC, SDS-PAGE, and 2D-differential gel electrophoresis (DIGE) [14,15,18], CE methodology offers numerous benefits and unique features in comparison to its chromatographic counterparts. Advantages of CE-separations comprise an outstanding separation efficiency due to the rectangular flow profile of the electroosmotic flow (EOF) and (ideally) the absence of protein interaction with the capillary surface, minute sample volumes used per analysis, low consumption of the separation medium, and abandonment of the mandatory use of organic solvents and non-convective polymers. In-capillary detection avoids dead-volume and the need for laborious staining/de-staining procedures in order to visualize protein zones. Moreover, the exceptional inherent single-instrument versatility allows for numerous orthogonal CE-based separations that can be run on the same equipment. Further advantages with a particular focus on pharmaceutical aspects are given elsewhere [19]. Moreover, the separation of proteins with different CE-techniques has been discussed in several reviews [20–23].

The ICH guideline Q4B Annex 11 explicitly refers to CE in pharmacopoeia texts [24], whereby in the related chapter of the USP, CZE, capillary gel electrophoresis (CGE), capillary isoelectric focusing (CIEF) and MEKC are itemized describing also the respective principle. This is harmonized with the sister organizations Ph. Eur. and JP [25]. With the exception of MEKC, these are the major modes applied also in the analysis of recombinant (therapeutic) proteins and they are thus addressed in this review. However, in terms of the analytical performance, CE still suffers from the undeserved reputation of an exalted diva. Nevertheless, a couple of inherent limitations have to be overcome in order to exploit the entire potency of CE-techniques (see Section 3.2).

This review discusses (i) current strategies in recombinant protein manufacturing and how they influence the final protein product as well as (ii) the important role CE and its different techniques progressively play in the characterization of recombinant products due to its exceptional analytical possibilities and versatility. This encompasses a comprehensive survey of successful CE strategies and applications over the past two decades. Differences in product profiles in combination with related therapeutic hazards caused by relevant/inappropriate manufacturing parameters will form a subject of discussion as well. A holistic view on the characterization of recombinant proteins with different CE techniques requires thus the inclusion and comprehension of general aspects of the preceding biotechnological manufacturing. Therefore, the initial part of the review focuses on the background of biotechnological protein manufacturing, e.g., host cell properties and selection, transfection, scale-up of cell cultures, cell culture media and cultivation conditions, and its relation to the product quality (Sections 2.1–2.9). These fundamentals prepare the propaedeutic background. Without this imparted knowledge, major aspects subsequently discussed in the analytical part would remain inapprehensible. The second part, which covers the core sections of this review, discusses advantages and limitations of CE, and addresses the applications of different CE-based separation techniques, such as CZE, (i)CIEF, CGE, μChip CE in the analysis of recombinant proteins (Sections 3.1-3.8). This is complemented by innovative strategies, such as affinity CE, in-capillary combination of CE with Western blot, CE methods hyphenated with MS detection in order to identify and characterize recombinant proteins and related variants (Sections 3.9-3.12), and the combination of complementary CE strategies (Section 3.13). CE-based separation and characterization of recombinant proteins will be discussed predominantly for therapeutic and diagnostic drug substances/drug products as well as for their production intermediates. Consistently, the contribution of CE to the optimization of upstream and downstream production processes of recombinant products will be highlighted as well. Moreover, this includes also the implementation of CE in quality control including related method validation according to the ICH guideline Q2 (R1) [26]. The principle of biotechnological production of recombinant proteins as well as the contribution of CE in optimizing the individual manufacturing steps and its role in the characterization of the final drug substance/drug product is shown in Fig. 1.

2. Manufacturing of recombinant proteins

2.1. Recombinant proteins

The extraction and purification of proteins from biological sources in sufficient quantity is mostly cumbersome, time-consuming and expensive. In some cases, the production of proteinaceous drugs with conventional methods failed, as for erythropoietin (EPO) or granulocyte colony stimulating factor (G-CSF) [27]. Moreover, isolation from

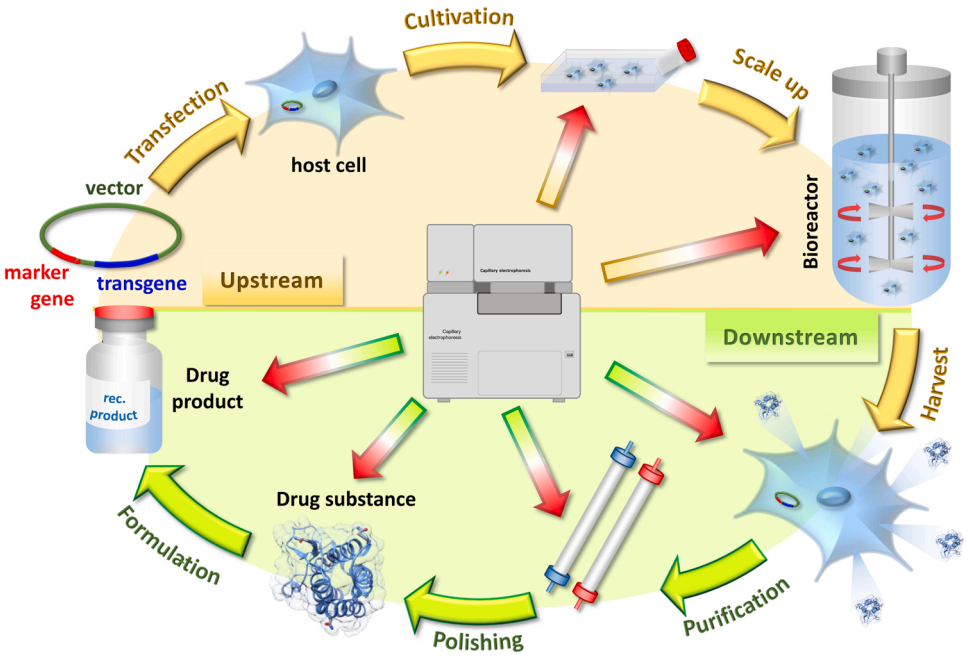

Fig. 1. Schematic representation of individual steps in the manufacturing of recombinant proteins. Arrows indicate the individual production steps that are currently covered by CE-based analyses and will be addressed in the review.

original biological sources bears the inherent risk for co-extraction of contaminants, which can serve as possible triggers for diseases or immune reactions [28]. This imposes a particular risk in case proteins are applied in disease prevention, e.g., as surface proteins acting as antigens in vaccines, or in human therapy [28]. Due to a prion contamination, the medical treatment with human growth hormone that was extracted and purified from corpses caused, for instance, iatrogenic transmission of Creutzfeld-Jakob disease (CJD) in several cases before the natural hormone became replaced by biotechnological products [29]. When proteins are biotechnologically expressed in host cells, most drawbacks related with the extraction from original human and animal sources are circumvented. In addition, large scale production in sufficient yield and standardized quality can be better guaranteed, thus conforming to clinical needs [1].

The first approval of a therapeutic protein, i.e., human insulin, recombinantly expressed in *E. coli* and launched to the market in 1982 [1] heralded a novel era. Since then, recombinant protein production has gained increasing importance in the biopharmaceutical industry [2]. According to their function, recombinant protein therapeutics have been classified as (i) therapeutics with enzymatic and regulatory functions, e.g., enzymes, hormones and growth factors, (ii) therapeutics with special targeting, such as monoclonal antibodies and antibody–drug conjugates, (iii) protein vaccines, and (iv) diagnostic proteins [30]. Moreover, recombinantly engineered therapeutic fusion proteins combine domains from different proteins, thus forming novel chimeric proteins, which merge the functionality of different individual proteins. In most cases, a so-called carrier domain and an effector domain are combined [31]. The carrier moiety may lead to high-life extension of the product, e.g., by a reduced renal clearance due to the increased protein mass [32], and thus improve also pharmacokinetics. Mostly, the Fc part of human immunoglobulins is used for this purpose. The effector domain carries the various functions of the engineered fusion protein [31]. Alternatively, a similar decrease in renal clearance and improved protection from proteolytic degradation with concomitantly increased circulating half-life can be induced by covalent attachment of polyethylene glycol (PEG) to recombinant proteins. In parallel, a decrease in the immunogenicity of PEGylated proteins was reported [33]. Further details are discussed in Section 3.5.2. The CE part (Section 3) will cover all these biotherapeutic classes, with the exception of mAbs and antibody-drug conjugates. This is due to the expansive number of publications in this field, which would go beyond the scope of the review.

2.2. Host cells

Different host cells are disposable for the (industrial) expression of heterologous proteins, including bacteria (*E. coli*), unicellular protozoa (*Leishmania tarentolae* (LEXSY)) [34], yeast (*Pichia pastoris* – meanwhile taxonomically identified as *Komagataella phaffii* [35,36], *Saccharomyces cerevisiae*) [4,37], filamentous fungi (*Aspergillus spp.*) [38,39], plant cells (e.g., different *Nicotiana tabacum* strains, *Oryza sativa*) [28,40], insect cells [4,41] (e.g., from *Spodoptera frugiperda* (Sf9, Sf21) [41,42] or from the moth *Trichoplusia ni* (=High Five™ cell line) [43]), and mammalian cell lines, for instance Chinese Hamster Ovary (CHO) cell lines [5,44,45], Baby Hamster Kidney (BHK) cells [4,46,47], and murine myeloma cells (SP2/0, NS0) [4]. In case of *E. coli*, overexpression of the target protein may lead to its accumulation in intracellular protein aggregates, so-called insoluble inclusion bodies. Multistep preparation from these inclusion bodies including solubilization with denaturing agents (e.g., with guanidine HCl or urea [48–51]), purification and refolding into the native state by removal of the denaturing agent is required followed by another purification step [48,51] (see Section 3.3.12). Furthermore, human cells, such as human embryonic kidney cells (HEK 293) [4,52] or human fibrosarcoma cells (HT-1080) [4,41,53] are used for biotechnological protein production. Other human cells, such as HKB-11 (a hybrid of kidney and B-cells), PER.C6 (human embryonic retinal cells) and HuH-7 (a hepatocyte derived cellular carcinoma line) are used in (pre) clinical phases [53] (see Table 1). Human cell lines might acquire human virus infections, explaining the need for virus clearance during the downstream processing [4,54] (see Section 2.8). A schematic survey of host cells used for the production of glycosylated recombinant proteins is provided in Fig. 2. Moreover, cell-free protein synthesis platforms, e.g., based on crude extracts of *E. coli*, have been applied [55].

The selection of appropriate expression systems is driven by several aspects, covering a cost-efficient manufacturing and storage [56], the quality and consistency of the final product, the potency for an authentic protein glycosylation, the capacity for scaling-up the protein production

Table 1
Comparison of host cells most frequently employed in the expression of recombinant proteins[a].

Host cells	Advantages	Disadvantages	References
Non-mammalian cell lines			
Bacterial cells	Rapid cell growth and high protein yield; easy, fast and cheap cultivation; cost-effective carbon sources	Production of simple proteins; inefficient PTMs; no glycosylation; propensity for protein aggregation (in form of inclusion bodies) due to absence of chaperons; contamination risk with endotoxins	[4,28,41,47,53]
Yeast cells	Fast cell division and high protein yield; glycosylation possible; sharing the N-glycan core structure with humans; cultured in chemically defined media; low contamination risk	Human glycoprofiles difficult to achieve; hypermannosylation: immunogenic for humans; low/no fucose content; complete lack of sialic acids	[4,28,47,53]
Filamentous fungi	High growth rate and high productivity; extracellular secretion of proteins; correct folding of eukaryotic proteins; compared to yeast higher similarity of glycosylation pattern with mammals	Lower production of heterologous proteins (e.g., mammal proteins); secreted fungal proteases degrading recombinant proteins and thus yields; causing high viscosity of culture media; expression rate and secretion of fungal proteases determined by morphology during cultivation; glycosylation pattern different to mammals with altered terminal carbohydrate residues	[38,39]
Plants and plant cells (molecular pharming) various species e.g., tobacco maize, potato, rice	Cost-effective; agricultural scalability; fast scaling-up; improved safety (avoiding mammalian viruses); high product quality; versatile cultivation options (bioreactor, greenhouse, field)	Slower growth (compared to microbes) with medium to long production time-scale; plant vacuole contributing to cell size, but not to productivity; PTM differences to humans: lack of terminal Gal and sialic acid residues; α(1,3)fucose and β(1,2)xylose (both missing in humans); regulatory challenges	[28,65,66]
Insect cell lines	Cost-effective cultivation; all major fermentation strategies possible including suspension; simple synthetic media applicable; PTMs and glycosylation possible with higher similarity to humans (compared to bacteria, yeast, fungi); disulfide bond formation; no human pathogens, no endotoxins; no contamination with pesticides and herbicides (compared to whole plants)	No efficient secretion of proteins > 30 kDa to culture medium; genetic instability in continuous cultures; α(1,3)fucose[b] (immunogenic for humans); no sialic acids; no galactose; high fractions of oligomannose and paucimannose (with 3–7 mannose moieties); N-glycosylation simpler than in mammal cells; genes for related enzymes have to be implemented in the genome for complex glycosylation	[4,40,41,47,53]
Non-human mammalian cell lines			
CHO	Most common expression system: expression of > 70% of recombinant biopharmaceuticals; easy to transfect; growth in suspension; adaptable to serum-free and chemically-defined media, therefore low background; no human viruses / human virus genes not expressed, thus low biosafety risk; cell lines commercially available, e.g., ExpiCHO.	Lacking full proteolytic processing for some proteins; non-human glycan structures: Gal-α(1,3)-Gal (=α-Gal; <2%) and N-glycolneuraminic acid (Neu5Gc; <0.2%), both immunogenic; no production of α(2,6) sialic acid; lower sialic acid content (compared to humans); lack of α (1,3/4)-fucosyltransferases.	[4,41,45,47,53,59, 87]
BHK	Advantages as for other mammalian, but non-human host cells; cost effective vaccine production; adaptable to suspension cultivation and serum-free conditions	Not all BHK cell lines adaptable to suspension conditions; microbeads/microcarriers might be required; cell aggregation in serum-free culture medium; expression of α-Gal and Neu5Gc (both immunogenic)	[377–379]
NS0, SP2/0	Stable transfection; NS0 growth in suspension cultures; sialic acids mostly in α(2,6)-linkage	Production of α-Gal and Neu5Gc (both immunogenic) – even at higher levels than in CHO; NS0: cholesterol in culture medium required	[47]
Human cell lines			
HEK293, HT-1080, PER.C6	Endogenously no immunogenic glycans produced: no α-Gal, no Neu5Gc; compared to CHO: higher homogeneity of glycans (tetra-antennary); higher sialic acid content (compared to CHO); different transfection modes applicable	Human viral infections; lower clinical experience in comparison to other host cell lines	[47,59]

[a] A comprehensive survey of approved biotherapeutics together with the host cells applied in their manufacturing and their approval/non-approval by the EMA and FDA are given elsewhere [59].
[b] α(1,3)fucose occurring in the glycan core, contrary to α(1,6)fucose in the glycan core synthesized by mammals [47].

in concomitantly short time-frames as well as a risk reduction for product contaminations derived from host cells or the applied cell culture medium [28].

2.2.1. *Stability of host cells*

The long-term stability of host cell lines constitutes a relevant aspect for the quality of recombinant products. The genetic plasticity of CHO cells represents an advantage in the context of their adaptation to different cultivation conditions and scales, but imposes also a challenge in terms of maintaining the cell productivity and the (critical) quality attributes of the recombinant biotherapeutics over an extended cultivation period. Instability has been reported for up to 63% of recombinant CHO cells and can be caused by silencing or loss of genes, but also in response to external stressors, e.g., cultivation conditions. Genes coding for glycosylation enzymes, proteases, protein folding and chaperones can thereby be affected. In general, cell lines are considered stable, if ≥ 70% productivity is retained over 70 generations [57]. General aspects are reviewed elsewhere [28,54].

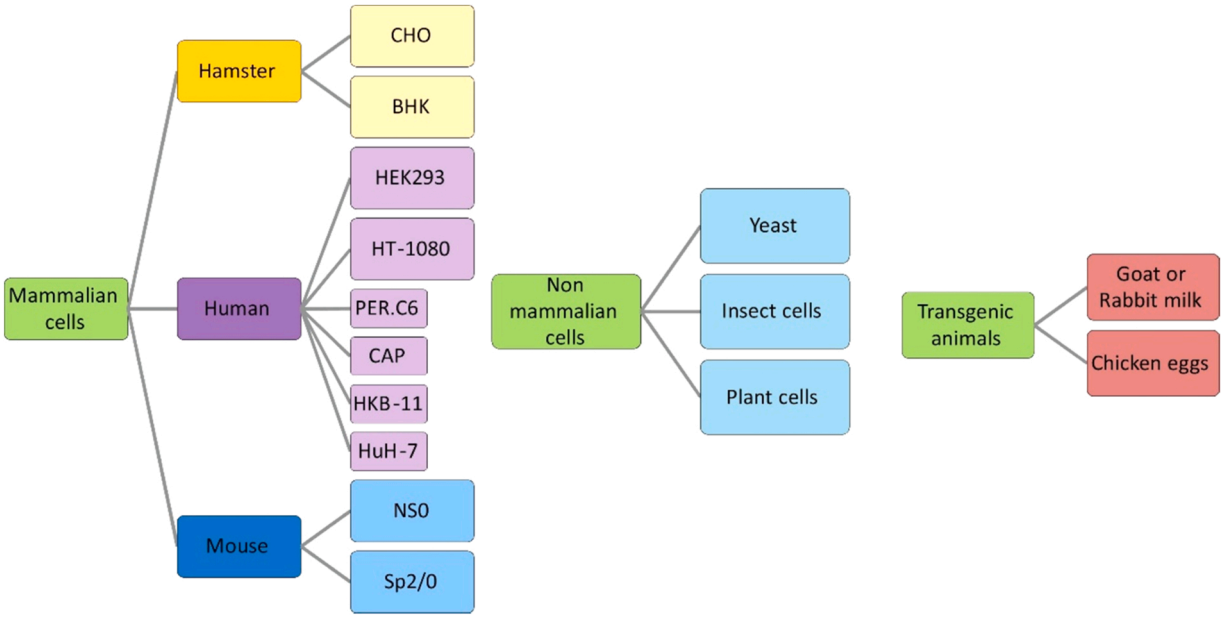

Fig. 2. Expression systems used for glycoprotein production by biopharmaceutical industries.
Reprinted from [53], with permission from Elsevier.

2.2.2. *Non-human and immunogenic protein modifications and contaminations*

Depending on the selected host cell line, the glycosylation pattern of recombinant biotherapeutics might deviate from natural human profiles. Non-authentic glycosylation by non-human host cells imposes a safety risk due to the potential immunogenicity of these products. Carbohydrate moieties that are not endogenous in human comprise α(1,3)-fucose and β(1,2)-xylose in plant cells [47,53] as well as Gal-α(1,3)-Gal (=α-Gal) and N-glycolneuraminic acid (Neu5Gc) in non-human mammalian cells, e.g., CHO and murine cell lines [4,47,53]. In comparison to CHO, murine cell lines (NS0, Sp2/0) express even higher percentages of α-Gal and Neu5Gc [47,53]. Contrary to other mammalians, humans lack Neu5Gc since the gene for the related enzyme converting N-acetylneuraminic acid (Neu5Ac) in Neu5Gc is irreversibly mutated [47,58]. Consistently, humans possess antibodies against Neu5Gc with up to 0.2% of the immune globulin G (IgG) directed against this immunogenic glycan variant. As shown in animal models, this can affect the clearance rate and thus the efficacies of recombinant biotherapeutics. Immune reactions against repetitively or even chronically administered recombinant therapeutic products carrying Neu5Gc might cause chronic inflammations paving the way for the progress of more serious diseases, such as atherosclerosis or cancer. In addition, a Neu5Gc contamination of recombinant products might also result from cell culture media, which are derived from animals (see Section 2.4). The competitive offer of the human sialic acid Neu5Ac in culture media could favorably shift the glycoprofile by reducing the Neu5Gc content in glycans in CHO, but not in murine cell lines [58]. Insect cells produce immunogenic glycans with fucose α(1,3)-glycosidic bound to a GlcNAc residue of the glycan core contrary to the core α(1,6) fucose linkage present in mammals. Yeast cells share the N-glycan core, i.e., Mannose $(MAN)_3GlcNAc_2$, with humans, but produce hypermannosylated N-glycans, which are immunogenic for humans [47].

Moreover, some glycans present in humans are not expressed in host cells. CHO cells for instance cannot produce α(2,6)sialylation and α(1,3/4)fucosylation (see Table 1) [4,53,59]. Insect cells produce glycans of the paucimannose type, which comprises the human core structure of N-glycans ($Man_3GlcNAc_2$), but lack further carbohydrate moieties, especially terminal galactose (Gal) and sialic acids. The paucimannose type occurs also in plants together with high-mannose variants (Table 1). For these reasons, *E. coli*, yeast and plant cells are primarily used as hosts for the expression of aglycosylated proteins in industry [47]. A depiction of the host-cell specific glycosylation pattern indicating differences from authentic human profiles is provided elsewhere [47].

Recombinant products may contain contaminations, comprising endotoxins (from bacteria), oncogenic DNA, viruses [28], such as endogenous retroviruses in murine hybridoma and CHO cells or viruses stemming from fetal bovine serum (e.g., adenovirus, bovine polyomavirus) [54], and prions [4,28,60]. Moreover, host cell proteins (HCPs) contained in the final recombinant product may pose another health risk for patients. HCPs may affect the product quality by degrading the biopharmaceutical and/or the contained excipients (e.g., polysorbates) via enzymatic reactions, but can also induce immune reactions of the patient either against the HCP per se or by triggering a response against the recombinant therapeutic protein with HCPs acting as adjuvants [61].

2.3. *Vectors and transfection of host cells*

2.3.1. *Methods of transfection*

Transfection is realized by the transfer of the recombinant gene into the selected host cell using a vector (e.g., a plasmid or a viral vector), which serves as a vehicle for the recombinant gene [4,62]. Ideally, transfections should be affordable straightforward and reproducible with high efficiency, exert low cytotoxicity and not compromise cell physiology [63]. Transfection methods have been classified as chemical, physical (both non-viral) and biological (=virus mediated) (see Table 2) [62,63]. Chemical transfection strategies apply calcium phosphate precipitation, cationic lipids (=lipofection) or cationic polymers, such as diethylaminoethyl (DEAE)-dextran or polyethylene imine (PEI). Electroporation, a physical approach, induces a transient membrane permeability of host cells via the generation of pores by electric pulses. These pores serve as entrance gates for vectors. Finally, viral delivery systems, e.g., adeno-associated viruses (AAV; for transient transfection) and lentiviruses (for stable transfection), can be used. Viral transfection is also called transduction [4,62,63]. However, the primary field of virus-based transfection is gene therapy (trials) to combat for instance monogenic diseases. This strategy has also been applied in cell cultures to produce for instance AAV recombinantly (without encapsulated DNA) [4,64] (see Section 3.12.4). The different transfection modes are

Table 2
Survey of selected transfection modes [62,63,380,381].

Transfection mode	Advantages	Disadvantages
Non-viral		
I. Chemical		
Calcium phosphate	High efficiency, cost-effective	Efficiency depending on cell type and condition
Cationic lipid	Straightforward; commercial products available; no limitation in package size	Limitation in targeting specific cells
Cationic polymer	No viral vector required	Cell specific cytotoxicity, lower transfection efficiency
II. Physical/Mechanical		
Direct injection	Straightforward	Special equipment required (micro needle, Gene Gun)
Electroporation	No vector required; applicable to cells cumbersome to transfect	Laborious, challenging technique; risk of cell damage and cell death
Sonoporation	High specificity; deep gene penetration; low cost; no cytotoxic effects	Risk of cell damage and cell death
Viral (transduction)		
III. Virus-mediated transfection	Straightforward, efficient	Potential hazard to staff; risk of induction of mutagenesis and gene disruption; virus depending packaging size

surveyed in Table 2. A discussion of factors that determine the transfection efficiency is beyond the scope of this review, but is compiled elsewhere [62].

Molecular farming, i.e., the expression of recombinant proteins in whole plants, represents another option for biotechnological production. The transfection of plants is done either by *Agrobacterium tumefaciens* [65] or by bombardment with micro-particles that are coated with DNA. If the DNA of chloroplasts is transfected instead of the genome contained in the cell nucleus, the protein yield is increased substantially, since the transgene copy number is raised due to the high number of chloroplasts in single plant cells. The transcription of the target gene in plants can be realized during a specific development phase or in defined tissues. Both strategies target to avoid pronounced accumulation of the recombinant proteins and to maintain their stability. In addition, "expression construct" design by employing promoters for high-level transcription boosts the yield. Promotors can also be triggered by external stimuli. As for plant cell lines, differences compared to human post-translational modifications (PTMs) occur also in molecular farming (Section 2.2.2; Table 1). Moreover, proteins with masses > 20–30 kDa have a pronounced tendency to remain in the apoplast instead of being secreted [28]. However, molecular farming has not reached the level of a widely-accepted routine expression strategy for biopharmaceutical means. This limitation is also related to environmental biosafety concerns particularly in open-field cultivation fueling worries about transgene spread via pollen or seed and horizontal gene transfer, which constitutes also a challenge for regulatory authorities and framework [28,66]. A survey of products manufactured by molecular farming is given elsewhere [28,65].

Transgene integration in the host cell genome is mostly random and occurs preferably in heterochromatin sections. This results in a low transcription efficiency. Therefore, screening for cells with successful transfection in active DNA regions, so-called hot spots, is essential. Different strategies are pursued in targeting site-specific integration including specific recombinases, endonucleases, such as zinc finger nucleases (ZFN), transcription activator like effector nucleases (TALEM), and recently also CRISPR/Cas 9 approaches. Further details are provided elsewhere [45,53].

2.3.2. Transient vs. stable transfection

For short-term expression and thus a transient production of the recombinant target protein, an integration of the vector in the host cell genome is not required. However, the vector is then lost in the course of cell division [4,53]. Depending on the frame conditions (target protein, host cell line, cultivation) harvest is done after 2–14 d [41]. This approach is primarily employed in research and for candidate screening. For industrial large-scale production with high yields, stable cell lines are required and the vector has to become integrated in the host cell genome in order to assure increased protein yields in consistent quality [4].

2.3.3. Regulatory elements, selector genes and clone selection

Besides the actual transgene, vectors contain regulatory elements that increase the expression of the target gene and thus the yield of the recombinant protein. These supportive elements include promotor and enhancer sequences, multiple cloning sites and elements that modulate the DNA architecture and thus the accessibility of the desired gene for the transcription machinery. In addition, a so-called selection system is required for the identification and selection of successfully transfected cells. The selector genes are also transferred to the host cell and may be localized on the same plasmid that carries the recombinant gene or on a separate vector [46]. The selector gene codes for an enzyme that allows transfected cells to survive and grow in cell culture media (i) lacking a selected essential nutrient and/or (ii) containing an inhibitor agent. Mostly, genes for dihydrofolate reductase (DHFR) or glutamine synthetase (GS) are applied as selectors [46,53,67]. In absence of hypoxanthine and thymidine or glutamine only transfected cells, which contain the DHFR or the GS selector gene, respectively, will survive [46,68,69]. Besides, resistance genes to antibiotics can be applied as well [4,70]. The DHFR system is frequently used in CHO cells [4,46]. For the selection of transfected cells, an additional inhibition of DHFR with methotrexate (MTX) or of GS with methionine sulfoximine (MSX), an inhibitory glutamate analogue, has been applied in CHO cells as well as GS knock-out cell lines [53,68]. Application of knock-out cell lines is due to the endogenous GS activity of CHO cells [53]. Moreover, selection of successfully transfected cells via MTX was also shown to foster transgene amplification, but is also a reason for instability in protein production [45]. The propensity for gene amplification increases for transgenes situated close to a short inverted-repeat sequence. The proposed mechanism for transgene amplification has been described exemplarily for CHO cells. In a nutshell, DNA double-strand breaks induced close to an inverted-repeat sequence lead to a DNA intra-strand connection via a hairpin formation. Subsequent bi-directional DNA replication forms a palindrome structure that carries the amplified gene [71].

Recently, Sun et al. [69] described an alternative proline-related selection, since CHO cells show proline auxotrophy. With the employment of Δ-pyrroline-5-carboxylate synthase as a selection marker, transfected cells were selected in proline deficient cell culture media within two weeks. In addition, this strategy prevented the application of toxic reagents that have to be removed otherwise [69].

2.3.4. Transcription efficiency and gene silencing

After the successful transfection, surviving host cells are isolated and single cells serve then as parent cells of derived cell clones. Cell clones with highest protein yield represent promising candidates for subsequent production of recombinant proteins. The site of transgene integration in the host cell genome determines the transcription efficiency and thus the yield of the desired target protein. This refers to DNA sections of different compactness, namely tightly packed

heterochromatin and lightly packed euchromatin. Gene silencing represents a general problem in mammalian host cells. This well-known effect is most likely caused by condensed DNA sections adjacent to the transfection site triggered by changes in the PTMs of histones, e.g., changed acetylation and methylation, and methylations in the transgene promoter region [46,57,72]. This detrimental effect can be counteracted by inhibiting adverse PTMs on the histone level [46]. Moreover, genes involved in the glycosylation of recombinant biopharmaceutics were affected by their silencing during long-term cultivation this way causing a decrease in sialylation. Transcriptional changes can also be induced by an altered composition of offered nutrients or by released metabolites [57].

2.4. Cell culture media

Cell culture media are composed of a basal medium fraction, e.g., Minimum Essential Medium (MEM) or Dulbecco's Modified Eagle's Medium and added nutritional constituents [73]. The latter might be added via human- or animal serum, platelet-, animal- or plant hydrolysates or directly in form of recombinant proteins [60,73]. Nutrients comprise trace elements, carbohydrates, amino acids, proteins, vitamins, lipids, fatty acids, hormones, growth factors, carrier proteins and proteins for cell adhesion required in cell cultivation [73]. The composition of the cell culture medium has a major impact on the physiology, growth pattern and transgene expression of transfected cells and thus also on the properties and especially the CQAs of the final recombinant product. Batch consistency is a matter of concern if poorly characterized/standardized media are used. Thus, standardized raw material, i.e., culture medium, contributes to an improved control of the final product [73].

For the cultivation of transfected cells, different types of culture media are applied. Initially, media based on biological material, i.e., biological fluids, were used. These (i) serum-based media mostly contain fetal bovine serum (FBS) and a complex mixture of growth supporting constituents. However, these media lack consistency with variations between different suppliers and batches and show a seasonal and geographical variability [74–77]. For cGMP conformance of serum, it has to be traceable and the source has to be verifiable BSE free. However, this statement and the certificate "cGMP-grade" serum has been controversially discussed since the raw material is not produced under cGMP conditions [73]. Moreover, a blending of FBS-based media with adult BSA was revealed in commercial media [78]. In calf serum, ~1500–1900 metabolites were addressed with ~800 metabolites annotated [79]. In addition, 660 proteins were covered in calf serum [80]. For comparison, in human plasma, 980 proteins have been experimentally identified. However, low abundant proteins even might have been missed [81]. Altogether, the variability of the composition of serum-based culture media contributes to different product qualities and thus makes a general inter-laboratory/inter-manufacturer comparability questionable [4,73,77]. In addition, these media bear the inherent risk of a contamination with viruses, microorganisms, yeasts and prions [60,82,83] (see Section 2.2.2). Moreover, serum collection from bovine fetuses has raised ethical concerns [78,83]. This caused the OECD and the EMA to recommend the replacement of FBS-containing media [77,84,85].

(ii) Xeno-free media include nutrients and proteins of only human origin excluding animal sera. They have been employed successfully to substitute FBS [60,73,86]. This can be extended to reagents that are applied in the production of the recombinant target protein [73]. In the case of (iii) serum-free media, animal or human serum as a whole is replaced by proteins from plants or from animal sources other than serum. (iv) Animal component-free media contain neither sera nor proteins derived from animals or humans. However, the composition of this medium is still poorly defined. (v) Protein-free media substitute proteins by digests or hydrolysates of proteins, but still lack a true chemical definition due to the presence of other non-proteinaceous biological constituents [73]. However, protein-free culture media make the purification of the target product more straightforward compared to media, which contain proteins or even serum, and result in a reduced background [41]. (vi) In contrast, chemically-defined media possess a distinct composition since they are composed of a mixture of defined components, including proteins, hormones, growth factors and cytokines, all with known structure and produced recombinantly in defined cell lines [73]. CHO and HEK cell lines can be cultivated in such chemically-defined media [41]. Chemically-defined media provide batch consistency and combine therefore comparability of results with ethical standards. However, this goes along with increased pricing and the need for a cell-specific adaptation of the composition [4] since there is no universally applicable formulation for chemically-defined media [74].

2.5. Scale-up of cell cultures

Expression systems of recombinant proteins are initially established in small scales of a few mL due to cost- and time efficiency of early stage development and optimization. The cell culture dimension is then scaled-up to commercial production scales, e.g., stir-tank bioreactors of stainless steel with up to 20,000 L [4,87]. This is done by increasing the culture volume and cell number stepwise via several passages. Duration and number of the steps of this so-called seed train should be kept low [88]. Moreover, yield and quality of the recombinant protein should not suffer from the scale-up [89]. What sounds straightforward is in fact a challenging and time-consuming process since the relevant parameters cannot simply be adjusted in a linear manner and the risk to fail in the scale-up process is high [7,89]. Mostly, scale-up is done by trial-and-error and requires experience [88,89]. The performance of host cells was shown to be scale-specific [4,7] with optimal time points for a cell passage to the next higher scale [88]. Different parameters have been considered in the scale-up process, including for instance shear stress, impeller tip velocity, volume average, power input, energy dissipation, and maximum shear rate [7]. Mathematical and computer models that allow for a prediction of optimized values for key parameters in defined culture scales have been derived, respectively [7,88,89].

Host cells are sensitive to shear stress. The shear environment in bioreactors is locally different with considerably higher shear rates close to the impeller compared to the bulk medium. Thus, a computational fluid dynamic simulation was done for different bioreactor configurations, generating a 3D space in order to result in a predefined cell viability. This space was defined by the acceptable ranges of three shear related parameters providing optimal rpm. Higher agitation speeds might cause cell damage, whereas too low rpm caused cell aggregation with concomitant limitation in nutrient transfer [7].

O_2 supply and CO_2 removal represent further critical parameters in the scale-up of cell cultures, and depend on the specific host cell line and the cell culture stage. For a high surface-to-volume ratio of the medium, the gas transfer via the liquid-air headspace surface in the bioreactor is sufficient. However, higher volumes in reactors of increased height will reduce this ratio unfavorably and require an additional oxygen sparge flow, which increases the shear stress. Thus, sparge flow rates have to be adjusted to prevent cell damage, but equally assure sufficient transfer rates of O_2 and CO_2. An increase in the CO_2 concentration of cell cultures will affect cell growth and the glycosylation of recombinant proteins [89]. A computer tool for optimizing the seed train based on the determination of the optimal time point for cell passage to the next culture scale was developed and compared to experimental results. This model considered inter alia uptake rates of glucose and glutamine, but also production rates of lactate and ammonia [88] (see also Section 2.6.3).

2.6. Cultivation of transfected cells

2.6.1. Modes of cell cultivation

Two different platforms are applied in the cultivation, namely (i) adherent cell cultures and (ii) suspension cell cultures. In adherent cultures, cells grow as monolayers on an artificial substrate. The product yield is limited by the available surface area. This format is preferably applied in research. (ii) In suspension cultures, cells float freely in the

culture medium. This format is mainly used for protein bulk production and the yield is restricted by the cell concentration. Cells have to be compatible with this type of cultivation, which is the case for CHO, NS0, BHK, HEK-293 and PER.C6 cell lines [46,53]. Other host cells have to be adapted to this cultivation platform [46]. Industrially, mammalian cells are mostly cultivated in suspension [4].

Based on the supply and exchange of the medium in cultivation reactors, non-continuous, semi-continuous and continuous cultivation modes can be distinguished. (i) Batch reactors use a non-continuous strategy in cultivation, whereas (ii) fed-batch fermenters apply a semi-continuous cultivation strategy. (iii) Perfusion systems pursue a continuous approach [46,87]. In batch cultures, nutrients and host cells are added to the fermenter with the start of the cultivation. Afterwards, no further nutrients are added nor dead host cells or metabolites produced or released from host cells are withdrawn. This causes the cultivation conditions to change over the entire production period. Cells grow in stirred reactors until the cell density declines due to the consumption of nutrients and the accumulation of detrimental products. Then the recombinant product is harvested [87,90]. In fed-batch processes, feeds that are specifically adapted to the individual stages and thus to the related needs of the cell culture are delivered at defined time-points from a connected feed hold tank (Fig. 3**A**). This promotes an extended cell viability and thus increases the final protein yield compared to a simple batch approach. In both cases, the final product is harvested at the end of the cultivation period and remains until then in the bioreactor [4,87].

In perfusion cultures, fresh medium is continuously supplied to the bioreactor at constant rate [4]. Culture medium influx to and efflux from the bioreactor occur with the same flow rate [87] and the exchanged medium volume may comprise several reactor volumes per day [46]. Recombinant products are withdrawn via a harvest line, which is equipped with a device for the retention of host cells. Thus, only medium containing the recombinant product is taken from the reactor this way (Fig. 3B). Contrary to fed-batch reactors, host cells are removed from the reactor in the perfusion mode via a separate bleed stream to keep a constant cell density in the reactor. Together with abundant cells some recombinant product will be removed, which reduces the final protein yield. Thus, the bleed rate should be kept small. Importantly, fast cell growth will entail an increased bleed flow rate and result in smaller protein yields. A comparison of cell density, target protein concentration and the total production for the discussed cultivation strategies is given elsewhere [87]. Karst et al. [91] showed a more or less stable viability and density of host cells in perfusion cultures, whereas both declined over time in fed-batch reactors. Based on the discussed aspects, this resulted also in a lower PTM heterogeneity of recombinant products under perfusion conditions [91].

2.6.2. *Influence of cultivation conditions on the recombinant product*

The cultivation mode influences the quality of the target product. This may be related to generated product-related impurities, produced by changes in the PTMs (N- and O-glycosylation, oxidation, deamidation, amino acid variations in the *C*- and *N*-terminus) as well as by higher order changes, e.g., aggregation and fragmentation, but also to process-related impurities, including HCPs, host cell DNA and other leachable compounds [5,91,92]. If CQAs are affected by these changes, this may induce infusion reactions, immunogenicity, anaphylaxis or reduced efficacy in patients [4]. A comprehensive survey of CQAs and how quality attributes are assessed for their criticality is given elsewhere [92,93]. CQAs are primarily considered of relevance for recombinant proteins, but can also be extended considering the criticality of process-related impurities and of raw materials applied in the production of the final (pharmaceutical) product [92].

Industrial production of recombinant proteins is nowadays mostly done in fed-batch and also perfusion reactors [87]. In case of fed-batch reactors, recombinant proteins remain in the fermenter from the time point of their synthesis until the end of the production period. This results in different residence times of individual protein molecules depending on their respective time point of translation [87,91]. The total cultivation duration in fed-batch reactors depends also on the host cell type: CHO cells typically spend 14–21 days, whereas the time interval is reduced to 7–10 days for yeast or filamentous fungi [35]. During this period, the composition of the cell environment changes due to an accumulation of detrimental cell metabolites, like ammonia and lactate, and other constituents released after apoptosis. This results in different PTMs, which increases the heterogeneity of the final product [46,87,91].

Perfusion cultivation offers numerous benefits in comparison to a fed-batch cultivation: the residence time is shorter and less variable for

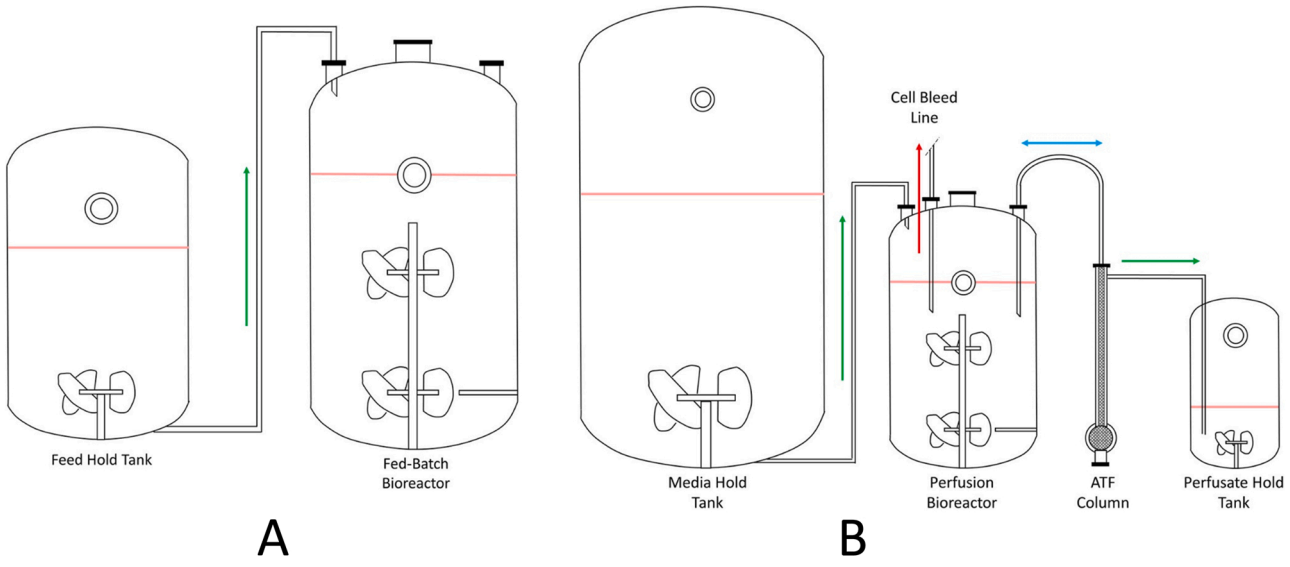

Fig. 3. Comparison of (A) fed-batch and (B) perfusion fermenter. (A) In fed-batch reactors a feed source is added from the feed hold tank to the bioreactor on predetermined time-points to prolong the viability of the culture. (B) In the perfusion reactor, a large media hold vessel is needed to supply perfusion media at the required rate over the duration of the culture.
Reprinted from [4], with permission from Elsevier.

individual protein molecules due to their continuous removal via the harvest line. In parallel, the continuous supply of fresh medium leads to a stable microenvironment. This improves the long-term consistency of the recombinant product [91]. Further advantages include an increased density of viable cells and an improved viability over a longer cultivation period, an improvement in CQAs, such as reduced aggregation and product clipping, but also a reduction in the variability of CQAs, as shown for the distribution of charge variants and glycosylation pattern in a CHO-K1 cell line. ChipCE, CGE and iCIEF were employed in addressing clipping and glycosylation pattern [94].

Despite the described benefits of perfusion reactors, fed-batch reactors still dominate the (bio)pharmaceutical production. This is mostly since the development and optimization of cultivation was focused on the latter over the past decade. Moreover, for a transition towards perfusion an adaption of cultivation platforms is required, including for instance the optimization of the host cell line, of culture media, flow rates and of the operation time. This requests time- and cost-intensive investments. In addition, the product batch is well defined in fed-batch cultivation since it is related to the defined time point of harvesting. In case of perfusion with a continuous harvesting of products, a timely stable cultivation process is required to assure batch consistency [87].

Traditionally, CQAs are measured off-line at an advanced production stage. Currently, tendencies for real-time monitoring at early manufacturing stages are reinforced. This covers not only CQAs, but also critical process parameters targeting to decode their interrelation. This knowledge can then be used to predict the final product quality in early production stages, but also to intervene well-timed via relevant process variables to counteract prognosticated disturbances of the product quality, this way also improving the product consistency [95]. As stated previously, non-human host cells may provide simplified or non-human glycosylation pattern and may fail to produce some human glycosylation structures (see Section 2.2.2). A more consistent product glycosylation can be targeted by glyco-engineering. In this context, an adaptation of the cell culture medium and of cultivation parameters have been used as well as the in vitro and in vivo implementation of enzymes that are involved in the appropriate glycosylation pathway in order to “humanize” the glycosylation profile [4,28]. This process is supported by mathematical modelling via stoichiometric and - more relevant - kinetic models. Mathematical models are trained and improved in an iterative process by the input of experimental data derived from a portfolio of analytical tools including also CE-based methods [96].

2.6.3. Cultivation conditions

Metabolic products, such as lactate and ammonia, which are produced by viable cells and released from dead cells as well, progressively deplete cell growth and protein production due to their accumulation in the culture medium. The effect of lactate is indirect via a decrease in the pH of the medium and the required addition of bases leading to an increase in osmolarity. Ammonia directly affects the product quality via induction of cell apoptosis and a concomitant release of glycosidases and proteases. Moreover, the induced pH change in the Golgi apparatus results in reduced glycosylation and sialylation of recombinant proteins [5].

The quality of recombinant proteins is determined by various cultivation-related factors including for instance the culture environment per se, and HCPs. Mammalian cells, such as CHO, show highest growth rates at 37 °C. A temperature reduction to 32–33 °C decreases the growth, but improves the cell viability and thus the productivity. In addition, less metabolic products, such as ammonia and lactate, and enzymes are released from dead cells [5]. This was shown to increase the sialylation of EPO. The concomitant increase in the negative net charge of EPO increased the electrostatic repulsion and reduced the aggregation propensity. The pH of the culture medium also influences cell growth, release of cell metabolites, protein yield and quality. Deviations from the optimum cultivation pH, which is mainly kept in the neutral domain, may cause protein aggregation and influence glycosylation [5].

2.7. Viability of host cells and host cell proteins (HCPs)

2.7.1. Viability of host cells

The viability of host cells is essential in their cultivation since metabolites and enzymes become released from dead cells (see Sections 2.6.3 and 2.7.2). This is of general concern in long-term cultivation. The cell viability is related to the increased expression of specific transcription factors and to anti-apoptotic and pro-proliferative genes. Thus, forced expression of beneficial genes and silencing or even knocking out genes deteriorating viability are appropriate strategies to foster cell viability [45].

2.7.2. Host cell proteins (HCPs)

HCPs are secreted by proliferating cells and released from dead cells [57,97]. The HCP profile encountered in the supernatant of cell cultures depends on the host cell line, the duration and the mode of cultivation [5,97,98]. Moreover, HCPs might also be released from cells that have been damaged mechanically by the impeller required for media agitation in bioreactors [99] (see Section 2.5). In general, an extension in the cultivation duration leads to an increased accumulation of HCPs in the medium. Due to their longer cultivation duration, fed-batch cultures showed higher HCP concentrations and increased numbers of different HCP species compared to batch-cultures, i.e., ~2100 HCPs vs. ~1900 HPCs, respectively [97]. In both cultivation modes, HCPs increased and the fraction of HCPs stemming from intracellular compartments grew with the duration of cultivation when entering the declining phase of host cell growth with progressive lysis of dead cells [97]. Secreted and released proteases and glycosidases constitute important HCP classes and can affect the CQAs [57,99]. In media of CHO cells derived from bioreactor batch cultures, HCPs that are involved in apoptosis, in cell death, proteolysis and in the processing of N-glycans have been identified. Other HCPs act as autocrine growth factors promoting the growth of host cells [99]. For some CHO cell lines, HCPs caused an increase in acidic variants of the recombinant protein species due to deamidation, increased sialylation, reduction of disulfide bonds and C-terminal lysine clipping [97]. In other CHO lines acidic isoforms and sialic acid content decreased by an increase in the neuraminidase concentration, with a concomitant increase in the fraction of neutral glycans [98]. Changes in the protein charge may also lead to an altered aggregation propensity of the recombinant product [5]. HCPs with protease function, such as cathepsins, serine- and cysteine proteases, were shown to cause degradation and even fragmentation of recombinant proteins, e.g., for EPO or IFN-γ [97,98]. The discussed effects may change the isoelectric point (pI) and/or the size of the target proteins. Both properties are addressed in CE-techniques and can be used to distinguish closely related protein variants electrophoretically (see Sections 3.1 and 3.7). Some HCPs, such as acidic proteases from CHO cells, can escape downstream purification (see Section 2.8), co-elute with the recombinant protein and pass to the final drug substance. This can compromise the stability of the final drug product especially during long-term storage [98,100]. Moreover, HCPs were shown to evoke inflammation and immunogenicity in combination with a recombinant protein, thus acting as undesired adjuvants in the described case [101]. In chemically defined cell culture media (see Section 2.4), growth factors, such as insulin, are required to increase cell viability and growth. Insulin degrading enzyme (IDE) was secreted by CHO cell lines and accumulated over time. This degraded insulin, reduced the cell viability and thus the titer of the recombinant protein [102]. Added inhibitors of proteases, such as pepstatin A, or IDE inhibitors were able to eliminate/inactivate challenging HCPs. This was also realized by knocking out the related genes in host cells [98,102]. Consequently, HCPs have to be considered as CQAs as well [100]. USP and Ph. Eur. recommend HCP concentrations as low as technically feasible, but currently do not specify thresholds for reasons outlined elsewhere [61,103,104]. CE cannot only be used for the characterization of recombinant proteins, but also of HCPs (see Section 3.14). Among the electrophoretic methods of the USP applied in the HCP characterization, CE-SDS with laser induced fluorescence (LIF) detection is listed [103].

2.8. Downstream processing

After the harvest of recombinant proteins, downstream processing is required, which comprises the isolation of the target protein from the residual cell culture biomass and protein purification by removal of remaining impurities. Downstream processing covers the majority of the production costs [40] and has to be tailored to the respective properties of the target protein as well as the contained impurities. For economic reasons, the biopharmaceutical industry progressively applies downstream platforms for related products. This streamlines not only their development, but allows for the operation with templates in quality control. As a result, the commercialization, but ideally also the admission by regulatory authorities is accelerated [8]. Comprehensive strategies and protocols for specific purification and isolation of recombinant proteins are surveyed elsewhere [105]. Different challenges are encountered in downstream processing, depending whether proteins are secreted in the culture medium or remain in the host cells. This entails either a higher protein dilution in the medium or requires cell disruption with subsequent removal of cell debris and high HCP concentrations [40]. A typical downstream scheme comprises (1) a purification step with capturing of the recombinant protein, e.g., via affinity chromatography, (2) inactivation of possible viral contaminants with low pH, (3) multistep product polishing, (4) viral filtration/clearance, and (5) ultrafiltration/diafiltration. Multistep polishing assures that final products meet their specifications. Commonly, flow-through approaches, such as anion-exchange-, cation-exchange- and hydrophobic interaction chromatography, where impurities are retained and the target protein passes, are combined with a bind-elute strategy [8,51,91,106]. In the latter strategy, the desired recombinant protein and remaining impurities are subjected to a chromatographic separation and the target protein is recovered either with a wide or a narrow retention window cut, depending whether high recovery or high purity is the ultimate goal [91]. Analytical methods, e.g., CE-techniques, can be applied to test for the efficacy of downstream processing by comparing aliquots taken from individual steps and batches (as shown in Sections 3.3.1, 3.3.4, 3.3.10), but constitute also monitoring tools assuring the consistency of downstream purification over time.

2.9. Perspectives and novel strategies in target host cell selection

CHO cell lines are widely applied in industrial manufacturing of recombinant products, which is due to their approval by regulatory authorities, such as FDA and EMA [3]. Novel approaches in product-related host cell selection target on comprehensive Omics, combining genomic, transcriptomic, proteomic and metabolomic data in order to understand the genetic landscape of individual CHO cell lines. This may support the selection/adaption of CHO cells to specific needs, e.g., required PTM profiles, and is of particular importance in glycosylation microheterogeneity and profiles of charge variants. Understanding the cell line specific PTM profiles is relevant for two reasons: it (i) ensures the synthesis of desired PTM profiles tailored for the intended use of the recombinant products and (ii) helps to decode, how cellular PTMs influence bioprocess-related CHO phenotypes. Ideally, the recognition of the genetic configuration together with pinpointing target genes for specific PTM decorations would either allow for a selection of appropriate CHO cell lines or for their genetic engineering in order to home on a tailored product. The latter strategy could employ CRISPR/Cas 9 [3]. This concept could also be applied in adapting alternative non-mammalian host cells that offer general advantages over CHO and human cell lines, e.g., faster growth, reduced HCP secretion, more robust and cost-effective cultivation, but presently suffer from the disadvantage of non-human like and possibly immunogenic PTMs (see Section 2.2.2; Table 2). In this context, protozoa, yeasts and filamentous fungi have been proposed recently [35]. Moreover, in combination with platform approaches [8] this strategy can reduce timelines for transferring biopharmaceutical candidates to phase 1 clinical studies [35].

3. Capillary electrophoresis techniques

3.1. Principle of CE

CE-based analysis systems separate analytes in fused-silica capillaries of miniaturized dimensions, i.e., an inner diameter of preferably 50–75 μm. Analytes move in the separation capillary under the influence of an external electrical field with their migration order governed by their charge and hydrodynamic radius (r_H). The relationship between these parameters and the electrophoretic velocity v_i^o is given by the following equation

$$v_i^o = \frac{z \bullet e \bullet E}{6 \bullet \pi \bullet \eta \bullet r_H} \quad (1)$$

where z is the charge number of the analyte, e is the elementary charge, E represents the electric field strength and η the viscosity of the separation medium.

Dividing v_i^o by E provides the so-called limiting or absolute electrophoretic mobility, which corresponds to the electrophoretic velocity standardized to the unit of the electric field. Eq. (1) assumes infinite dilution and a fully charged analyte. However, the analyte interaction with counterions present in the separation medium, i.e., the background electrolyte (BGE), reduces the mobility in comparison to Eq. (1) due to the electrophoretic relaxation and retardation force resulting in the so-called actual mobility [107,108]. Moreover, depending on the pH of the applied BGE, analytes/proteins may take different charge states and cycle between these charge states during their migration. Since charge states differ in their electrophoretic mobility, the mobility over the migration distance is the average weighted over the time fraction that an individual analyte spends in the respective charge state. This is the effective electrophoretic mobility (μ_{eff}). A comprehensive discussion and a survey of the different electrophoretic mobilities is given by Jouyban and Kenndler [108]. Protein states of the same species and charge, but differing in their r_H as small as 26 pm were resolved in CZE [109]. This would allow for the distinction of different conformations, even on a cis/trans level, of the same protein [109,110] (see Section 3.3.12).

The pH of the applied BGE governs the protonation/deprotonation state of the silica surface, i.e., of the silanol groups, and thus the net charge. These negative charges are compensated by cations of the BGE, which are arranged in an electrical double layer [111,112]. The related zeta-potential (ζ) determines the velocity of the electroosmotic flow (v_{EOF}) according to the following equation [113].

$$v_{EOF} = \frac{\varepsilon \bullet E \bullet \zeta}{4 \bullet \pi \bullet \eta \bullet} \quad (2)$$

with ε representing the electric permittivity. Fundamentals of the EOF and the ζ-potential have been discussed comprehensively in numerous papers [114–116]. Corresponding electrical double layers will also form on the surface of charged particles and are thus also present on protein surfaces [117] (see Section 3.3.9.2).

Contrary to chromatographic separations, where analyte interaction with the stationary phase is a prerequisite for successful analyte resolution, in CE even short-time interactions of the analytes with the capillary surface entail a pronounced detrimental effect on peak width and thus separation efficiency. Retention factors < 0.1 reduced plate numbers of proteins by a factor of 20 [118–120]. The adhesion propensity increases with protein size and is more pronounced for proteins with alkaline pI [121]. Therefore, protein-wall interactions have to be counteracted. This represents a key aspect for successful protein separations with CE. Appropriate means to combat protein adhesion are addressed in the next section.

3.2. Strategies to prevent protein adhesion

3.2.1. Protein adsorption

Besides the inherent conformational stability, i.e., whether proteins are classified as "hard" or "soft" [122], the protein isoelectric point (pI) and its relation to the pH of the BGE determines the adhesion onto the capillary surface [123]. If the pH equals the protein pI, protein attachment is most pronounced due to the minimized lateral repulsion between adhered proteins [123,124]. In case of pH<pI, protein electrostatic adsorption occurs since the silica surface and the protein are countercharged. However, if the pH approaches the pI of silica, which is around 2.2 [125], protein adsorption progressively diminishes by reducing the silica net charge to virtual zero. Concomitantly, this will also suppress the EOF [126]. With pH>pI, both protein and silica surface are co-charged and prevention of adsorption is expected due to an electrostatic repulsion. The guanidine moiety of arginine and the ε-amino group of lysine are protagonists of electrostatic attachment, due to their positive charge even under alkaline conditions [127,128]. Actually, patch-like accumulation of these basic amino acids on the protein surface may cause adsorption even under repulsive conditions [129,130]. Moreover, hydrophobic proteins also show a pronounced adhesion tendency (see Sections 3.3.1 and 3.3.7) [131,132]. Principles and molecular mechanisms of protein adsorption as well as counteracting strategies have been comprehensively discussed in a couple of reviews [133,134]. One has to keep in mind that an entire prevention of protein adsorption in CE is a myth and thus utmost restriction has to be the ultimate goal. Consistently, separation efficiency is not only determined by axial protein diffusion, but – besides other factors (e.g., thermal and instrumental contributions to band dispersion) – also by protein adsorption onto the capillary wall. This refers to a mass transfer to the capillary surface. Leclercq et al. [135] showed in this context that even low retention factors (<0.05) exert an influence on the achieved separation efficiency and an optimal apparent electrophoretic velocity (and thus separation voltage) can be addressed. In fact, the chromatographic world enters CZE under these conditions.

3.2.2. Preventive strategies

Different strategies have been applied either alone or in combination to combat detrimental protein adsorption.

(1) One approach refers to an appropriate conditioning of fresh separation capillaries, since the conditioning protocol and the applied rinsing solutions have to be adjusted to the BGE and the separation problem [130].
(2) An appropriate rinsing protocol between consecutive CE runs helps in minimizing protein adsorption and promotes the desorption of adhered protein residues prior to the next CE run. Capillary rinsing with acidic solutions, such as HCl, reduces the negative charges of silica by protonation of silanol groups. This effect will continue during the subsequent separation step [136] due to the hysteresis effect described by Lambert and Middleton [137]. Alternatively, multistep rinsing with alternate cycling between alkaline and acidic rinsing solutions supports the detachment of proteins [130]. This is essential, since post-adsorption processes, e.g., conformational changes leading to multipoint contacts [133,138], may turn protein attachment (partly) into an irreversible event within 24 h [139]. This changes the capillary surface, the ζ-potential and thus the μ_{EOF} [121]. For some CE applications, rinsing with detergent solutions, e.g., SDS, was beneficial in the detachment of protein residues [123,139,140].
(3) Besides capillary rinsing, the composition of the BGE assists in counteracting adsorption. Some ions, such as phosphate, promote the taking of a native protein conformation [141], and mask or even change the charge of positive protein patches [122], which constitute primary contact points with the capillary [133]. Moreover, the protonation tendency of silanol groups was increased in the presence of phosphoric acid [142] via complex formation with phosphoric acid [143], this way apparently also screening the capillary surface [142]. Phosphate was also shown to improve the separation of rhEPO variants, even when contained in a mixed BGE [144].
(4) The influence of the selected pH of the BGE in relation to the protein pI was already discussed in the previous section. However, one has to be aware that operations at highly acidic or alkaline pH reduce protein adsorption, but reduces charge differences [142] and may entail protein unfolding [145,146] thus diminishing the resolution of closely related protein variants by abating minute differences in net charge and r_H. Moreover, quaternary protein structure and prosthetic groups may get lost under extreme pH conditions [130,147]. Besides, an increased risk for aggregation and precipitation has been reported especially under highly acidic conditions [126].
(5) An increase in the BGE concentration will promote the competition of electrolyte ions with proteins for available adhesion sites on the capillary surface, but simultaneously increase Joule heating, which results in peak broadening and impaired resolution [148]. The application of acidic isoelectric buffers with zwitterionic properties was shown favorable in this context [123, 133].
(6) Some authors applied repetitive sample injections with several virtual analyses prior to the actual CE measurements in order to saturate possible adhesion sites on the capillary surface [132].
(7) The by far most effective strategies employ a masking of silanol groups and thus shielding of negative charges on the capillary surface by capillary coating with some recent solutions compiled elsewhere [149]. Information about the influence of deposition and rinsing solutions on the topography of the coating as well as their effect on protein adsorption were not accessible by direct in-capillary measurements on the coating level, but had to be deduced from separation results [121,130]. Atomic force microscopy (AFM) filled this information gap, but was applied under operations that simulate separation conditions and was refined to topographic aspects [150,151]. Recently, a consortium of research groups established an AFM mode with combined topographic and recognition (TREC) imaging in the characterization of coatings inside the capillary by addressing charge distribution in combination with topography [152,153]. This novel imaging strategy will support a refined direct visualization of surface mechanisms in coated and bare fused-silica (bfs) capillaries when separating proteins.

Capillary coating is realized by (i) physically adhered and (ii) covalently linked coating. The first case (i) can be sub-classified in (a) dynamic and (b) static (semi-permanent) coating. In dynamic coating, small reagents adhere to the capillary surface thus masking the negative capillary charges. Since their attachment is weak and thus only temporary, gaps in the coating have to be filled continuously. Therefore, dynamic coating constituents have to be added to the BGE to assure continuous renewal of the coating. This type of coating is not compatible with CE-MS. Examples for dynamic coating agents are given elsewhere [123]. In static coating, neutral or polyionic polymers of high molar mass are applied. The preparation of the coating is realized by rinsing the capillary with a polymer solution of appropriate composition. Since the adhesion of the coating agents is stronger than in dynamic coating, an addition of coating polymers to the BGE is not required anymore. However, coatings can still be regenerated by another rinsing step once degradation occurs over time. Static coatings are either prepared in monolayer or multilayer architecture. For the latter case, the so-called successive multiple ionic polymer layer (SMIL) coating has to be mentioned, which combines alternating polycationic and polyanionic polymer layers thus boosting the durability [154,155]. The principles of

SMIL coating have been recently reviewed [156]. With appropriate polymer combinations and tailored coating protocols, a durability of > 70 runs (corresponding to >42 h voltage application) could be realized without a need for recoating in between as shown by our group [157].

In addition, covalent coatings can be applied and numerous synthesis protocols are available as compiled elsewhere [158]. However, due to the laborious multistep preparation, mostly commercial capillaries with covalent coating are applied in the CE separation of recombinant proteins (see Table 3).

3.3. Capillary zone electrophoresis

3.3.1. Interleukins

Human interleukin-7 (hIL-7) constitutes a 32–35 kDa glycoprotein with three N-glycosylation sites and one O-glycosylation site. IL-7 is involved in B- and T-cell lymphopoiesis including also maturation, mobilization and maintenance of cells responding to IL-7 [48]. It is applied in the therapy of cancer and of diseases causing chronic infections [131,159]. Initially, rIL-7 was mainly expressed in *E. coli*, *Pichia pastoris*, and insect cells (see Section 2.2). Non-glycosylated IL-7 from *E. coli* is bioactive, but immunogenicity concerns have been discussed. Thus, expression is done in CHO cells meanwhile [131,159]. Tavernaś group [159] separated glycosylated rhIL-7 from CHO in a 25 mmol/L citrate buffer, pH 2.6, resolving rhIL-7 in four peak clusters. The improved separation compared to other BGEs tested by the group has been attributed to an selective ion-pair formation between citrate and the respective glycovariants of rhIL-7 [160,161], this way influencing the individual charge-to-r_H ratio [161] (see Eq. 1). When NaOH was replaced by triethanolamine in the BGE preparation, the resolution was improved due to an EOF reversal and a reduction of protein adhesion. A rinsing procedure with 50 mmol/L SDS between runs was essential to improve the precision of both t_m and relative peak areas (see Section 3.2.2). Different production batches were compared: whereas a scale-up from 12 L to 200 L in the production was without effect on the profile of rhIL-7, improved downstream processing (see Section 2.8) revealed an increase of higher glycosylated and sialylated variants [159]. The same group optimized an alkaline BGE with 25 mmol/L borate and 12 mmol/L diaminobutane (DAB), pH 10, for rhIL-7. Seven glycovariants were resolved [131]. Complexation of borate with carbohydrates has been described to influence the μ_{eff} [162]. Moreover, DAB was added for dynamic capillary coating. Capillary storage in 0.1 mol/L NaOH overnight and a capillary conditioning that included also the performance of five “pre-analyses” with rhIL-7 prior to the actual CZE-UV measurements improved the precision of μ_{EOF} and t_m. This has been attributed to an improved adhesion of DAB on the inner capillary wall. The analysis of non-glycosylated rhIL-7 from *E. coli* provided a broad peak and the signal did not return to the former intensity of the baseline [131], which is indicative for pronounced protein adsorption [121]. This has been related to the accessibility of a hydrophobic patch on the protein surface that was not shielded by the missing carbohydrate chains anymore. Finally, three rhIL-7 batches from CHO cells were compared, where a modified downstream purification resulted in different profiles [131].

rhIL-11 is applied in the treatment of thrombocytopenia induced by chemotherapy in order to increase platelet counts [163]. Since rhIL-11 is not glycosylated, it was expressed in *E. coli* with a theoretical mass of 19.2 kDa and a pI of 11.2. Its hydrophobicity complicates recombinant expression in *E. coli* due to an increased risk for the formation of inclusion bodies [164]. Different batches of two commercial rhIL-11 products were analyzed by CZE-UV. In addition, two reference rhIL-11 compounds, i.e., rhIL-11 WHO 92/788 and a biological reference substance (BRS) of rhIL-11, were analyzed. Separation was done in 50 mmol/L sodium dihydrogen phosphate, pH 3.0, which provided an improved peak symmetry (see Section 3.2.2) and an acceptable low separation current compared to all other tested BGEs. The method was validated [165] according to the ICH-guideline Q2(R1) [26] including also a comprehensive robustness testing. Based on the peak purity index and a concurrent comparison of slopes for external calibration and standard addition, interferences with excipients were excluded. Besides, the BRS was subjected to forced degradation including acidic, alkaline, oxidative, UV and thermal stress with subsequent separation of related degradation products. Different batches of commercial rhIL-11 products (Plaquemax® and Neumega®) were analyzed with the validated CZE-UV method and content/potency was compared to results delivered by RP-HPLC with C_4-columns and by an in-vitro bioassay. The encountered differences were statistically non-significant on a 5% significance level applying analysis-of-variance (ANOVA) [165]. However, statements about homoscedasticity and normal distribution of data in order to justify this statistical approach were missing.

3.3.2. Interferon-α

Recombinant interferon-α (IFN-α) is a cytokine approved in the treatment of hepatitis B and C, malignant melanoma, AIDS-related Kaposi sarcoma and hairy cell leukemia [166]. Catai et al. [167] analyzed a chemical reference substance (CRS) of rhIFN-α2b of the Ph. Eur. in SMIL capillaries coated with a bilayer of polybrene (PB) and poly (vinyl)sulfonate (PVS). With a BGE of 300 mmol/L Tris phosphate (pH 8.5), 125,000 plates were achieved [167].

3.3.3. Parathyroid hormone

Teriparatide is a recombinant 4.1 kDa fragment of the human parathyroid hormone (rhPTH 1–34) expressed in *E. coli*. It is applied for bone formation in order to treat osteoporosis and has been applied off-label for treatment of hypoparathyroidism [168,169]. A CZE-UV method was optimized based on a commercial formulation of rhPTH. CZE separations were done with 50 mmol/L sodium dihydrogen phosphate, pH 3.0. The capability of the CZE method for stability testing of rhPTH 1–34 products was evaluated by means of forced degradation studies on an rDNA-derived WHO reference product of the hormone. Therefore, the product was subjected to acidic and alkaline stress conditions. Moreover, thermal degradation, photo-degradation with UV light and oxidation with 3% H_2O_2 were done. In either case, the height of the primordial peak decreased, and one to three novel peaks, representing the resulting degradation products, were induced. For acidic stress, resulting degradation product(s) were not detectable at the selected wavelength. After its validation, the CZE-UV method was applied to commercial teriparatide formulations and results were compared to RP-HPLC, SEC-HPLC and an in vitro bioassay (n = 10, respectively). The mean difference to the CZE-UV method was < 1.4% in either case and not significant on a significance level of 0.05 as shown by ANOVA [168].

3.3.4. Recombinant 18 kDa and 24 kDa glycoproteins

CZE-UV in polyvinyl alcohol (PVA) coated capillaries was applied to separate variants of a highly glycosylated 18 kDa protein recombinantly produced in CHO. Unfortunately, the protein identity was not revealed in the publication. The protein possessed seven N- and one O-glycosylation site with 60% of the molecular weight related to the carbohydrate moieties. The pI of the protein was ~2.0 and thus highly acidic. CZE separation was done in 25 mmol/L β-alanine/acetic acid with 0.01% (v/v) Tween 20, pH 3.3. A low BGE concentration was selected to restrict the separation current and Joule heating (compare Section 3.2.2). The protein carried up to 30 sialic acid residues with major glycovariants possessing 26–30 sialic acids. This was corroborated by a spectrophotometric assay with ninhydrin. The specificity of the CZE method was addressed by comparative measurements of two commercial EPO products, i.e., Epogen® (epoetin α, pI ~4.4) and Aranesp® (synthetic EPO = Darbepoetin α; pI ~3). Intermediate precision was determined by testing different batches of PVA capillaries, application of different CE instruments, and different operating analysts in the analysis of the 18 kDa glycoprotein. Moreover, the CZE method was successfully applied as an in-process assay in selecting an appropriate CHO clone

Table 3
Analysis of recombinant proteins with different CE techniques.

Recombinant protein/ product	Host cell	CE-technique	Detection and MS interface	Capillary coating	BGE and SL	Separation and ESI conditions	Validation	Comments	Ref.
CZE-UV									
rhIL-7	CHO	CZE	UV 214 nm	Presumed dynamic (triethano-lamine)	25 mM citrate/ triethanolamine, pH 2.8	15.0 kV, 25 °C Inj. 3.45 kPa, 5 s	Intra- & interday precision (t_m, peak area)	Analysis of HPLC fractions; batch testing	[159]
rhIL-7	CHO *E. coli*	CZE	UV 214 nm	dynamic (DAB)	25 mM borate, pH 10, with 10 mM DAB	20.0 kV, 25 °C Inj. 0.5 psi, 5 s	Specificity, LOQ, linearity, precision, robustness	System suitability test; testing of batch-to-batch consistency	[131]
rhIL-11 (WHO 92/788; BCR; Plaquemax®, Neumega®); rhIL-11 in human plasma	*E.coli* n.s.	CZE	UV 196 nm	bfs	50 mM NaH_2PO_4, pH 3.0 adjusted with phosphoric acid	20 kV, 25 °C Inj. 50 mbar, 45 s	Linearity, trueness, precision (t_m, % peak area), LOD, LOQ, robustness, stability	System suitability test; forced degradation studies; Rupatadine fumurate used as ISTD	[165]
rhIFN-α2b (Ph. Eur. CRS)	*E. coli*	CZE	UV 205 nm	SMIL (PB-PVS)	300 mM Tris phosphate, pH 8.5	30 kV, 25 °C Inj. 34.5 mbar, 5 s	/	HSA affecting t_m; rinse with 0.1 M NaOH	[167]
rhPTH (Teriparatide) (WHO 04/200; Fortéo®)	*E. coli*	CZE	UV 200 nm	bfs	50 mM sodium dihydrogen phosphate, pH 3.0	20 kV, 25 °C Inj. 50 mbar, 45 s	Specificity, linearity, precision, trueness, LOD, LOQ, robustness	System suitability test; forced degradation studies; application of ISTD (ranitidine)	[168]
rhEPO (WHO 88/574; Eprex®; Dynepo®; Binocrit®; Retacrit®)	n.s.	CZE	UV 214 nm	dynamic (DAB)	10 mM sodium chloride, 10 mM Tricine, 10 mM sodium acetate, 7 M urea and 2.5 mM DAB, pH 5.5 (=Ph. Eur. BGE for rhEPO)	15.7 kV, 25 °C Inj. 0.7 psi, 60 s	/	Testing biosimilars vs. originators	[178]
rhEPO (Ph. Eur. BRP; human urinary EPO)	CHO	CZE	UV 214 nm	dynamic (DAB)	Ph. Eur. BGE for rhEPO with 3.9 mM DAB, pH 5.5	15.4 kV, 35 °C Inj. 0.5 psi, 30–80 s	/	Comparison rhEPO and urinary EPO	[179]
rhEPO (Ph. Eur. BRP lot 2; Aranesp® (=darbepoetin α))	CHO	CZE	UV 214 nm	dynamic (DAB)	Ph. Eur. BGE for rhEPO, pH 5.5 (for Ph. Eur. BRP), with pH 4.5 for Aranesp®	15 kV, 35 °C Inj. 33.5 mbar, 15 s	Intra- and inter-day precision (t_m, μ_{eff}, corrected peak areas)	Darbepoetin α misuse in sport	[180]
rhEPO (Ph. Eur. BRP; Eprex® (EPO-α), NeoRecormon® (EPO-β))	CHO	CZE	UV 214 nm	dynamic (DAB)	Ph. Eur. BGE for rhEPO with 3.9 mM DAB, pH 5.5	25 kV, 35 °C Inj. 0.5 psi, 15 s	/	Removal of HSA excipient	[181]
rhEPO	CHO	CZE	UV 200 nm	dynamic (methyl-chitosan)	10 mM sodium acetate-HAc, 7 M urea, 2.5 mM DAB and 0.2 mg/mL methylchitosan, pH 4.5	-12 kV (reversed polarity), 25 °C Inj. 0.5 psi, 3 s	/	/	[182]
rhEPO (Ph. Eur. BRP; samples from five manufacturers – not specified)	n.s.	CZE	UV 214 nm	SMIL (commercial double layer coating)	nitrilotri(trimethyl) phosphonic acid, pH 4.4, with 7 M urea	30 kV, 25 °C Inj. 0.5 psi, 15 s	Resolution, repeatability (t_m, %peak area)	Comparison with Ph. Eur. method	[183]
rhEPO (BRP batch 4, EDQM; 8 different production batches)	CHO	CZE	UV 214 nm	dynamic (DAB)	Ph. Eur. BGE for rhEPO, pH 5.5	15.4 kV, 25 °C Inj. 33.5 psi, 15 s	/	Relation between bioactivity and aggregation	[187]
rhEPO (NESP® (darbepoetin-α); JR-131 (biosimilar))	CHO	CZE	UV 214 nm	dynamic (DAB)	DAB, sodium acetate, urea, pH 4.5 (no further specification)	20.0 μA, 35C Inj. 0.5 psi, 20 s	/	Cell culture medium without animal derived material; comparison biosimilar vs. originator	[188]
rhEPO (Ph. Eur. BRP; different batches of various drug products and formulated products)	n.s.	CZE	UV 200 nm	commercial coating (amine coated eCap capillary)	200 mM or 300 mM NaH_2PO_4, both with 1 mM $NiCl_2$, pH 4.0	-8.0 kV, 20 kV Inj. 0.5 psi, 8 s	Linearity, range, precision (t_m, corrected peak area), LOD, LOQ, matrix effect	No sample pretreatment required; comparison with Ph. Eur. method	[190]
rhCG (commercial CRS; illegal hCG samples)	n.s.	DICZE	UV 200 nm	dynamic (DAB)	8.2 mM DAB, 85 mM ammonium phosphate, pH 6.0	15 kV, 20 °C Inj. 0.5 psi, 5 s (double injection mode, DICZE)	Repeatability (t_m, relative t_m)	Method applied to illegally distributed products	[199]
rhGF (=somatropin) (CRS from EDQM)	n.s.	MICZE	UV 200 nm	SMIL (PB-chondroitin sulfate)	100 mM ammonium phosphate dibasic, pH 6.0	10 kV or 17.4 kV, 30 °C Inj. 0.8 psi, 10 s (multiple-injection mode, MICZE)	Inter-day precision (t_m, % peak area)	Comparison with Ph. Eur. method; SMIL coating regeneration every 5 CZE runs	[132]

(*continued on next page*)

Table 3 (*continued*)

Recombinant protein/ product	Host cell	CE-technique	Detection and MS interface	Capillary coating	BGE and SL	Separation and ESI conditions	Validation	Comments	Ref.
rhG-CSF (reference substance from NIBSC; seven batches from commercial manufacturers)	n.s.	CZE	UV 195 nm	bfs	50 mM di-sodium tetraborate decahydrate, pH 9	15 kV, 15 °C Inj. 50 mbar, 6 s	Inter-day precision (concentration of rhG-CSF); repeatability, inter-day precision (t_m, %peak area); trueness, LOD, LOQ, robustness of CZE; stability	System suitability test; Leuprorelin acetate used as ISTD; standard prepared daily, storage under light protection; forced degradation studies; content evaluation of pharmaceutical formulations	[202]
VLPs – rotavirus (dlRLPs, tlRLPs)	Baculo-virus/ High Five® insect cells	CZE	UV 205, 260, 280 nm	bfs	10 mM sodium phosphate, 10 mM SDS and 10 mM sodium deoxycholate, pH 7	25 kV, 20 °C Inj. 68.9 kPa, 10 s	Trueness, specificity, linearity, LOD, LOQ, repeatability and inter-day precision (μ_{eff}, peak area)	Phtalic acid used as ISTD	[205]
VLPs – rotavirus (dlRPLs, tlRLPs) – from 25 cell lysate lots and purified vaccine preparations	Green monkey Vero cells	CZE	UV 200 nm	dynamic (DAB)	Commercial eCAP Chiral high pH (pH 8.0) buffer with 10 mM DAB	18 kV, 20 °C (with 0.5 psi applied on both capillary ends Inj. 0.1 psi, 4 s	/	Application of serum-free, low protein medium; analysis of RLPs from strains contained in pentavalent vaccine RotaTeq®; tlRLP content in lysate and after purification	[209]
VLPs – human papilloma virus	Baculo-virus/ High Five insect cells	CZE	UV 254 nm	dynamic (PEO coating)	10 mM Tris HCl, 10 mM HEPES-Na, 100 mM NaCl and 0.1% PEG 6000, pH 7.4, with 1.5 mM SDS	10 kV, 15 °C Inj. − 50 mbar, 15 s (short-end injection)	Linearity, trueness, repeatability, intermediate precision (all for VLP concentration), LOD, LOQ	Phthalic acid used as ISTD; regeneration of PEO coating prior to each CZE run	[213]
VLPs – human papilloma virus (batches of in-lab preparations; commercial VLP-based vaccines: Gardasil®, Cervarix®)	Baculo-virus/ Sf9 insect cells	CZE	UV 205, 260, 280 nm	dynamic (PEO coating)	10 mM Tris HCl, 10 mM HEPES-Na, 100 mM NaCl and 0.1% PEG 6000, pH 7.4, with 1.5 mM SDS	10 kV, 15 °C Inj. − 50 mbar, 15 s (short-end injection)	Intra-day, inter-day precision (t_m)	Regeneration of PEO coating prior to each CZE run	[214]
Intact recombinant adenovirus type 5	HEK or PER. C6	CZE	UV 214 nm	Covalent (PVA coating)	25 mM sodium phosphate, pH 7.0	-29.5 kV, 20 °C Inj. 3.4 kPa, 30 s	/	Capillary with 150 μm bubble cell	[215]
Recombinant adenovirus (RM; commercial vaccines; drug substance, drug product; crude/ lysed/clarified harvest; AEX and diafiltrated product – all with different batches)	n.s.	CZE	UV 214 nm	Covalent (PVA coating)	25 mM Tris, 338 mM tricine (pH 7.7), and 0.2% polysorbate 20	-25.5 kV, 15 °C Inj. 50 mbar, 5 s (short end)	Precision (between & within run; total intermediate); bias; total error (bias and intermediate precision); correlated bivariate least square regression	Capillary with 150 μm bubble cell; system suitability test	[220]
Recombinant oncolytic vaccinia virus (JX-594 strain)	n.s.	CZE (qCE)	LIF Exc. 488 nm, Em. 520 nm	bfs	50 mM sodium tetraborate (borax), pH 9.2	10 kV, 20 °C Inj. 0.5 psi, 5 s	/	Intercalation of fluorescence dye	[223]
rβ2-M (WT; five point mutants; two truncated variants)	*E. coli*	CZE	UV 200 nm	bfs	50 mM ammonium bicarbonate, pH 7.4	25 kV, 15 °C Inj. 50 mbar, 8 s	/	Folding variants	[230]
Recombinant birch pollen allergen (Bet v 1a) (three commercial batches)	*E. coli*	CZE	UV 210 nm	dynamic (TEPA)	100 mM $Na_2HPO_4.2\ H_2O$, 2 mM TEPA, pH 6.50	15 kV, 35 °C Inj. 35 mbar, 10 s	Precision (repeatability, intermediate precision for different capillaries: t_m, μ_{eff}), purity, linearity, LOQ	Distinction of carbamylated variants	[246]
Recombinant birch pollen allergen (Bet v 1a; one commercial batch)	*E. coli*	CZE	UV 210 nm	dynamic (TEPA)	100 mM MES, 0.4 mM TEPA, pH 6.50	25 kV, 35 °C Inj. 35 mbar, 10 s	Purity of product	Distinction of carbamylated variants	[251]
Recombinant birch pollen allergen (Bet v 1a: WT and hypoallergen; commercial batches)	*E. coli*	CZE	UV 210 nm	SMIL (4-layer PDADMAC-DS)	75 mM or 100 mM NH_4HCO_3, pH 6.70	8 kV or 14 kV, 30 °C Inj. 35 mbar, 10 s	Precision (intra- und inter-day for t_m)	Durability of SMIL coating for > 70 runs without recoating	[157]

(*continued on next page*)

Table 3 (*continued*)

Recombinant protein/ product	Host cell	CE-technique	Detection and MS interface	Capillary coating	BGE and SL	Separation and ESI conditions	Validation	Comments	Ref.
Recombinant human β-secretase	HEK 293	CZE (with enzyme reaction)	UV 200 nm	bfs	5% HAc	30 kV, 37 °C Inj. 30 mbar, 3 s (for consecutively injected plugs)	Selectivity, precision, robustness, stability, calibration and linearity, sensitivity, trueness; recovery for TDLFP- and EMMA-based method	Kinetic studies and inhibition assays	[257]
CGE-UV									
Tuberculosis recombinant fusion protein HyVac (H4) – vaccine candidate (combination of two antigens)	n.s.	CGE	UV 220 nm	bfs	Commercial SDS-MW gel buffer	500 V/cm, 25 °C Inj. 0.7 psi, 240 s or 170 V/cm, 20 s	Trueness, linearity (relative purity and relative peak area), precision	Samples spiked with HSA to mimic impurity	[261]
PEG-IFN-α and IFN-α	n.s.	CGE	UV 220 nm	bfs	Commercial CE-SDS run buffer	15 kV, 20 °C Inj. 10 kV, 10–20 s	/	Monitoring of PEGylation reaction	[263]
PEG-IFN-α (native; branched and trimer-PEG-IFN-α)	n.s.	CGE	UV 220 nm	bfs	Commercial CE-SDS run buffer	10 kV, 20 °C Inj. 5 kV, 60 s	/	Mono-PEGylated IFN-α, different PEG-lengths	[264]
dl- and tl-RLPs	Sf9 cells	CGE	UV 220 nm	bfs	Commercial CE-SDS run buffer	15 kV, 20 °C Inj. 34.5 kPa, 50 s	LOD	Separation of virus proteins contained in RLPs	[42]
Insulin (bovine pancreas)	/	CGE	UV 214 nm LIF: Exc. 494 nm, Em. 522 nm	Coated (PHEA)	0.5% or 1% PHEA separation matrix	15 kV, 25 °C Inj. 0.5 psi, 8 s (UV) Inj. 10 or 12 kV, 12 s	LOD (UV and LIF)	Separation of insulin monomer, oligomers, and aggregates; FITC-labeled insulin	[266]
Recombinant human insulin product (Humuline®)	*E. coli*	CGE	UV 220 nm	Coated (PEO)	0.6 M Tris-borate buffer (pH 8.1), 5 mM EDTA, 10% (w/v) dextran, 0.2% (w/v) SDS or 0.2% (w/v) sodium deoxycholate, 10% (v/v) glycerol	30 kV, 25 °C Inj. − 2 bar, 2 s	Intra-day precision (t_m); stability testing (−20 °C, 4 °C, room temperature)	Insulin dimers and polymers; PEO coating regenerated prior to each run	[260]
μChipCGE									
rhG-CSF (commercial product), PEG-rhG-CSF	n.s.	μChipCGE	Fluorescence	Protein 80 or 230 Labchip	Commercial kit (gel-dye mix)	n.s.	Linearity	Optimization of PEGylation conditions	[271]
rFVIII and PEGylated-rFVIII; rVWF and PEGylated-rVWF	both in CHO	μChipCGE	Fluorescence	Protein 230 Labchip	Commercial kit (gel-dye mix)	Inj. 68 s	/	Deglycosylation of (PEG)-rVWF with PNGase F	[272]
CIEF									
rhEPO (BRP Ph. Eur.)	CHO	CIEF	UV 280 nm	Coated (PAA, in-lab; commercial eCAP neutrally coated)	Pl 3–10 & 2–4; 7 M urea & commercial cIEF gel Anolyte: H_3PO_4 Catholyte: NaOH	Focusing: 25 kV, 6 min Mobilization: pressure with parallel kV application	Precision – intra- and inter-day (t_m, t_m corrected with ISTD; area, area corrected with ISTD)	β-lactoglobulin used as ISTD	[290]
rBet v 1a (non-modified, carbamylated)	*E. coli*	CIEF	UV 280 nm	Coated (PAA, in-lab; commercial eCAP neutrally coated)	BE 3–10, Pl 5–6 and Al 5–7 & commercial cIEF gel Anolyte: H_3PO_4 or glycine Catholyte: NaOH or CHES	Inj. 2069 mbar, 90 s (entire capillary) Focusing: 15 kV, 6 min Mobilization: pressure (48 mbar) with parallel kV application	Product purity	Linearity of pH gradients	[251]

(*continued on next page*)

Table 3 (*continued*)

Recombinant protein/ product	Host cell	CE-technique	Detection and MS interface	Capillary coating	BGE and SL	Separation and ESI conditions	Validation	Comments	Ref.
rBet v 1a (non-modified, carbamylated)	*E. coli*	CIEF	UV 280 nm	Coated (commercial eCAP neutrally coated)	BE 3–10, Pl 5–6 and Al 5–7 & commercial cIEF gel Anolyte: glycine Catholyte: CHES	Inj. 2069 mbar, 90 s (entire capillary) Focusing: 15 kV, 6 min Mobilization: pressure (48 mbar) with parallel kV application	Relative purity, specificity, repeatability and intermediate precision (relative t_m, relative purity); linearity (Mandel fitting test); LOQ; robustness	System suitability test	[292]
Equine and swine influenza virus (different purification procedures)	Allantoic fluid/egg	CIEF	UV 280 nm	bfs	Bl 3–10, Al 3–4.5 and Al 2–4 or only Bl 3–10 Anolyte: H_3PO_4 with EtOH Catholyte: NaOH	Inj. Δh 100 mm, 5–40 s, segmental injection Focusing and moblization: 20 kV	Purity	Comparison to real-time PCR; profiling of different purification stages	[293]
iCIEF									
rhEPO (Ph. Eur. CRS; recombinant preparations from 12 manufacturers)	CHO	iCIEF	UV 280 nm	Coated (commercial FC capillary)	Pl 3–10 and Pl 2.5–5 Anolyte: H_3PO_4 Catholyte: NaOH	Focusing: 1.5 kV, 1 min then 3 kV, 6.5 min	/	Manufactured in bioreactors or roller bottles	[295]
rhEPO (8 commercial drug products)	n.s.	iCIEF	UV 280 nm and fluorescence Exc. 280 nm, Em. 350 nm	Coated (commercial FC capillary)	Pl 2.5–5 and Pl 5–8 with 4 M urea Anolyte: H_3PO_4 Catholyte: NaOH	Focusing: 0.75 kV, 2.5 min then 3 kV, 12 min	Precision - intra- and inter-day (pI, peak area), trueness (by spike-and-recovery), linearity, range, LOQ, and robustness	Detection by native fluorescence; comparison UV 280 and fluorescence 280 nm	[296]
Commercial therapeutic rFc-fusion proteins (etanercept, abatacept, aflibercept, human tumor necrosis factor-α receptorII: IgG Fc fusion protein, conbercept, belatacept, VEGFR-Fc fusion protein, thrombopoietin mimetic peptide-Fc fusion protein, glucagon-like peptide-1-Fc fusion protein)	n.s.	iCIEF	UV 280 nm and fluorescence Exc. 280 nm, Em. 350 nm	cIEF cartridge (coating not specified)	Sl 2–9, Sl 3–5 and Sl 5–8 with SimpleSol or optional up to 4 M urea	Focusing: 1.5 kV, 1 min then 3 kV, 12 min	Repeatability (peak areas, pI)	Application of iCIEF platform method for different fusion proteins	[31]
rHPVs (5 commercial HPV products	*P. pastoris*	iCIEF	UV 280 nm	Coated (commercial FC capillary)	Pl 3–10, 2 M urea	Focusing: 1.5 kV, 1 min then 3 kV, 4 min	Specificity, trueness (pI for pI marker); repeatability and intermediate precision (pI), LOD, LOQ	Testing of rHPVs	[210]
Affinity CE									
rβ2-M (interaction with inhibitors of fibrillogenesis)	*E. coli* (inclusion bodies)	ACE (CZE)	UV 200 nm	bfs	100 mM phosphate buffer, pH 7.4	18 kV, 15 °C; 13 °C (for refolding experiments) Inj. 0.7 psi, 8 s	/	Tested inhibitors dissolved in different concentrations in BGE for ACE; binding constants for native and inter-mediate rβ2-M conformations; refolding	[299]
Recombinant birch pollen allergen Bet v 1a (interaction with specific mAbs)	*E. coli*	ACE (CIEF)	UV 280 nm	Coated (commercial neutrally coated)	BE 3–10, Al 5–7, Pl 5–6 Anolyte: glycine (with H_3PO_4) Catholyte: CHES (with NaOH)	Inj. 2068 mbar, 90 s (entire capillary filled) Focusing: 15.0 kV, 6 min Mobilization: pressure (48 mbar) with parallel kV application	Linearity of unbound Bet v 1a (corrected peak area)	ACE with two in-house prepared specific anti-Bet v 1a mAbs (IgGs); distinction of mono- and divalent immune-complexes	[300]

(*continued on next page*)

Table 3 (*continued*)

Recombinant protein/ product	Host cell	CE-technique	Detection and MS interface	Capillary coating	BGE and SL	Separation and ESI conditions	Validation	Comments	Ref.
rHPV16-VLP (interaction with H16.V5, i.e., anti- rHPV16-VLP mAb)	Baculo-virus/ High Five insect cells	ACE (CZE)	UV 254 nm	Dynamic (PEO coating)	10 mM Tris HCl, 10 mM HEPES-Na, 100 mM NaCl and 0.1% PEG 6000, pH 7.4, with 1.5 mM SDS	10 kV, 15 °C Inj. − 50 mbar, 15 s (short-end injection)	Specificity by testing a non-specific antibody	Pre-equilibration (1 h at room temperature prior to ACE analysis); regeneration of coating prior to each CZE run; phthalic acid used as ISTD	[213]
Human rhinovirus (serotype 2 and 14) (interaction with mAbs 8F5 and 17-IA against both serotypes)	Infected cell pellets	ACE	UV 205 nm, 260 nm	bfs	100 mM boric acid, 10 mM SDS, pH 8.3	25 kV, 20 °C Inj. 50 mbar, 9 s	/	Pre-incubation (prior to ACE analysis 60 min at room temperature); o-phthalic acid used as ISTD	[301]
CE-online Western blot									
9 crude lysate samples of vaccine candidates (not specified)	*E. coli* or baculo-virus / insect cells	CGE & Western blot	Chemi-luminescence	Commercial (UV-activated coating for Western blot) multichannel	Solutions from commercial kit (ProteinSimple)	250 V Inj. sequence of separation- and stacking matrix, then sample	Calibration/linearity, precision - repeatability and intermediate precision (total peak area), LOD, LOQ	Comparison with RP-HPLC; crude lysate analysis	[304]
Drug substances and cell culture harvest (not specified)	n.s.	CGE & Western blot	Chemi-luminescence	Commercial (UV-activated coating for Western blot) multichannel	Solutions from commercial kit (ProteinSimple)	275 V Inj. sequence of separation- and stacking matrix, then sample	Calibration/linearity, repeatability (concentration)	Comparison of cell culture harvest and purified drug substance	[303]
BSA in four batches of virus vaccine final drug substances and in four process intermediates of vaccine	Human cell substrate	CGE & Western blot	Chemi-luminescence	Commercial (UV-activated coating for Western blot) multichannel	Solutions from commercial kit (ProteinSimple)	n.s.	Calibration/linearity, intermediate precision (concentration), LOD, LOQ, trueness (recovery from spiked samples)	Application to monitor BSA clearing in downstream processing; BSA (monomers, dimers, aggregates)	[310]
CZE – glycosylation analysis									
rhEPO (commercial product) – released oligosaccharides	CHO	CZE-LIF	Fluorescence Exc. 488 nm, Em. 540 nm	bfs	150 mM sodium phosphate, pH 2.5 or pH 7.0	21 kV, 25 °C Inj. 0.5 psi, 5 s	/	Derivatization with rhodamine 110; glycan analysis after PNGase F digest	[313]
rhEPO (BRP batch 2 and 3) – analysis of N- and O-glycopeptide	CHO	CZE	TOF-MS coaxial SL sprayer	bfs	50 mM HAc and 50 mM FA, pH 2.2. SL: 50% iPrOH/50% H_2O with 0.05% FA; 3.3 µL/min	18 kV, 25 °C Inj. 0.5 psi, 5 s	/	Digest with trypsin, Glu-C and/or neuraminidase	[328]
PSA	/	CZE	QqTOF-MS CESI	bfs	10% (v/v) HAc, pH 2.3	20 kV, 25 °C Inj. 1 psi, 60 s	/	Digest with PNGase F, and sialidase; in-capillary pre-concentration	[329]
r-αhCG	Murine cell line	CZE	LTQ-FT-MS liquid junction interface (home-made)	Coated (PVA)	2% HAc, pH 2.5	8 kV, temperature n.s. Inj. 10 cm height difference, 30 s	Repeatability of relative mass for most intense glycoforms	Glycoform profiling of α-subunit	[330]
CE-MS of intact recombinant proteins									
rhGF (=somatropin) (CRS from EDQM) rhIFN-β1a (commercial product)	n.s.	CZE	micrOTOF-MS coaxial SL sprayer	SMIL (PB-PVS, PB-DS-PB)	BGE: 75 mM ammonium formate, pH 8.5 SL: 75% ACN/25% H_2O with 5% FA; 4 µL/min BGE: 50 mM HAc, pH 3.0 SL: 25% iPrOH/75% H_2O with 0.5% HAc; 2 µL/min	+ 30 kV or − 30 kV Inj. 1 psi, 12 s	/	Characterization of glycovariants of rhGF and rhIFN-β1a	[336]
rhEPO (NeoRecormon®) rhIFN-β1a (Avonex®)	CHO (both)	CZE	micrOTOF-MS CESI	Coated (commercial: neutral)	BGE: 2 M HAc, pH 2.1, BGE: 50 mM HAc, pH 3.0	30 kV, 20 °C Inj. 5 psi, 10 s 15 kV, 20 °C	/	Characterization of glycovariants	[320]

(*continued on next page*)

Table 3 (*continued*)

Recombinant protein/ product	Host cell	CE-technique	Detection and MS interface	Capillary coating	BGE and SL	Separation and ESI conditions	Validation	Comments	Ref.
rhIFN-β1a (Avonex®)	CHO	CZE	LTQ Orbitrap ELITE Velos CESI	Coated (commercial: PEI)	BGE: 3% HAc, pH 2.5	-20 kV Inj. 1 psi, 10 s or 0.5 psi, 5 s	Repeatability of t_m	Sialidase and galactosidase treatment; characterization of glycan structure	[337]
rhEPO (BRP batch 3 from Ph. Eur) rhGH (commercial product)	n.s.	CZE	micrOTOFQ-MS or maXis qTOF-MS coaxial SL sprayer	Semipermanent (commercial solution: Ultratrol™ LN)	BGE: 1 M HAc 40 mM ammonium bicarbonate, pH 8.5 SL: 50% iPrOH/50% H_2O with 1.0% HAc; 4 μL/min	+ 30 kV Inj. 50 mbar, 12 s or 100 mbar, 6 s,	/	Isotopic resolution of glycoforms with increased mass resolution due to extended flight paths	[338]
Somatropin with NOTA-labeling	n.s	CZE	micrOTOFQ-MS coaxial SL sprayer	SMIL (PB-PVS)	BGE: 75 mM ammonium hydroxide, pH 8.5 SL: 75% iPrOH/22% H_2O/ 3% HAc; 4 μL/min	30 kV, 20 °C Inj. 1 psi, 12 s	/	Somatotropin labeled with p-SCN-Bn-NOTA; marker for cancer	[339]
rhEPO (BRP batch 2 from Ph. Eur; commercial product)	n.s.	CZE	micrOTOFQ-MS coaxial SL sprayer	Coated (PB)	BGE: 1 M HAc with 20% MeOH, pH 2.4 SL: 50% iPrOH/50% H_2O; 4 μL/min	-30 kV Inj. 50 mbar, 60 s	/	Daily recoating required; distinction of glycoforms and proteoforms	[340]
rhEPO (Eprex®, NeoRecormon®)	CHO (both)	CZE	micrOTOFQ-MS coaxial SL sprayer	Coated (PB)	BGE: 1 M HAc with 20% MeOH, pH 2.4 SL: 50% iPrOH/50% H_2O; 4 μL/min	-30 kV Inj. 50 mbar, 20 s	/	Distinction of glycoforms between α- and β-epoetin	[172]
Fusion protein (Fc-FGF21 WT and Fc-FGF21 RG)	Bacterial expression system	CZE	TOF-MS EMASS-II	Coated (LPA)	BGE: 30% HAc	30 kV; 960 mbar after 10 min CZE co-applied Inj. sample stacking (no details)	/	Purification with offline immune-affinity; eluate directly injected	[32]
Three VPs of recombinant AAV (commercial products AAV2 and AAV2tYF)	n.s.	CZE	Q Exactive HF ZipChip	n.s.	n.s.	500 V/cm Inj. 2 Pa, 30 s	/	Characterization of VPs for serotype identification	[345]
rβ2-M	*E. coli*	CZE	6210 LC/MS TOF MS with coaxial SL sprayer or maXis HD Ultra high resolution QTOF with CESI	bfs	BGE: 50 mM ammonium bicarbonate, pH 7.4 (for either equipment) SL: 49.5% iPrOH/49.5% H_2O/1% FA; 4 μL/min	30 kV, 15 °C Inj. 50 mbar, 150 s Inj. 5 psi, 20 s	Precision of t_m and peak area	Distinction of conformations	[348]
Recombinant pollen allergen (nitrated variants of Bet v 1a)	*E. coli*	CZE	micrOTOF-MS coaxial SL sprayer	bfs	BGE: 10 mM ammonium bicarbonate, pH 7.50 SL: 75% MeOH/24.9% H_2O /0.1% FA; 6 μL/min	25 kV, 25 °C Inj. 35 mbar, 10 s	/	In-lab nitration; distinction of nitrated variants and positional isomers	[352]
Recombinant pollen allergen (nitrated variants of Bet v 1a)	*E. coli*	CZE	LTQ Orbitrap XL coaxial SL sprayer (in-lab designed)	bfs	BGE: 10 mM ammonium bicarbonate, pH 7.50 SL: 75% MeOHl/24.9% H_2O /0.1% FA; 3 μL/min	20 kV, 25 °C Inj. 35 mbar, 10 s	Repeatability for t_m, peak area and peak height (based on tryptic peptides of nitrated Brt v 1a)	Combination of intact, top-down and bottom up results (with MS^2); distinction of nitrated variants and positional isomers; identification of nitration hotspots	[353]
Recombinant pollen allergen (Art v 3 – heat stressed)	*E. coli*	CZE	UV or micrOTOF-MS coaxial SL sprayer	bfs	BGE: 100 mM $NaH_2PO_4{\cdot}H_2O$, pH 2.50 (UV) BGE: 1 M FA, pH 1.80 (CE-MS) SL: 75% MeOH/24.9% H_2O /0.1% FA; 6 μL/min	15 kV, 25 °C (UV) 25 kV, 25 °C (CE-MS) Inj. 35 mbar, 10 s (UV) 35 mbar, 50 s (CE-MS)	/	Allergen thermally stressed at two pH domains; in-capillary pre-concentration for CE-MS	[357]

(*continued on next page*)

Table 3 (*continued*)

Recombinant protein/ product	Host cell	CE-technique	Detection and MS interface	Capillary coating	BGE and SL	Separation and ESI conditions	Validation	Comments	Ref.
Combination of CE strategies									
rhCG (Ovitrelle®; commercial rhCGβ) commercial urinary hCG (Pregnyl®)	CHO (Ovitrelle®) *P. pastoris* (rhCGβ)	A: CGE B: CIEF C: CZE-UV D: CZE-MS	UV (A-C) or triple quad 6400 MS (D) coaxial SL sprayer (D)	A,C,D: bfs B: Coated (HPC)	A: commercial SDS-MW Kit B: commercial kit; CA (3–10), with 6 M urea C, D - BGE: 800 mM FA/ 800 mM HAc, 20% MeOH D: SL 50% MeOH/50% H_2O with 0.1% FA; 0.6 µL/ min	A: − 15 kV, 25 °C Inj: - 5 kV, 20 s B: Focusing: 25 kV 25 °C Mobilization: with 350 mM HAc, 25 or 30 kV C: + 30 kV, Inj. 50 mbar, 20 s D: + 30 kV, 60 °C Inj. n.s.	B: Repeatability of t_m D: repeatability of t_m and signal intensity of major peaks	Application of orthogonal CE methods; comparison of recombinant and urinary hCG	[359]
rhG-CSF (commercial product) – PEGylated variants	n.s	A: CZE B: CGE	UV 214 nm (both)	A: bfs B: Coated (commercial eCAP)	A - BGE: 100 mM phosphate, pH 2.5 B: Commercial eCAP SDS Kit	A: 10 kV, 20 °C Inj. 0.5 psi, 5 s B: 15 kV, 20 °C Inj. 0.5 psi, 30 s	Calibration for CZE-UV	Distinction of different PEGylation variants	[360]
Fusion protein (RC28E, i.e., eflimrufusp alfa)	CHO	A: CGE B: iCIEF	UV A: 220 nm B: 280 nm	bfs	A: Commercial SDS Kit B: SI 5–9 (commercial)	A: 30 kV, 25 °C Inj. 5 kV, 20 s B: Focusing: 1.5 kV, 1 min then 3 kV, 6 min	/	Comparison of batches	[362]

Al = Ampholyte; BE = Beckman carrier ampholyte; Bl = Biolyte; Em. = emission; Exc. = excitation; FA = formic acid; FC = fluorocarbon; HAc = acetic acid; iPrOH = iso-propanol; MeOH = methanol; n.s. = not stated; Pl = Pharmalyte; Sl = Servalyte; SimpleSol = non denaturing stabilizer.

after the transfection and successfully guided the optimization of the cell culture conditions as well as the downstream purification strategy in order to achieve the desired glycosylation profile [170].

Berkowitz et al. [171] analyzed a 24 kDa recombinant glycoprotein (identity not revealed), which possessed one glycosylation site. Separation was done in a commercial 100 mmol/L triethanolamine-phosphoric acid buffer with pH 2.5 in bfs capillaries. Due to the suppression of the EOF under these conditions, migration was governed by μ_{eff} of the individual protein variants. Major species carried a disialylated biantennary structure. With a sialidase digest, presumptive glycovariants that were specified according to the antennary sialylation level have been assigned. With increased sialylation and higher antennary structures, the μ_{eff} was retarded. This has been related to a loss of positive charges and an increase in r_H (see Section 3.1; Eq. 1). In addition, deamidated variants were revealed, which resulted in doublet peaks corresponding to non-deamidated/deamidated pairs. In total, 60 variants were resolved. The method was applied to demonstrate the influence of different CHO strains, different cultivation media and storage conditions on the recombinant product in terms of sialylation, antennary structures and deamidation [171].

3.3.5. *Erythropoietin (EPO)*

EPO is a complex glycoprotein with three N- and one O-glycosylation site. N-linked glycans possess 2–4 branches, where each branch may end with sialic acid [172]. rhEPO differs from endogenous hEPO in the glycosylation pattern since hEPO shows a higher content of sialic acids [172]. rEPO is applied in the clinical therapy of anemia in the context of chronic renal failure [173]. In addition, rEPO is administered as a supportive therapy in cancer patients with cancer-related or chemotherapy induced anemia. This explains, why rEPO causes the largest single drug costs in the US and has besides its health- also a large economic impact [174]. The therapeutic effect of rEPO has been controversially discussed and seems to be related to the hemoglobin concentration of patients. Besides the expected effect on erythrocyte number and hemoglobin concentration, rEPO exerts also a direct effect on tumor cells. The increase in tumor oxygenation is assumed to improve the efficacy of radio- and chemotherapy and to reduce tumor growth and metastasis by shutting down a related pathway [174]. On the other hand, inhibition of apoptosis of tumor cells, tumor progression and metastasis by stimulated angiogenesis, as well as a detrimental modulation of the effect of therapeutics was discussed, which is in contradiction to the beneficial effects discussed before [174–176]. In fact, responses might differ depending on the respective patient population [175] and may also be cancer specific [176]. Moreover, an increased thromboembolic risk is induced by EPO, but seems to depend on the hemoglobin level at the time of rEPO administration [174]. rhEPO is also applied in illegal blood doping in sports. The method of the IOC and WADA for antidoping controls refers to isoelectric profiles of EPO sampled from urine [177].

Four approved EPO products were compared by the CZE method of the Ph. Eur. Thereby, two originator products (Eprex® and Dynepo®) were compared with two biosimilars (Binocrit® and Retacrit®). SDS-PAGE and SEC proved the absence of EPO aggregates and fragments. The BGE of the Ph. Eur. method is composed of 10 mmol/L NaCl, 10 mmol/L Tricine, 10 mmol/L sodium acetate, 7 mol/L urea and 2.5 mmol/L DAB, pH 5.5. Due to the presence of urea in the BGE, the separation is done under denaturing conditions and thus based on charge differences generated by the sialic acid content. Nine glycoforms were distinguished in Dynepo®, whereas for all other tested EPO products six charge variants were resolved. The different glycosylation pattern was due to the expression of Dynepo® in a human fibrosarcoma cell line, whereas all other products were produced in CHO (see Section 2.2). Dynepo® possesses no Neu5Gc (see Section 2.2.2). Moreover, differences in the relative intensity of glycoforms between Eprex® and Binocrit® were related to the more pronounced high-mannose structures in the latter [178]. De Frutos et al. [179] identified different glycoform profiles when comparing rEPO (i.e., BRP of the Ph. Eur.) and

urinary human EPO with three additional acidic variants revealed for the latter. Thus, a distinction between recombinant and native EPO seems possible with the Ph. Eur. CZE method. However, inter-individual variability of endogenous EPO has to be considered as well as manufacturer/host cell related differences [179].

The Ph. Eur. method was inappropriate for a hyperglycosylated EPO product, i.e., Aranesp®, which differs in five amino acids from human EPO. This creates two further N-glycosylation sites with oligosaccharide chains carrying up to four sialic acids, respectively, and results in an increased molecular mass of 37 kDa. In comparison to the BRP, the glycoprofile of Aranesp® was shifted to higher t_m and lacked baseline resolution. Due to the lower pI of Aranesp® (see Section 3.3.4), the pH of the BGE had to be reduced from 5.5 to 4.5 in order to restore baseline resolution [180].

When EPO products contained human serum albumin (HSA) as an excipient, the separation of glycovariants was impaired or entirely prevented, depending on the HSA concentration. This has been assigned to an adsorption of HSA on the capillary surface and its incomplete detachment in subsequent rinsing steps. With an immunochromatographic purification, HSA could be removed from the EPO formulation and a subsequent concentration step resulted in profiles corresponding to the BRP of Ph. Eur. For a correct assignment of glycoforms to individual peaks, μ_{eff} turned out to be the most reliable parameter [181]. Recently, rhEPO variants were separated in capillaries dynamically coated with methyl chitosan applying 10 mmol/L sodium acetate-acetic acid, 7 mol/L urea, 2.5 mmol/L DAB and 0.2 mg/mL methyl chitosan as BGE. The composition partly resembles the BGE of the Ph. Eur. standard method. The CZE analysis was completed within 9 min [182]. Others applied a commercial kit with a bilayer coating of the capillary and nitrilotri(trimethyl)phosphonic acid, pH 4.4, including 7 mol/L urea to analyze the rhEPO reference from the European Directorate for the Quality of Medicines and Health Care (EDQM) and compared EPO samples from different manufactures. Compared to the Ph. Eur. standard method, the analysis time was accelerated two-fold [183]. However, it is not clear whether the described double layer shielding refers to a true dynamic coating, as the authors claim, or represents a SMIL coating.

3.3.5.1. CZE quality assay for EPO. CZE data for EPO have been employed in the introduction of novel quality parameters, i.e., the isoform number (=I-number) [184] and the Ibio-number [185]. Both assays are based on peak area percent shares of individual isoforms of EPO. Whereas the I-number assay multiplies the percent of individual peak areas with the isoform number and sums the individual products, the Ibio-number assay considers the bioactivity of the individual isoforms by a so-called isoform factor. Further details are given elsewhere [184–186]. Both parameters were proposed to replace criteria currently applied in the characterization of EPO products. The author claimed an improved accuracy and precision and thus a superior quality tool in the evaluation of EPO batches [184,185]. Different I-numbers have been assigned to different glycosylation profiles in CZE and were used in the classification of the EPO bioactivity, i.e., increased terminal sialic acid residues entailing a higher bioactivity [187]. This concept was tested and refined by considering additional factors, such as the secondary and tertiary protein structure, hydrophobicity, conformation, and possible aggregation. The latter was evaluated via the r_H. The charge profiles of eight rhEPO batches produced in CHO cells were analyzed with CZE-UV using the Ph. Eur. method with subsequent calculation of the I-number, respectively. The biological activity was derived from an in vivo bioassay standardized to the results of an EPO BRP from the EDQM. Results revealed that the I-number and bioactivity did not show a pronounced relation for the tested batches, as some batches with a lower I-number possessed a higher bioactivity than other batches with higher I-numbers. Instead, the authors found a stronger correlation between particle size (r_H) and bioactivity, pointing to the (additional) detrimental effect of aggregated species. This was also reflected by differences in protein structure for rhEPO batches of diverse bioactivity as revealed by CD, DLS and fluorescence [187].

3.3.5.2. Darbepoetin and its biosimilar. JR-131, a biosimilar of darbepoetin-α, was compared against its reference product, i.e., the originator, NESP® with CZE-UV. Compared to native hEPO, darbepoetin-α possesses five changes in the amino acid sequence and carries two additional N-glycans. CZE was embedded in a comprehensive portfolio of analytical tools applied in testing the biosimilarity of JR-131. Seven charge variants were distinguished with CZE-UV with no difference in the resolved profile between NESP® (six batches) and JR-131 (seven batches). This was in accordance with results of the other applied tools, with the exception of some minor differences in the extent of O-acetylated sialic acid [188].

3.3.5.3. Alternative CZE method for EPO without mandatory pre-purification. The Ph. Eur. standard method does not allow for direct analysis of commercial EPO products, but requires a pre-purification in order to get rid of excipients (e.g., trehalose, urea, Tween 20, polysorbate 20 and 80, various amino acids, sodium chloride, sodium phosphate). This is done by passing the rhEPO products through a 10 kDa cut-off filter prior to their analysis [179,189]. While this works for small molecules, removal of high-mass excipients may compromise resolution and EPO recovery [190]. Boucher et al. [190] presented a different CZE-UV method, which allowed for direct analysis of EPO products by combining a commercial capillary with permanent amine coating (eCAP amine) with a BGE composed of 200 mmol/L NaH_2PO_4 and 1 mmol/L $NiCl_2$, adjusted to pH 4.0 with acetic acid. The applied method was optimized previously and $NiCl_2$ was added to the BGE in order to separate rhEPO and HSA, which was used as an excipient in early EPO products until it became replaced by polysorbate [190]. As possible mechanisms for the improved separation a reversible complex formation between nickel ions and HSA, a masking of active capillary sites by nickel ions or their involvement in a HSA interaction with active capillary sites have been discussed [191]. The CZE-UV method was applied in the characterization of commercial rhEPO formulations containing HSA, polysorbate 20 or 80. Results were compared to the Ph. Eur. method. The number of resolved glycovariants for a Ph. Eur. BRP corresponded, but the resolution was impaired. The migration order was reversed due to the positive capillary coating and the required polarity shift of the separation voltage (Fig. 4). Despite the lack of sample pretreatment, matrix effects were absent. Thus, quantification by interpolation via two-point calibration was done. The method was applied to α- and β-EPO and darbepoetin-α with different excipients (HSA, polysorbate 20 and 80). Products were compared to the corresponding drug substances and met the manufacturer specifications. Only one EPO batch showed a complete loss in resolution of glycovariants - most likely due to compromised product integrity [190].

3.3.6. Recombinant human chorionic gonadotropin (rhCG)

hCG is a heterodimer of 37 kDa composed of an α- and a β-subunit non-covalently linked by hydrophobic and ionic interactions. The α-subunit carries two N-glycosylation sites, whereas the β-subunit contains two N- and four O-glycosylation sites [192]. hCG is produced by specialized cells of the placenta, so-called trophoblasts. The pituitary gland produces a sulfated hCG variant. Moreover, a hyperglycosylated hCG variant was identified, which acts as an autocrine factor. The latter is produced in early pregnancy and stimulates placenta growth, but was also shown to play a role in some cancer types by promoting cancer growth and invasion [193,194]. Moreover, it is also secreted by some tumors, e.g., ovarian cancer. hCG serum levels are tumor stage dependent [195]. Free α- and β-subunits were detected in serum and urine of cancer patients [194]. The therapeutic use of rhCG comprises the promotion of ovulation in infertility treatment [196], and the treatment of hypogonadotropic hypogonadism [197]. However, hCG has also been

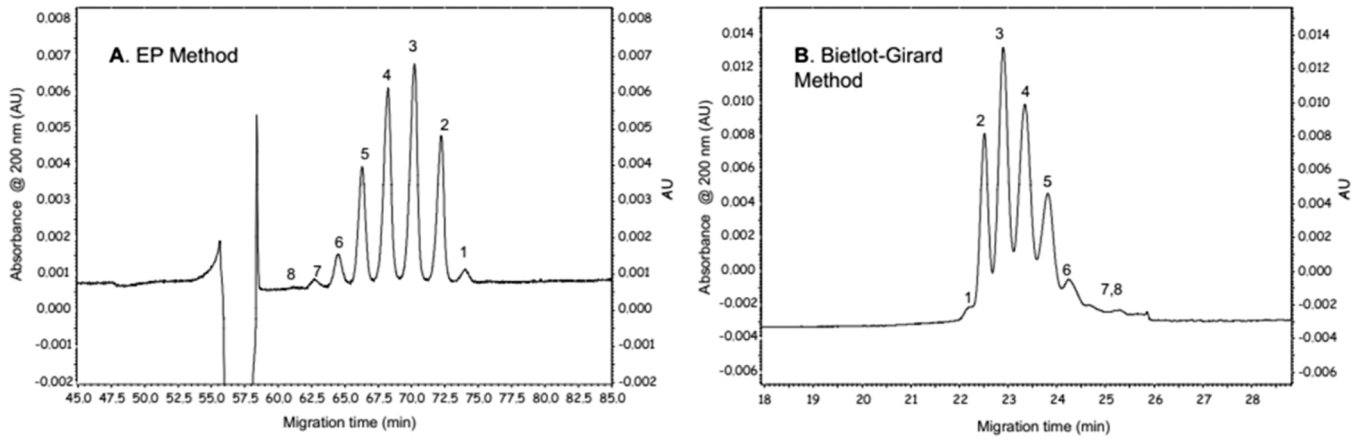

Pk #	Bietlot-Girard Method % Corrected Peak Area	EP Method % Corrected Peak Area
1	1.36	1.76
2	16.95	18.57
3	29.23	30.18
4	27.61	27.6
5	17.13	16.06
6	5.49	4.55
7	2.23 (7+8)	1.28
8	-	<0.3
Totals	100	100

Fig. 4. Electropherograms of the European pharmacopoeia biological references preparation for EPO by (A) the Ph. Eur. monograph method and (B) an alternative novel method.
Reprinted from [190], with permission from Elsevier.

abused to stimulate endogenous testosterone production exploiting anabolic effects [198].

A double injection CZE (DICZE) mode was used to analyze products suspected to contain rhCG. Thereby, first a commercial rhCG CRS was injected and separated for 35 min before the second injection of the investigated product was done. The selected time interval between the injections prevented a mutual influence of the injected plugs. Identification of possible rhCG content in the second injection was done by the closeness of agreement to the calculated and observed t_m of the CRS using the relative t_m of three major rhCG variants [199]. The theoretical background of this injection mode is explained in detail elsewhere [200]. CZE separation was done in dynamically coated capillaries using 85 mmol/L ammonium phosphate (pH 6) including 8.2 mmol/L DAB resulting in a cluster of 10 partially resolved peaks for the rhCG CRS. Peaks were assumed to represent variants of α- and β-subunits. Variants have been assigned to the microheterogeneity of rhCG due to the variable number of sialic acids. Peptide mass finger printing with MALDI-TOF-MS was established as a complementary tool for rhCG confirmation. Individual acceptance criteria defined for both methods had to be met, respectively, for a positive hCG identification in an investigated sample [199]. Previously, pharmaceutical hCG was analyzed in 200 mmol/L borate with 12.5 mmol/L DAB (pH 9) providing a glycoform cluster composed of six major peaks and 8 minor peaks flanking the main cluster [201]. Unfortunately, the authors did not state whether hCG was recombinant or extracted from urine.

3.3.7. Recombinant human growth hormone (rhGH)

rhGH (=somatropin) is a hydrophobic protein due to its high number of hydrophobic amino acids (tryptophan, tyrosine). Lyophilized products and aqueous solutions of rhGH, all derived from *E. coli*, showed deamidated and oxidated variants, a cleaved form and a mutated form with His exchanged against Gln in position 18. Due to its hydrophobicity and adsorption to the capillary wall, rhGH generated pronounced peak tailing in bfs capillaries. Prior to the actual CZE-measurements, several injections were required in bfs capillaries in order to saturate adhesion sites on the capillary surface with proteinaceous material [132]. This effect was described previously for other protein species as well [121]. Thus, capillaries were shielded with a SMIL bilayer coating composed of polycationic PB and negatively charged chondroitin sulfate A providing appropriate peak shapes already with the first injection. However, the SMIL coating had to be refreshed every five runs due to some t_m drift otherwise occurring by a degradation of the SMIL coating. Certified rhGH from EDQM was analyzed in 100 mmol/L ammonium phosphate dibasic (pH 6.0), which allowed for a distinction of four minor variants in addition to the major rhGH species. A sequential injection of two sample plugs allowed for a simultaneous analysis of two samples within one CZE run and accelerated the total analysis time by 30 min [132].

3.3.8. Recombinant human granulocyte colony-stimulating factor (rhG-CSF)

Non-glycosylated rhG-CSF was expressed in *E. coli*. CZE-UV separation was done in capillaries coated with polyethylene oxide (PEO) of a molar mass of 8000,000 g/mol [202]. The coating is non-covalent and occurs via hydrogen bonds formed between ether oxygens of the PEO chain and silanol hydrogens on the capillary surface. The high molar mass of PEO improved the stability of the coating [203]. Separation conditions were optimized with best results for 50 mmol/L di-sodium tetraborate decahydrate, pH 9. Leuprorelin acetate was applied as an internal standard (ISTD) for injection correction. An in-house reference preparation of rhG-CSF was subjected to forced degradation studies

including acidic, alkaline or thermal (55 °C) stress. Moreover, oxidative stress was simulated by 3% (v/v) H_2O_2. In either case, the area of the original rhG-CSF peak decreased, but only under alkaline and thermal stress a novel peak was detected within the selected analysis time of 30 min. The method was validated including a robustness testing and provided an LOD and LOQ of 0.22 and 0.75 μg/mL, respectively, both derived from the slope and the standard deviation of the intercept of three calibration curves. The validated CZE-UV method was then applied to seven commercial rhG-CSF batches from different manufacturers. The results were compared to data from SEC and RP-HPLC and an in-vitro cell culture bioassay performed in parallel on these samples. All provided corresponding results both for the mean relative rhG-CSF content and the SD [202].

3.3.9. *Virus-like particles - vaccines*

Virus-like particles (VLPs) mimic the authentic structure of native viruses and represent safe and cost-effective vaccine candidates since they contain only the protein virus capsid, but lack the genetic material [204–207]. VLP based vaccines – applied either preventive or therapeutic - are highly immunogenic and trigger innate and adaptive immune responses. Therapeutic VLP-based vaccines target to combat chronic and metabolic diseases as well as defined types of cancer. Moreover, they may serve as carriers for specifically delivering drugs for instance in cancer therapy, and are promising candidates for gene therapy [207]. Currently, five VLP-based vaccines have been approved - inter alia against papilloma virus/cervical cancer -, others are in the clinical trial phase. Moreover, VLPs against various cancers are tested pre-clinically [207].

The majority of recombinant viral proteins that form VLPs is expressed in bacteria and yeast, but also in insect and mammalian cell lines [206,207]. *E. coli* offers a cost-efficient and high yield expression system, but possesses also inherent obstacles related to protein solubility and PTMs (see Section 2.2). A comparison of different expression systems for VLPs is provided elsewhere [206]. One or more protein species of the virus capsid can be expressed simultaneously in host cells. These proteins assemble then spontaneously to VLPs, either intra- or extracellular [207]. Thereby, native-like epitopes have to be maintained. This has to be evaluated by appropriate analytical methods [206]. Besides non-enveloped VLPs, which are only composed of capsid proteins, so-called enveloped VLPs contain also a lipid membrane (from the host cell), with the virus proteins anchored therein. VLPs can be composed of a single layer or of several layers. A more comprehensive description as well as a discussion of upstream and downstream processing of VLPs is given elsewhere [207].

3.3.9.1. Rotavirus VLPs. Castro-Acosta et al. [205] analyzed VLPs of the rotavirus, the pathogen that causes diarrhea. The native rotavirus capsid contains three layers of proteins. Four prominent structural proteins of the virus capsid were expressed in shake flasks by coinfections using a baculovirus-insect cell system. The virus proteins assembled in rotavirus-like particles (RLPs). As the process was not entirely efficient, different RLPs formed, including single-layered, double-layered (dl) and triple-layered (tl) RLPs as well as unassembled monomers [205]. tlRLP is the preferred species since it contains the immunogenic glycoprotein of the outer capsid layer and induces the immune response [204,205,208,209]. A separation of dlRLP and tlRLP species was achieved with CZE-UV in 10 mmol/L sodium phosphate containing 10 mmol/L SDS and 10 mmol/L sodium deoxycholate, pH 7.0. The CZE-UV method was validated and provided an LOQ of 2.11 and 4.10 μg/mL for dlRLP and tlRLP, respectively [205]. Mellado et al. [204] investigated in vitro conditions that induced disassembly of tlRLP in dlRLP and vice versa, i.e., reassembly. The addressed parameters comprised temperature, buffer, chelating species (EDTA, EGTA) and Ca^{++} in different concentrations as well as reagents, which stabilize protein structures, i.e., glycerol. Dis- and reassembly was monitored with CZE-UV via formed dlRLPs and tlRLPs and results were compared with data from DLS. CZE separations were done in capillaries dynamically coated with DAB using a commercial chiral separation buffer. The understanding of the assembly of viral proteins (VPs) will allow for improved strategies in the high-yield formation of tlRLPs [204]. Indeed Mathis et al. [209] applied CZE-UV to demonstrate and evaluate consistent manufacturing of RLP-based vaccines. Rotavirus strains are divided in protease sensitive types (=P types) and glycoprotein types (=G types). The investigated rotavirus vaccine contained five vaccine strains (G1-G4 and P1). The standard methods applied so far in the distinction of dlRLP and tlRLP, i.e., CsCl isopycnic gradients and agarose gel electrophoresis, were complemented by CZE-UV by the authors. Different BGE compositions and pH-values were tested with a commercial eCAP chiral high pH buffer modified with 10 mmol/L DAB providing best separation (see also [204]). DAB was shown to reduce protein adhesion onto the capillary wall [123] and to modify the EOF [209]. dlRLPs and tlRLPs purified with a CsCl gradient were resolved in CZE as distinct peaks with a t_m-difference of ~3 min. However, the migration order of dlRLPs and tlRLPs depended on the rotavirus strain. This has been assigned to (i) different interactions between the two protein species that form the outer capsid layer, and (ii) differences in the number of glycosylation sites (1–3 sites), this way changing the net charge of tlRLPs. With the addition of EDTA, tlRLPs were converted in dlRLPs as evident from CZE-UV electropherograms. In infected cell lysate batches only for the virus type P1 tlRLPs migrated ahead of dlRLPs. When the results of CsCl gradients and CZE-UV were compared, the averaged relative tlRLP content in individual virus strains was 1.3–2.2 times higher in CsCl. This was related to the presence of two upper bands in the CsCl gradient that were previously not considered, but contained dlRLPs associated with lipids. When these bands were injected in CZE-UV, a signal at the dlRLP position was recorded, since lipids apparently dissociated under the CZE separation conditions. Thus, the rotavirus vaccine could be characterized by the dlRLP and tlRLP composition of the contained virus strains, which allows for the application of CZE as an analysis tool to evaluate the consistency of vaccine batches [209]. This is a requirement in the quality control of commercial products [42].

3.3.9.2. Human papillomavirus - VLPs. Human papillomavirus (HPV) is related with cervical cancer, the second frequent cause in female cancer deaths worldwide [210] and the most common in developing countries [211]. Vaccines are mainly based on the major HPV protein L1, which shows self-assembly to pentameric capsomers. 72 of these pentameric L1 capsomers finally form the VLP. This sort of vaccine production is straightforward and results in high yield [212]. Low and high-risk HPV types have been distinguished, with HPV types 16 and 18 eliciting the majority of cervical cancer cases [210–212]. Both HPV types are included in approved bivalent and quadrivalent HPV vaccines [207,211]. Currently, further multivalent vaccines are developed. Moreover, the next vaccine generation targets to replace current host cells (i.e., insect cells and *S. cerevisiae*) by *E. coli* [212].

HPV-VLPs composed of the L1 capsid protein were recombinantly produced in a baculovirus-Sf9 insect cell system. CZE analysis was done in a PEO coated capillary applying a BGE composed of 10 mmol/L Tris, 10 mmol/L 4-(2-hydroxyethyl)piperazine-1-ethanesulfonic acid (HEPES), 100 mmol/L NaCl and 0.1% PEG 6000, pH 7.4, including also 1.5 mmol/L SDS. Under these conditions, HPV-VLPs migrated as anions. Sample injection at the short end of the capillary minimized the separation length to 8.5 cm and accelerated the analysis [213,214]. With increasing concentrations of HPV-VLPs, their μ_{eff} was reduced. This effect was explained by overlapping electrical double layers of neighbor HPV-VLPs at increased concentrations. Concomitantly, the ζ-potential at the VLP surface (see Section 3.1) became less negative with increasing HPV-VLP concentrations, which explains the observed reduction of μ_{eff}. At HPV-VLP concentrations $\leq$ 50 μg/mL, the μ_{eff} became independent from the VLP concentration. The assumed mass of individual HPV-VLPs

was given with 20.3 MDa [213]. SDS apparently adhered to the PEO coating thus leading to an electrostatic repulsion of anionic VLPs, which prevented their adsorption and aggregation. The integrity of VLPs was not compromised by the applied SDS concentration. This was explained by the formation of disulfide bonds between the capsomers forming a VLP. Different batches of HPV-VLP samples were analyzed and compared to a WT-sample. The major peak in VLP samples was not present in the WT-sample. Due to the high molecular mass and the small diffusion coefficient of VLPs, plate numbers around 350,000 were realized. In addition, an approved tetravalent VLP vaccine, i.e., Gardasil®, which is based on the L1 capsid protein of four different HPV types, was successfully analyzed with the method. Contaminants stemming from Sf6 cells, which were observed in in-lab manufactured HPV-VLP samples, were not detected in Gardasil® [214].

3.3.10. Intact recombinant viruses

Mann et al. [215] analyzed recombinant adenovirus preparations by CZE-UV. Adenovirus type 5 was recombinantly manufactured in HEK 293 or PER.C6 cells in a serum-free medium and carried a fibroblast growth factor transgene (FGF-4). The virus is composed of at least 11 different protein species, which assemble to a capsid of ~2500 proteins by non-covalent interactions. CZE separation was done in commercial capillaries with PVA coating. Moreover, capillaries were equipped with an extended light path (="bubble cell") of 150 μm in order to enhance the signal intensity [215]. The improved S/N and resolution for a wide variety of proteins was shown by direct comparison to straight bfs capillaries [130]. Geometry and commercial manufacturing of the bubble cell is described elsewhere [216]. However, a bubble cell-like geometry of the inner diameter in the detection region of the capillary can also be prepared in-lab [217,218]. CZE separation was done in 25 mmol/L sodium phosphate buffer, pH 7.0, with reversed polarity. Besides a major peak, also some minor peaks were resolved. The observed minor peaks were induced by a freeze-thaw cycle as virus preparations were frozen after their purification. Viral fractions were collected after their CZE separation and showed infectivity, thus proving preserved viral integrity [215]. Van Tricht et al. [219] analyzed adeno-based vaccines (adenovirus type 26 and 35) during their manufacturing and monitored the product quality during the individual steps of upstream and downstream processing. They also applied a PVA capillary with bubble cell and compared it to SMIL-coated and commercially neutral coated (eCAP) capillaries. A high ionic strength BGE, i.e., 125 mmol/L Tris, 338 mmol/L Tricine with 0.2% (v/v) polysorbate 20, pH 7.7, was applied for the CZE separations. Together with an appropriate rinsing protocol, protein adsorption could be restricted. Sample injection was done at the short end of the capillary, which allowed for $t_m < 3$ min. Lysed and clarified harvests resulted in interfering matrix peaks stemming from the DNA of lysed host cells. A digest with benzonase cut DNA in smaller fragments thus solving the matrix problem. The μ_{eff} depended on the capsid proteins building the adenovirus types, but was independent from the type of the incorporated DNA. When compared to standard methods, i.e., quantitative polymerase chain reaction (qPCR) and anion exchange-HPLC, the CZE-UV method provided a higher throughput and improved precision and accuracy [219]. In a follow-up publication, the CZE separation method was applied to downstream samples. Results were compared to qPCR, which constitutes the standard method for quantification. Evaluation was done by correlated bivariate least square regression and proved corresponding results for both methods. The in-process control of the virus concentration with CZE-UV is considerably faster providing results within 2 h contrary to 3 d required by qPCR. Importantly, the production process is in the waiting loop until results are achieved [220].

3.3.11. Oncolytic viruses

Oncolytic viruses represent a promising tool for future targeted cancer treatment due to their safety and considerably lower toxicity compared to conventional cancer therapies [221,222]. These viruses have been modified and cannot replicate in healthy cells, but in tumor cells [222]. In the described case, virions of a defined oncolytic strain (JX-594) of vaccinia virus were obtained from the manufacturer and quantified by CZE-LIF [223]. This virus strain combats cancer cells by their lysis, reduces tumor vascularization and promotes an anti-tumor immune response [222]. The virus and free DNA fractions were separated in 50 mmol/L sodium tetraborate, pH 9.2. For quantification an intercalating fluorescence dye, i.e., YOYO-1, was applied and virus particles were lysed with proteinase K. The ratio of free DNA before and after virus lysis was determined and a calibration with λ DNA was done. Together with the molar mass of the viral DNA, the concentration of intact virions was determined providing an improvement in comparison to nanoparticle tracking analysis [223].

3.3.12. Conformational changes of recombinant β2-microglobulin

The appropriate function of proteins in vivo, but also of recombinant biologics is related to their native folding. Changes in the protein conformation will lead to an impairment or even entire loss in function and may trigger the onset of conformational diseases, such as Alzheimer's disease or amyotrophic lateral sclerosis [224,225]. These diseases progress via folding intermediates, which possess an increased propensity for oligomerization and aggregation [225]. This might entail intra- or extracellular self-association leading to protein aggregates. Similarly, this effect is of concern in host cells with high expression of heterologous proteins, for instance in *E. coli*, where proteins accumulate in inclusion bodies (see Section 2.2). From there, proteins have to be resolubilized and refolded in their functional state. Moreover, (partial) unfolding may also occur during downstream purification or storage [51].

Recombinant β2-microglobulin (β2-M) is a 11.8 kDa protein rich in β-sheets [226]. It has been applied as a model protein in order to gain first insights in the in vivo progress of amyloidosis [227]. The protein is also responsible for dialysis-related amyloidosis (DRA), which affects the majority of patients with long-term hemodialysis. In healthy people, glomerular clearance of β2-M occurs in the kidney followed by reabsorption and catabolism in the proximal renal tubules. However, membranes applied in dialysis have a 200 Da cut-off and may lead to an up to 60-fold increased plasma concentration of β2-M in the final stage. Besides, dialysis constitutes an inflammatory trigger, which stimulates the expression and release of β2-M by cytokines [228]. Altogether, this generates amyloids, which deposit in the musculoskeletal systems due to the apparent affinity of β2-M for type I and II collagen [228,229]. Under pathological conditions, partial unfolded forms, i.e., intermediate misfolded conformation, of β2-M were reported due to a trans isomerization at Pro32 and hold responsible for fibril formation [228].

WT-β2-M and seven mutated or truncated β2-M variants were recombinantly expressed in *E. coli*. One of the tested variants, D76Nβ2-M, occurs in vivo in autosomal dominant hereditary amyloidosis. Another N-truncated variant (ΔN6β2-M) is known to be present in the amyloids of DRA [230] and possesses a higher affinity for collagen than the WT [229]. Resolubilization and refolding of β2-M from inclusion bodies was done with acetonitrile (ACN), trifluoroethanol, urea and HCl. For all β2-M species tested with CZE, the native and the intermediate folding state could be addressed as distinct peaks, respectively, with the folding intermediate always possessing a lower electrophoretic mobility. This has been explained by a change in r_H and/or changes in the charge distribution or in the exposure of local charges due to structural changes. CZE separations were done under native conditions, i.e., 50 mmol/L NH_4HCO_3, pH 7.4, in order to avoid induction of artificial unfolding during the separation. For some species, another folding variant was revealed. Most remarkable, onset of aggregation was observed for D76Nβ2-M at a separation temperature of 37 °C, contrary to the WT, which possessed still an intact structure at the highest temperature tested (42 °C). This underpins the role of CE in deciphering the unfolding properties of recombinant proteins under different frame conditions. In addition, the different responses of β2-M variants to

selected denaturants were tested [230].

3.3.13. Recombinant allergens in diagnosis and therapy

Contrary to all recombinant proteins discussed so far, non-human and even non-mammalian proteins can be used in diagnosis and therapy. This is exemplified by means of allergens. Allergens are applied in diagnosis [231,232], but also for therapeutic treatment of established allergies by allergen immunotherapy [233–235], better known as hyposensitization, which induces an immuno-modulatory effect that ideally prevents allergy progression from rhinitis to asthma [236]. In addition, preventive therapeutic vaccines based on the allergy-eliciting allergen may be administered in early childhood [237]. Initially, diagnosis and therapy was based on allergen extracts derived from natural biological sources. However, this product type is ill-defined and batches are highly variable between and even within manufacturers [238,239]. Thus, standardization of these products is extremely challenging/impossible. An international collaborative study produced a standardized birch pollen extract, which became a WHO standard [240]. However, once consumed, novel batches will differ in their composition. The outlined limitations have been remedied by recombinant allergens, which provide defined quality, batch consistency, defined shelf-life and potency [241–243]. This allows for a component-resolved diagnosis and a therapy offering the option to prepare isoform cocktails tailored specifically to individual patients in their immune therapy [231,238]. As a consequence, unintentional *de novo* sensitization against allergens/isoforms the patient was not reacting so far - as shown for natural extracts – is prevented [244]. However, recombinant allergens have to conform properties of the WT-allergen cognate [241]. The EMA issued a guideline for developing products for specific immunotherapies [245].

3.3.13.1. Pollen allergens. The major isoform 1a of the birch pollen allergen (Bet v 1a) was expressed in *E. coli* since the WT allergen carries no PTMs. Three commercial batches were compared by CZE-UV. Two batches used only the soluble allergen fraction, whereas the third batch combined the soluble and insoluble allergen fraction in order to increase the yield. For the latter, 4 mol/L urea was applied in the production for re-solubilization [246]. However, as urea degrades to ammonium and cyanate [247], carbamylation of α- and ε-amino groups occurred taking place on the N-terminus and lysine side chains [248]. Single and double carbamylated species were revealed by ESI-QTOF-MS measurements. Since carbamylation causes an incremental loss of positive charges and thus a change in the pI, related variants could be resolved with CZE [246]. In addition, conformational changes in response to carbamylation have been discussed as well [247,249], altogether resulting in a possible decline of bioactivity as shown for EPO [250]. Protein carbamylation in general has also been associated to diseases, such as rheumatoid arthritis, atherosclerosis and Alzheimer's disease [249]. Thus, this CZE approach provides also a strategy for other recombinant proteins that have been carbamylated during their manufacturing. Best separation was achieved with 100 mmol/L sodium hydrogen phosphate, pH 6.50. The addition of 2.0 mmol/L tetraethylene pentamine (TEPA) provided dynamic capillary coating. In addition, TEPA improved the electrophoretic resolution of different positional subspecies of single- and double carbamylated variants due to a retardation of the EOF and a selective interaction with side chains of aspartic and glutamic acid. In total, eight Bet v 1a variants were resolved. The determined purity was ~40% for the carbamylated batch and > 85% for the non-carbamylated products. Instead of t_m, μ_{eff} was applied for identification of variants, which improved the repeatability to < 0.6% (RSD) [246]. When 100 mmol/L 2-(*N*-morpholino)ethanesulfonic acid (MES) was applied in the BGE instead of phosphate, the optimized TEPA concentration was lowered to 0.4 mmol/L. This was attributed to a reduced ion-pair formation between TEPA and MES. The CZE separation of the carbamylated product was improved with this refined method: 17 variants were resolved and distributed in individual clusters for single and double carbamylated Bet v 1a species containing seven and six positional variants, respectively [251].

3.3.13.2. Hypoallergens. When used in therapy, an IgE boost in response to a treatment with recombinant WT-allergens cannot be excluded [236]. Hypoallergens may overcome this limitation. They can be prepared by chemical denaturation [233,243] or are genetically designed by selectively inducing mutations in relevant epitopes to reduce IgE binding, but maintaining their T-cell epitopes and thus strong T-cell activation [236,252]. This would reduce adverse reactions during hyposensitization, but allow for an increased dosage [232] and minimize the risk for unintentionally sensitizing genetically predisposed, i.e., atopic, patients [237].

The carbamylated birch pollen batch of Section 3.3.13.1 was resolved in SMIL-coated capillaries. The coating was composed of four layers with alternating charges, i.e., polycationic poly(diallyldimethylammonium chloride) (PDADMAC) and polyanionic dextran sulfate (DS). The terminal layer (i.e., DS) possessed the same charge as the allergens in order to guarantee electrostatic repulsion and combat protein adhesion. The elaborated non-covalent coating protocol provided an exceptional coating durability without the need for re-coating steps contrary to others (see Section 3.3.7). Durability testing of the SMIL coating comprised 70 runs performed over 23 days with the SMIL coating still intact when the test was stopped. Separation was in 100 mmol/L ammonium bicarbonate, pH 6.70. 14 variants were resolved including even a triple-carbamylated variant. Plate numbers up to 685,000 were realized. Inter-day precision for t_{EOF} and t_m was < 0.35% and < 0.80%, respectively. In addition, a commercially available recombinant hypoallergen with six mutations deliberately introduced in order to reduce IgE responses was analyzed. The hypoallergen was clearly separated from its recombinant major WT-like variant [157]. In addition, two in-house Bet v 1a hypoallergens, initially designed *in-silico* before expressed in *E. coli*, were characterized in terms of their purity by CZE-UV in bfs capillaries [253].

3.4. CZE with enzymatic in-capillary reactions

3.4.1. Recombinant human β-secretase (rhBACE1)

β-secretase (=beta-site amyloid precursor protein cleavage enzyme 1, BACE1) cleaves the β-amyloid peptide from its precursor protein. The resulting peptides aggregate thus forming oligomers and final amyloid plaques [254]. Early aggregation states, so-called prefibrillar structures, are associated with the neurotoxic effects in Alzheimer's disease [255]. The inhibition of β-secretase might retard or ideally even stop the progress of the disease [254]. The laborious testing of candidate inhibitors of enzymes can be automatized in the CE format. Moreover, multiplexing is possible with instruments that allow for the application of capillary arrays. By in-capillary reaction strategies, automatized testing under standardized and thus comparable conditions can be combined with fast throughput and minute consumption of enzyme, substrate and inhibitor solutions [256,257].

The research group of Z. Glatz [257] applied two different strategies for the characterization of the enzyme kinetic and the inhibition of recombinant human BACE1 expressed in HEK 293 cells: (i) transverse diffusion of laminar flow profiles (TDLFP) and (ii) a plug-plug-electrophoretically mediated microanalysis (EMMA). In the first approach, the enzyme and the substrate were injected as alternating zones with high pressure. The parabolic zone profile ensures the mixing of zones by diffusion (Fig. 5). In the plug-plug-EMMA approach reactants were injected in the order of their ascending μ_{eff}. Subsequent to the application of the separation voltage, fast migrating compounds invade the preceding zone of the slower migrating reactant (Fig. 5). Additionally, the voltage can be shut down to extend the contact and thus the reaction time. Both methods were tested using a decapeptide that contained the amyloid precursor cleavage site for BACE1 as a model

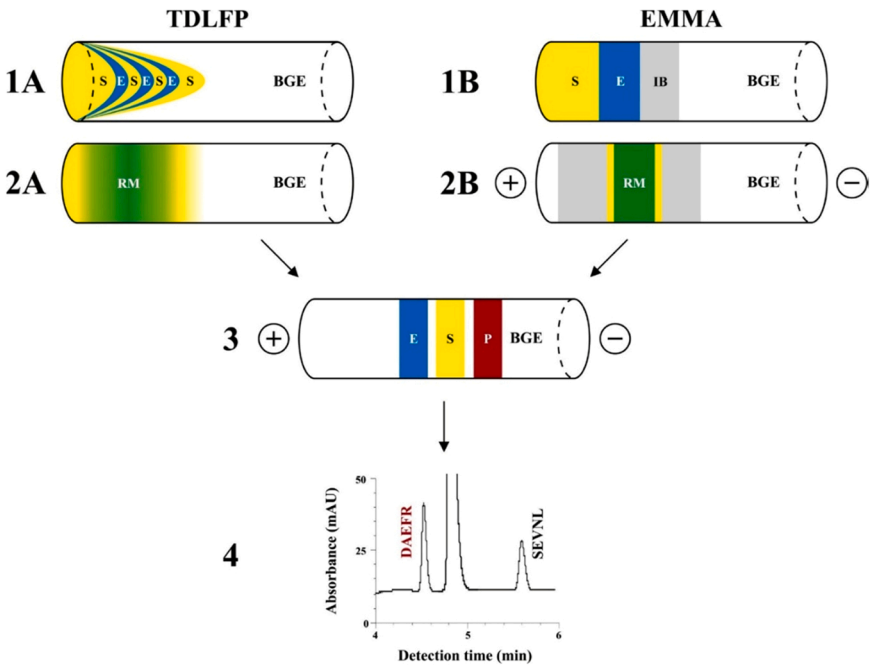

Fig. 5. Schematic representation of the configurations used in the β-secretase inhibitor screening. (1 A) In the TDLFP-based system, injection was accomplished by the alternating introduction of solutions of SEVNLDAEFR (S) and BACE1 (E). (2 A) The reaction mixture (RM) was then formed by transverse diffusion. (1B) The injection procedure of the system based on the EMMA methodology consisted of the plug introduction of the incubation buffer (IB), BACE1, and SEVNLDAEFR. (2B) Individually injected plugs were then merged by the application of a voltage. At the moment of full zone overlap, the voltage was turned off and the reaction mixture was incubated in order to accumulate enough reaction products (P) for detection. (3) In both methods, the reaction was terminated by the (re) application of voltage and separation of the SEVNLDAEFR and BACE1. (4) The reaction products were then detected and quantified using a UV–vis detector.
Reprinted from [257], with permission from Elsevier.

substrate. In TDLFP, four plugs of the decapeptide and three plugs of BACE1 were alternating injected. The seven plugs covered 8.6% of the total capillary length. In EMMA, the decapeptide was injected first, followed by BACE1. The capillary occupation of both EMMA plugs was equivalent to TDLFP. After an application of 30 kV for 28 s, the voltage was shut off and incubation was done for 12 min. Electropherograms of both methods corresponded and contained the initial decapeptide and the two pentapeptides resulting from enzymatic cleavage (Fig. 5). Intra-day and inter-day precision for peak areas was 1.5–2.2 times worse in case of TDLFP. Both strategies were applied in the determination of the apparent Michaelis constant and the apparent maximum reaction velocity. Moreover, both concepts were also employed as inhibition assays by testing inhibitors of BACE1. The derived half-maximal inhibitory concentration (IC_{50}) and the apparent inhibition constant were compared to literature data. Generally, TDLFP was applicable for fast initial screening, but lacks precision. Thus, for more precise studies, EMMA was the method of choice, but required a case specific optimization of the voltage-driven mixing step, which is related to the individual μ_{eff} of the reactants [257].

3.5. Capillary gel electrophoresis (CGE)

CGE separates proteins according to their size by application of a sieving polymeric network. Different polymers have been used to prepare sieving matrices. However, nowadays mostly commercial CGE kits (Table 3), which contain an appropriate polymer, are applied in the analysis of (commercial) recombinant proteins. In addition, capillary walls have to be coated in CGE. However, this is less related to protein adsorption [258] since proteins are mostly decorated with SDS-micelles (SDS-CGE) forming pearl-necklace like structures [259], but to suppress the EOF, this way improving the repeatability of results. Some sieving polymers simultaneously act as coating agents. This allows for an operation with bfs capillaries, which are coated when getting in contact with the polymeric solution. Further details are provided elsewhere [258].

Depending whether CGE is run with or without SDS, slightly different separation principles are realized. In SDS-CGE, proteins are denatured and decorated with SDS and migrate through the sieving polymer matrix according to their size. In absence of SDS, besides the size also the charge of proteins becomes relevant for the separation process. This explains why in some cases protein dimers may migrate faster than their monomers [260].

3.5.1. Fusion protein as vaccine candidate

Instead of SDS-PAGE, CGE was applied to analyze a vaccine candidate named HyVac (H4), which was intended as a booster for an extended protection against tuberculosis. The vaccine contained a recombinant fusion protein of 41.3 kDa composed of two protein antigens, i.e., Ag85B and TB10.4, which are expressed in the early infection state of tuberculosis. The sample preparation was described in detail and included inter alia mixing of H4 with 1% β-mercaptoethanol and a commercial SDS-MW gel buffer with subsequent heating to 75 °C for 3 min. Under non-reducing conditions, several oligomer species were separated in addition to the monomer, whereas in presence of β-mercaptoethanol only the monomer was detected. NIST-traceable BSA was applied as an ISTD. Peak areas of both H4 and BSA were corrected for their velocity [261] for reasons stated elsewhere [262]. For relative quantification, the corrected H4 peak area was divided by that of BSA. By this approach, the bias in quantification could be reduced 3-fold in comparison to quantification without correction. A calibration with BSA-corrected peak areas of H4 provided relative recoveries of 98.6–101.3% (for H4 concentrations between 20 and 110 μg/mL). For quantitation and purity determination two different CGE methods were developed. The CGE method for purity determination resulted in a relative H4 purity of 89% ± 0.14% (RSD), whereas SDS-PAGE provided 93%. The discrepancy has been attributed to the Coomassie staining in SDS-PAGE, which apparently resulted in an underestimation of minor impurities (Fig. 6) [261].

3.5.2. PEGylated IFN-α2a

PEGylation of biopharmaceuticals increases their water solubility and mass (due to PEG addition and disproportionate binding of water molecules), the shelf durability, the circulating half-life, and reduces protein immunogenicity (see Section 2.1). This is related to the increase in mass, which decreases renal clearance, but also due to the protective effect of PEG against thermal and pH stress, against proteolytic enzymes and a reduced immune-recognition caused by the PEG shielding of the protein surface. For IFN-α2a, which is applied in the hepatitis C therapy, the frequency of administration could therefore be reduced 3-fold compared to its native pendant. These advantageous effects can be

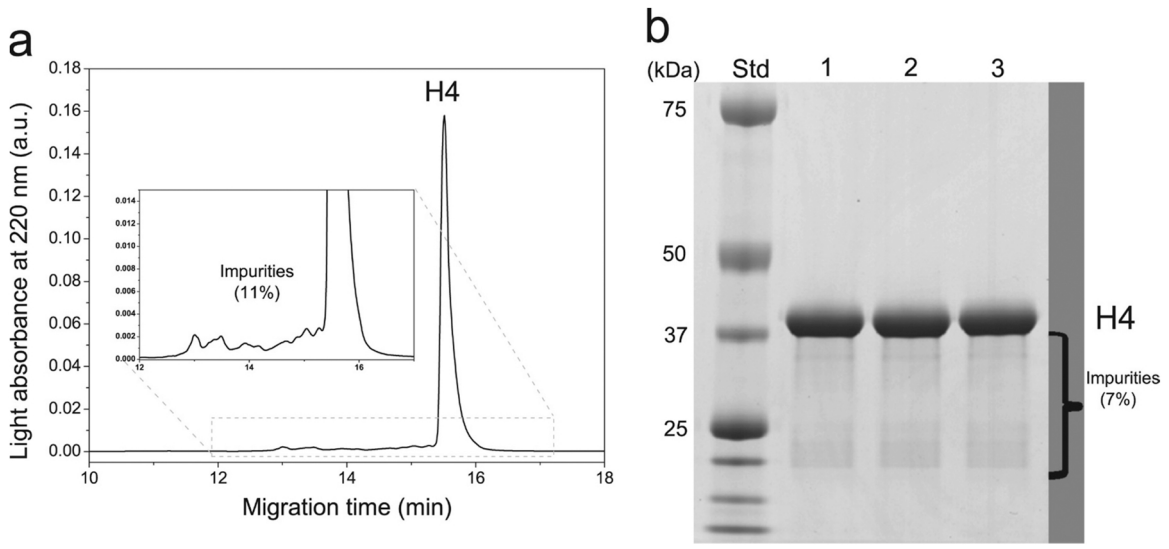

Fig. 6. Comparison of CGE (a) and SDS-PAGE (b) purity assays. CGE analysis was carried out under the following conditions: injected with 130 V/cm for 40 s, capillary cartridge temperature of 24 °C, and separation electric field of 530 V/cm, sample cooling garage temperature set to 10 °C and H4 concentration of 650 μg/mL. The inset shows the zoomed-in impurity region. SDS-PAGE conditions were: H4 load of 5 μg into lanes 1–3, Coomassie staining for visualization. Reprinted from [261], with permission from Elsevier.

further promoted by replacing linear with branched PEG [33].

Na et al. [263] applied SDS-CGE to separate IFN-α2a products after modification of amino groups, i.e., the N-terminus and ε-amino groups of lysine, with PEG. Depending on the applied excess of the PEGylation reagent, single- to hexa-PEGylated IFN-α2a species were generated and resolved by SDS-CGE. In addition, N-hydroxysuccinimide was detected. This group was released from the initial PEG reactant during the PEGylation reaction and can thus be employed as a reporter for the extent of the modification. SDS-CGE results were compared to SDS-PAGE and MALDI-TOF-MS data. Contrary to SDS-CGE, the conjugate with the highest PEGylation (i.e., tetra-PEG) was not detected with the other methods [263]. The same research group applied SDS-CGE to separate IFN-α2a PEGylation conjugates with branched or trimer PEG structures. Four lysine hotspots for PEGylation were identified. Besides mono- to tetra-PEGylated variants, also mono-PEG-conjugates with different PEG sizes (20,000−47,000) including branched and trimer structures were separated. Thereby, mass differences of 3500 could be resolved for mono-PEGylated variants presumably due to their different shape. Moreover, the method was used to check the quality of mono-PEGylated IFN-α2a variants after purification with SEC [264].

3.5.3. RLPs

dlRLPs and tlRLPs were produced in a baculovirus-insect cell (Sf6) expression system by co-infection. Purity and integrity of expressed and assembled RLPs were evaluated and confirmed by transmission electron microscopy, SDS-PAGE and Western blot. dlRLPs and tlRLPs were characterized by SDS-CGE. Injection parameters were critical for improved peak shapes and for the resolution of virus proteins. A temperature increase from 20 °C to 40 °C resulted in a decrease of the apparent mass by up to 7%. This was related to viscosity changes of the separation medium and altered sieving rather than to an actual mass shift. The virus proteins were separated in < 20 min with SDS-CGE. Profiles for the recombinant proteins of the rotavirus achieved with SDS-CGE, SDS-PAGE and Western blot were compared. MALDI-TOF-MS provided a higher mass accuracy for the virus proteins, but quantification was limited in comparison to SDS-CGE [42].

3.5.4. Protein aggregates in pharmaceutical insulin products

Insulin shows a high propensity for aggregation [265], which starts with destabilized monomers and proceeds via oligomeric species finally forming insoluble fibrillary aggregates [266]. The amyloidogenic region of insulin is localized in the N-terminal parts of the A- and B-chain, i.e., the so-called H-fragment, with major contribution to aggregation from the A-chain part [265]. Insulin aggregation has been observed both in vitro and in vivo [266]. Insulin aggregation can occur under agitation conditions and has been observed in pharmacological preparations. Resulting high-molecular mass insulin polymers are considered only partially potent and fibrils have a massive impact, particularly when injected subcutaneously [267]. In rare cases, insulin-derived subcutaneous amyloidosis has been observed in diabetes patients after repetitive insulin administration at the same injection site, observed as an “insulin ball” [268,269]. Analytical methods that are capable to distinguish between the different species evolved during the insulin aggregation progress are therefore essential.

Pryor et al. [266] were the first to separate early stage oligomers of insulin with CGE in capillaries coated with poly-N-hydroxyethylacrylamide (PHEA). PHEA was initially synthesized as a polymer matrix for DNA sequencing and simultaneously provides a hydrophilic capillary coating [270]. CGE was done in a matrix of 0.5% and 1% PHEA. The aggregation progress of insulin due to agitation at 185 rpm was followed over 24 h and besides aggregates between 30 and 50 kDa (i.e., 5–8-mers) even larger aggregates, which stayed below 100 kDa (17-mers), were detected. Contrary to the usual detection of aggregation with thioflavin, the CGE method allowed even for an early identification of initial aggregates [266].

Demelenne et al. [260] compared CGE as an orthogonal method to acidic SEC (pH 2.5) in order to analyze insulin aggregates in a pharmaceutical product. Separation was done in PEO coated capillaries. In parallel, neutral SEC at pH 7.4 was applied and the results were compared, respectively. A commercial insulin product, i.e., Humuline® Regular, was treated differently (untreated, acidic treatment, agitation (700 rpm for 24 h), agitation of acidified solution). Treated samples were then monitored for insulin aggregates with all three analysis methods. SDS-CGE addressed only the insulin monomer peak, whereas in CGE without SDS two peaks (insulin monomer and dimer) were detected proving the disruption of non-covalent forces between insulin monomers by SDS. When SDS was replaced by deoxycholate, both, the monomer and dimer peak were detected. Over 48 h agitation at 1200 rpm only insulin monomers and dimers were detected with CGE and neutral SEC in corresponding percentages. In acidic SEC, the dimer

peak was considerably smaller and remained nearly unchanged over time, but an additional oligomer peak occurred, which was absent in the other two methods. Apparently, the CGE and neutral SEC methods reflected the actual situation in the sample, whereas acidic conditions might have affected the net charge or the conformation of insulin and thus promoted aggregation [260].

3.6. μChipCGE

3.6.1. PEGylated rhG-CSF

Park et al. [271] analyzed rhG-CSF using μChipCGE with LIF detection after its modification with PEG reagents of 5000 Da and 20,000 Da, respectively. Different CGE configurations were tested covering mass ranges of 5–80 kDa (Protein 80 Labchip) or 14–230 kDa (Protein 230 Labchip). Reaction products prepared at different pH values were characterized. In terms of the PEGylation efficiency, two pH dependent maxima were revealed by the μChipCGE method, which were related to the different pK_a values of the α- and the ε-amino groups. The maximum at the lower pH was more appropriate since it addressed the N-terminal amino group resulting in a more homogenous reaction product. Mono- and di-PEG variants with 5 kDa and 20 kDa PEG modification were resolved simultaneously with the Protein 230 Labchip within less than 1 min [271].

3.6.2. (PEGylated) recombinant blood coagulation factors

Recombinant coagulation factor VIII (rFVIII) and recombinant van Willebrand factor (rvWF) were analyzed by μChipCGE. Both proteins were expressed in CHO. For rvWF a culture medium deficient of plasma and albumin was used (see Section 2.4). rFVIII is a heterodimeric glycoprotein composed of a light chain of ~80 kDa and a heavy chain with variable length (90–240 kDa) due to a flexible processing of its B-domain. rFVIII possesses 25 glycosylation sites, which are situated in the B-domain. The intact protein and monomer variants were separated using a commercial CGE separation kit including a gel-dye mix. Mass assignment was done by using two flanking markers with 4.5 and 240 kDa. The light chain and the heavy chain lacking the B-domain were not resolved and provided one sharp peak. Inclusion of the glycosylated B-domain resulted in numerous peaks due to the variable processing of the B-domain, all with increased peak widths caused by the extensive glycosylation of the B-domain. PEGylated rFVIII showed additional peaks due to PEGylated variants occurring at the expense of the original signals. The monomeric form of the rvWF resulted in a broad peak. PEGylation provided a series of six partially resolved signals, i.e., one- to six-fold PEGylated variants, at progressively higher masses. When rvWF was deglycosylated with PNGase F, the peak for the non-PEGylated species was shifted to lower t_m, whereas the resolution of the deglycosylated PEGylated variants was slightly improved and uncovered also a 7-fold PEGylated species [272].

3.7. Capillary isoelectric focusing (CIEF)

Contrary to CZE, which uses an uniform separation medium, analytes are separated in a pH gradient in CIEF. A primary pH gradient is formed by the migration of OH^- and H_3O^+ ions provided by the acidic anolyte and the alkaline catholyte [273]. Ampholytic compounds, so-called carrier ampholytes (CAs), stabilize the gradient by their buffer properties and generate a continuous pH gradient [274]. Different CAs are commercially available. By combining CAs covering different wide and narrow pH ranges, the pH gradient can be tailored to the respective composition of the sample [275]. The pronounced UV absorption of CAs at wavelengths usually exploited in protein detection (i.e., 190–210 nm) requires detection at 280 nm, which addresses aromatic amino acids [276]. The lower signal intensity at this wavelength is (partly) compensated by the exceptional protein concentrations, which are up to 200 mg/mL and achieved during the focusing step [129]. Under the influence of an electric field proteins migrate within the pH gradient until their pI equals the pH, where the protein acquires a net charge of zero and becomes focused. It has to be stressed that the formation of the pH gradient and protein focusing occur simultaneously. In CIEF, the r_H does not contribute to resolution, and separation is merely based on pI differences. Resolution is determined by the following equation[277,278]:

$$\Delta pI = 3 \bullet \sqrt{\frac{D\left(\frac{dpH}{dx}\right)}{E\left(-\frac{d\mu}{dpH}\right)}} \quad (3)$$

The resolution in CIEF can be improved by tuning the pH gradient with appropriate CA combinations and by reducing the analyte diffusion from the focused zones (see Eq. 3), which is mostly done by addition of polymers to increase the viscosity of the separation medium. An increased viscosity minimizes also band broadening during the mobilization [129]. The progressive decrease of the protein net charge during focusing enhances the risk for protein aggregation and even in-capillary precipitation resulting in stochastic profiles with spikes [279,280]. A major pitfall in CIEF with conventional CE instruments is the misinterpretation of insufficiently focused analytes as sophisticated separations [281]. Nowadays, two-step CIEF is the common format in conventional CE systems with single point detection: after the analytes have been focused, they are mobilized in a second step towards the detector, either by (i) pressure application or by (ii) chemical means [282]. The efficiency of different mobilization strategies was systematically investigated in a recent approach demonstrating that mobilization with zwitterions preserves analyte resolution acquired in the focusing step best [283]. Spacer compounds with well-defined pIs are added to the sample mixture to prevent anodic and cathodic losses of CAs and analytes due to isotachophoresis-driven drift processes [284,285].

Imaged CIEF (iCIEF) circumvents most of the problems described for conventional CE equipment by its whole-capillary imaging with a CCD camera and real-time detection of the focusing progress. This abandons the need for a mobilization step and allows for real-time monitoring of the focusing progress [286]. A comprehensive discussion of CIEF fundamentals is provided in several reviews [274,287–289].

3.7.1. EPO

CIEF-UV is a major CE separation technique in the analysis of EPO variants due to the influence of sialic acid residues on the pI. Different standard samples, including a BRP of the Ph. Eur., were analyzed by the group of de Frutos [290]. rEPO was produced in CHO. CIEF was done in capillaries coated with polyacrylamide (PAA) or in commercial capillaries (eCAP) with a neutral coating. For an improved separation, wide and narrow pH range CAs were combined including 7 mol/L urea. Bovine β-lactoglobulin was applied as an ISTD for normalization of mobilization times [290]. Cifuentes et al. [291] also analyzed a BRP of Ph. Eur. with CIEF using similar separation conditions and PAA coated capillaries. For a successful separation of EPO variants, some salt/excipients had to be retained in the CIEF sample. Seven glycovariants with pIs between 3.87 and 4.69 were resolved. CIEF results were compared to flat-bed IEF (5 bands) and the CZE method of the Ph. Eur. (8 glycovariants) [291].

3.7.2. Recombinant allergens

Recombinant Bet v 1a products (non-carbamylated and carbamylated batches; see Section 3.3.13.1) were analyzed with CIEF-UV either in commercial neutral coated or in-lab coated capillaries. Best separation results were achieved with a CA mixture that combined a wide pH range (3−10) with two narrow pH range (5–7 and 5–6) CAs, providing a resolution of 17 variants for the carbamylated product. One major and several minor subvariants could be distinguished for the single and double carbamylated species, respectively. Peak profiles and determined purity corresponded to CZE-UV results achieved for the same batch (see Section 3.3.13.1). The pI values for the major variants showed a stepwise decrease for carbamylated species due to the covalent modification of the N-terminus and the ε-amino groups of lysine [251]. The method was validated including linearity testing applying the Mandel fitting test and a comprehensive robustness test [292].

3.7.3. Influenza virus

Horká et al. [293] tested the purity of equine and swine influenza virus by means of CIEF-UV. Cultivation was on embryonated chicken eggs inoculated with allantoic fluid containing the virus. A lab-designed instrument was applied for CIEF measurements. Injection was done in a 100 μm i.d. capillary in three segments containing (1) a spacer (i.e., L-aspartic acid) dissolved in the catholyte, (2) virus and/or allantoic fluid, and (3) the CA mixture containing pI markers. Both virus types were separated from the allantoic fluid matrix prior to a purification step. Purification via precipitation with PEG 6000 and/or centrifugation through a 20% sucrose cushion reduced the matrix peak without compromising the intensity of the virus peak. Experimentally, pI values of 6.5 and 6.6 were determined for purified swine and equine influenza virus, respectively. CIEF separated also incomplete virus particles from the infectious virus [293].

3.8. Imaged CIEF (iCIEF)

The application of iCIEF in the (bio)pharmaceutical industry has been review recently [294] and advantages of iCIEF over conventional two-step CIEF were outlined in Section 3.7.

3.8.1. EPO

Cowper et al. [295] compared 12 commercial rhEPO originator and biosimilar products with a CRS of the EDQM. Commercial products were expressed in CHO cells and cultivated either in roller bottles or in bioreactors. Unfortunately, cultivation conditions were not specified further. Separation was done in fluorocarbon (FC) coated cartridges with a combination of wide and narrow pH range CAs under denaturing conditions (4 mol/L urea). The products differed in the relative abundance of sialic acids. In several products acidic variants (pI ~3.8–3.9) dominated, whereas in other products more alkaline EPO species (pI>4.65) were prevalent. No clear relation between the cultivation method (roller bottle, reactor) and the glycan profiles could be deduced. The authors assumed differences in cultivation conditions and media to be responsible for the observed variability. With two exceptions, all other products differed from the CRS in terms of their profile. Some products contained even penta- and hexa-anionic N-glycans [295].

Recently, an iCIEF-UV fluorescence method was applied to analyze eight different commercial rhEPO drug products under denaturing conditions (4 mol/L urea). Excitation was done at 280 nm with detection at an emission wavelength of 350 nm corresponding to protein native fluorescence. Contrary to the CE method of the Ph. Eur., analysis was done without sample pretreatment prior to CE analysis. In a first step, the composition of a drug product was simulated by combining 20 μg/mL rhEPO with 3 mg/mL HSA and 20 mmol/L citric acid. Relative areas and pIs of major peaks did not differ between this simulated "drug product" and the drug substance. iCIEF measurements were extended to commercial EPO products. Remarkably, the LOQ was 100-fold lower than in CZE-UV and CIEF-UV and still 10-times better than in CZE-LIF. Except for one commercial product, which showed a different pattern most probably due to different glycosylation, corresponding profiles were achieved (Fig. 7) [296].

3.8.2. Fusion proteins

For economic reasons, the biopharmaceutical industry progressively uses platform approaches in the development of cell lines and cell cultures, but also in downstream purification (as shown in Section 2.8) [8] and product formulation [297]. This platform concept is mostly applicable to a class of molecules sharing relevant physicochemical properties [297]. The idea of this concept is also transferred to analysis methods, where an optimized separation and detection strategy is applied to different analytes, and might only require minute amendments for a refined analysis. The applicability of this concept was

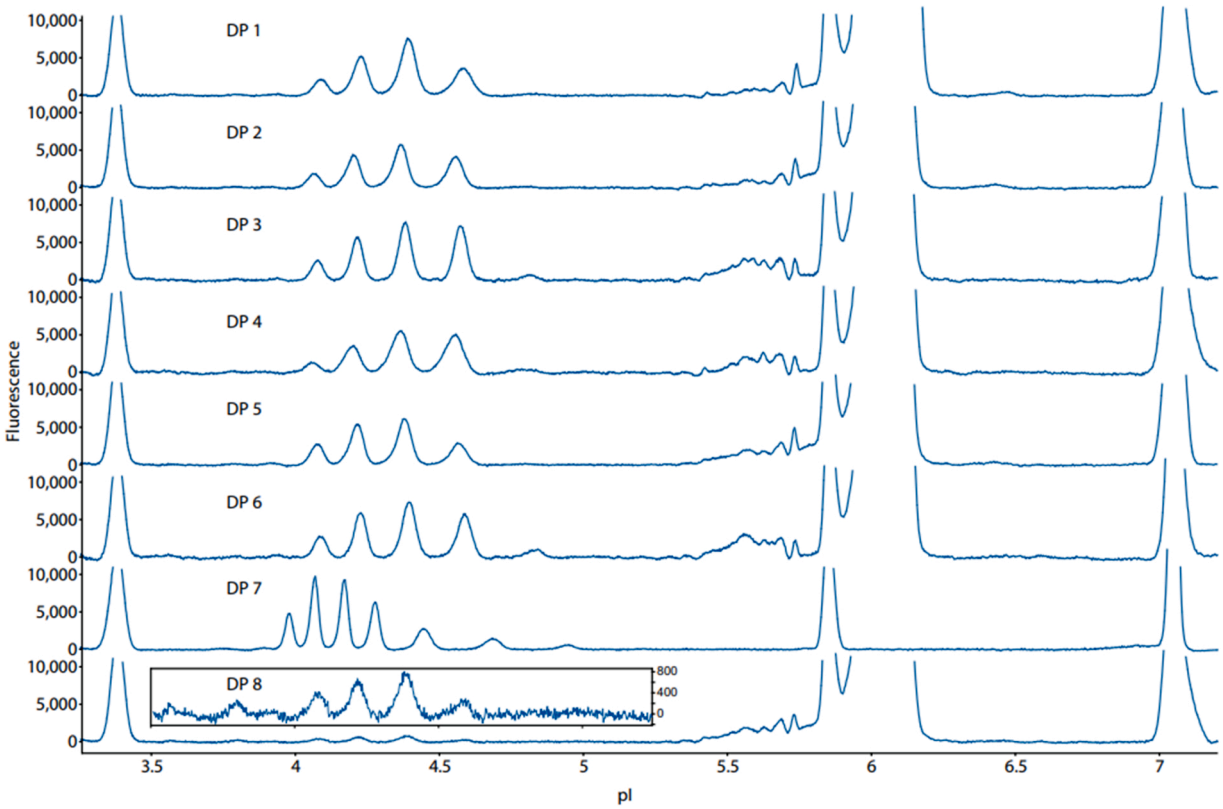

Fig. 7. Electropherograms resulting from the analysis of 8 different commercial drug products (DPs) with icIEF and native fluorescence detection. The inset shows DP 8 with the same X-axis scale, but with a narrower Y-axis scale to enhance the rhEPO peaks.
Reprinted from [296], with permission from Elsevier.

recently shown by our group for a CIEF-UV approach addressing therapeutic monoclonal antibodies under non denaturing conditions [298].

A similar strategy was also presented by Wu et al. [31] applying an iCIEF-based platform for 9 different fusion proteins. Since proteins are concentrated during the focusing step, an increased propensity for aggregation and even precipitation is observed (see Section 3.7). Therefore, additives that enhance protein solubility can be included [279]. In the current case, urea was tested. However, for the different fusion proteins, urea decreased signal heights and resolution, changed the apparent pI due to protein denaturation, or different urea concentrations had to be applied. These limitations were overcome by a commercial non-denaturing stabilizer. The tested fusion proteins covered a pI range between 4 and 8. A tailored use of narrow pH range CAs refined the separation. The instrumentation allowed for UV- and native fluorescence detection. The latter provided increased signal intensities and reduced the baseline noise. iCIEF provided peak pattern corresponding to slab gel IEF, but improved resolution and sensitivity, despite the fact that the injected protein mass was 4.4–8.9-times smaller in iCIEF [31].

3.8.3. Recombinant VLPs and viruses

iCIEF was applied in the characterization of HPV-VLPs (see Section 3.3.9.2) recombinantly produced in *Pichia pastoris*. The iCIEF optimization was done with HPV-VLPs composed of 18 L1-molecules due to their uniform assembly. In order to prevent aggregation and precipitation, which are recorded as spikes and irreproducible peak pattern [210, 279] (Sections 3.7), 2 mol/L urea was added, the CA content was reduced to 4% to restrict Joule heating, and the focusing time was limited to < 6 min. Disassembly with 50 mmol/L dithiothreitol at pH 8 was followed by a decrease to pH 6 in order to reassemble virus proteins. This procedure generated more uniform virus particles as evident from the iCIEF profile. pI values between 7.57 and 8.70 were determined for the five HPV-VLP variants [210].

3.9. Affinity CE

3.9.1. β2-M

Regazzoni et al. [299] applied affinity CE (ACE) to screen different sulfonated compounds for their anti-amyloidogenic activity applying recombinant β2-M as a model. The chemical names of the sulfonated fibrillogenesis inhibitors were not revealed, but provided in coded form. Increasing concentrations of the inhibitory ligands were added to the BGE, i.e., 100 mmol/L sodium phosphate, pH 7.4, and the respective changes in μ_{eff} were measured for (i) the native state and (ii) the folding intermediate of β2-M (see Section 3.3.12). Shifts in μ_{eff} proved ligand binding to both β2-M conformations. In addition, refolding of recombinant β2-M in native BGE was monitored after its unfolding under acidic conditions in presence and absence of the candidate inhibitory ligands. Results showed that ligand binding per se was not sufficient for an inhibition of fibrillogenesis, but had to address the protein domain involved in the formation of fibrils. Besides ACE, high-resolution MS and molecular modelling were combined to an integrated approach [299]. Aspects of ACE in probing the affinity of different ligands for β2-M are reviewed elsewhere [227].

3.9.2. Recombinant allergens

The epitope integrity of recombinant Bet v 1a was investigated by means of affinity-CIEF-UV applying two in-house produced monoclonal IgGs (mIgGs) from murine hybridoma cell lines. The ionic strength of the mIgG formulation was critical in order to assure solubility during product storage, but also to limit the CIEF current and prevent impaired resolution in CIEF. Affinity-CIEF used a mixture of one wide pH range CA and a blend of three narrow pH range CAs covering a pH domain of 5.0–7.7 in order to improve the resolution of IgG variants and of the immune-complexes formed between mIgG and Bet v 1a. The dissociation constant K_D of the immune-complexes was determined with 2–3 nmol/L by SPR. This high affinity binding allowed for pre-incubation with the formed complexes persisting during the focusing and subsequent mobilization step in CIEF. The concentration of mIgG was maintained during the experiments, whereas the concentration of added Bet v 1a was increased stepwise until the paratopes of mIgG were saturated and unbound allergen was measured in CIEF. Complexes with 1:1 and 1:2 stoichiometry were clearly resolved by their different pI-values caused by the binding of the acidic allergen. The heterogeneity of IgGs was reflected in the formed 1:1 and 1:2 immune-complexes. The work proved the feasibility of affinity-CIEF for evaluating the integrity of recombinant protein conformations/epitopes [300].

3.9.3. VLPs

Bettonville et al. [213] subjected recombinantly produced VLPs of HPV to affinity CZE-UV. HPV16, the most prevalent risk type for cervical cancer, was selected for this approach. CE capillaries were coated with PEO prior to each run, respectively. In addition, the BGE contained 0.1% PEG 6000. HPV16-VLPs were incubated with a 50-fold molar excess of a specific antibody (Ab), i.e., H16.V5, for 1 h at room temperature. The resulting complex migrated between free HPV16-VLP and H16.V5 and was clearly resolved from HPV16-VLP due to its lower μ_{eff}. This is related to the increase in molecular mass (from 20.3 MDa to 28.0 MDa). Due to some disintegration of the formed complexes, free HPV16-VLP was detected together with the complex, whereas free H16.V5 was not detected at the applied concentration. In the presence of a non-specific Ab no complex formation was observed, which proved the specificity of the method. Phthalic acid was employed as an ISTD to correct for variations in the injection volume. The approach allowed for identity confirmation of the HPV type and has thus the potential for the quality control of multivalent vaccines, where individual HPV types have to be distinguished [213].

The group of Kenndler [301] applied affinity-CZE to distinguish between two serotypes of the human rhinovirus by applying specific mAbs in excess. Virus-mAb complexes were formed by pre-incubation in absence of SDS and were then separated from free mAb in 100 mmol/L boric acid adjusted to pH 8.3 with 10 mmol/L SDS added. The detergent addition was required to prevent both virus aggregation and adsorption onto the capillary wall [301]. This BGE was previously optimized and applied to distinguish four serotypes of human rhinovirus and analyze crude virus preparations [302]. When a constant virus concentration was titrated with progressively increasing mAb concentrations, the μ_{eff} of the initial virus peak decreased until a plateau was reached. This was explained by the mAb-virus complex formation, which changed the mass and r_H, but also the pI by masking positive virus charges. Moreover, the peak related to the mAb-virus complex became initially broader before regaining its small width. In parallel, free mAb occurred at higher concentrations. This reflected an initially heterogeneous binding stoichiometry before all virus epitopes were saturated with mAbs. Similar effects were observed for extended pre-incubation times. This approach reflects the potential of affinity-CE in distinguishing different serotypes of viruses, but also a future option for screening virus-neutralizing agents [301].

3.10. CE with Western blot

Product monitoring in cell culture harvest samples is relevant for consistent manufacturing in order to allow for a prediction of the final drug substance and to correct for emerging quality constraints, for instance by adjustment of cultivation conditions and/or of the downstream purification [303]. In the biopharmaceutical industry, this sort of monitoring is traditionally done with SDS-PAGE in slab gel format followed by Western blot [303,304]. Western blot has been used for protein identification in early stage development, for the evaluation of the expression level of recombinant products, for the determination of the purity of the final product as well as for addressing HCPs [304,305]. However, drawbacks of this analysis strategy are manifold including the lack of automation, laborious handling steps, limited throughput and

insufficient quantitation both in terms of trueness and precision [303]. The latter was addressed by Koller and Wätzig [306] based on SDS-PAGE-Western blot analysis of rhEPO, where numerous error sources were outlined. When analyzing the same sample by different analysts, nearly 80% of the total error was assigned to the inter-operator variability. The related error source was apparently the color reaction, which is known to be delicate [306] and to limit quantitation [304]. The standardization of the gel-to-membrane transfer of proteins was reported another limitation [304].

CGE with in-capillary protein immobilization, followed by incubation with Abs and in-capillary detection represents an innovative concept and remedies most of the current pitfalls of SDS-PAGE-Western blot [303,304]. Major advantages of the CE-based approach cover the full automation of separation, blotting, incubation, washing and detection, and an improved quantitation. CGE separation is done in capillaries of 5 cm length in parallelized array format multiplexing 12 capillaries [303,304]. The capillaries possess a specific coating on the inner wall that allowed for non-specific covalent binding of separated proteins triggered by an UV photo-activation of the coating [304]. Capillaries are sequentially filled with a separation matrix, a stacking matrix (of lower ionic strength) and the protein sample. This causes the concentration of proteins as a narrow band at the boundary between the stacking and the separation matrix, before the separation is initiated [303,304]. After their separation according to size, proteins were immobilized by UV-exposure, followed by a washing step. Capillaries are then subjected to an Ab-diluent to prevent non-specific Ab binding. Subsequently, in-capillary Western blot is done either in a single step with the primary Ab conjugated with an enzyme [303] or in a two-step approach where incubation with a primary Ab is followed by a secondary Ab, which is directed against the first Ab and carries the enzyme [304,305]. In either case, horseradish peroxidase (HRP) is applied as the enzyme conjugate. After application of the substrate for HRP, i.e., luminol, the induced chemiluminescence is detected by a CCD camera and converted in electropherograms [303–305]. Instead of an in-capillary UV-immobilization, resolved proteins can also be blotted on a membrane after they have left the separation channel. Therefore, the blotting membrane is moved relative to the outlet of the separation channel by means of a translational stage and proteins are blotted in the order of their migration. The velocity of the stage movement determines the LOD and the resolution of blotted zones. An auxiliary liquid, which is fed to the electrophoretic effluent either by a microchannel integrated in the microchip or via a separate capillary surrounding the actual separation capillary, serves to stabilize the current and avoids bubble formation during the blotting process [307,308].

Rustandi et al. [304] applied the technique for screening and selection of appropriate Abs against recombinant vaccine proteins, which were expressed in *E. coli* or insect cells. In addition, the method was employed to evaluate the expression levels of membrane bound protein antigens in different host cell strains. Results proved the applicability for early-stage strain selection. When comparing the results of 11 parallel capillaries in a multiplexed array, the repeatability of peak areas was $< 10\%$ (RSD), whereas for independent runs the precision was $< 25\%$ (RSD). Quantitative results for crude lysates corresponded to RP-HPLC data, but provided improved specificity and faster throughput. The dynamic range covered two orders of magnitude with a LOQ of 0.23 μg/mL for the tested case [304]. Xu et al. [303] measured drug substances and related cell culture samples after a 1:100 dilution. The identity of the recombinant product was not revealed in the paper. Results showed three proteins with 100, 130 and 210 kDa. Their ratio constituted a decision tool for the release of drug substance batches: the relative peak area of the 210 kDa product was higher in the drug substance in comparison to the cell culture harvest proving the successful downstream enrichment of the recombinant protein. The effectual application of the method in the analysis of cell harvest material minimizes the risk for batch failure since the product quality can be predicted early in the production process, which allows for an intervention in due time [303].

Viral vaccines are produced in cell culture media containing FBS. However, due to the allergic potential of BSA, the WHO guidance requires ≤ 50 ng residual BSA in the final bulk per human dose, e.g., the final vaccine [309]. Loughney et al. [310] applied CE-based Western blot to quantify BSA in four batches of a final drug substance. With one exception, BSA was identified only in monomeric form in the products. The method was also applied for monitoring the BSA concentration in downstream process intermediate samples. Moreover, the method possessed the potential to differ between dimers and higher order aggregates of BSA based on their different size. A calibration curve between 5.2 ng/mL (=LOQ) and 420 ng/mL BSA was established. The realized LOQ complied with the requirement of the WHO. A trueness $> 80\%$ was determined for products spiked with 60 ng/mL BSA, and the precision was $\leq 15\%$ over a range of 700–2540 ng/mL BSA. Compared to ELISA, the CE-Western blot method was less affected by matrix interferences and provided a higher specificity [310]. Finally, automated CE-Western blot was used for the evaluation of CQAs of a recombinant drug product. The primary and secondary Ab that were applied in the recognition of separated and immobilized product constituents showed selective specificity for the subunits of the recombinant product. The recombinant protein was fractionated by SEC and the individual fractions were then analyzed with CE-Western blot. This allowed for a distinction and quantification of subunits, combinations of subunits and truncated fragments in heat stressed samples [311].

3.11. Analysis of glycosylation

The host cell line influences the glycosylation profile of recombinant proteins. Glycosylation controls the protein clearance time as shown exemplarily for a recombinant fusion protein expressed either in CHO or NS0 cells, and influences the in vivo binding affinity to the specific protein receptor [30]. Glycosylation can improve the protein stability by its protection against proteolytic decay, oxidation, denaturation and aggregation/precipitation. The latter may be due to a masking of hydrophobic protein patches or by steric repulsion. Moreover, a shielding of immunogenic epitopes by carbohydrate chains can lower the immunogenicity of recombinant protein products [30]. Different strategies have been pursued in the characterization of N-glycosylation of (recombinant) proteins addressing for instance intact glycoproteins, subunits of glycoproteins, glycopeptides, and glycans that have been released enzymatically from proteins [30]. A general survey of glycan analysis is given in a recent review [312].

3.11.1. Glycan analysis of recombinant proteins with CE

3.11.1.1. EPO. Ijiri et al. [313] characterized the structure of N-linked glycans of a commercial rhEPO product by CZE-LIF. After denaturation with SDS and β-mercaptoethanol, 10 μg EPO were digested either with PNGase F alone or in combination with neuraminidase. The released glycans were derivatized with the fluorescence dye rhodamine 110. Labeled glycans were excited at 488 nm and detected at 540 nm. Separation was done in 150 mmol/L sodium phosphate buffer. For sialo-oligosaccharides a pH of 7.0 was applied, whereas asialo-oligosaccharides were separated at pH 2.50. Separation was due to the different charge-to-r_H ratio, since asialo-oligosaccharides carry a positive charge at the selected pH due to the attached rhodamine 110. Differences in the r_H allowed even for a separation of 2,4- and 2, 6-branched 3-antennary isomers [313].

3.11.2. Analysis of glycans and glycopeptides of recombinant protein with CE-MS

Contrary to HPLC-MS, the hyphenation of CE to MS is more challenging and subjected to several constraints. This comprises the mandatory employment of volatile BGEs, which restricts the number of applicable electrolytes [314]. The major challenge of the CE-MS

hyphenation refers to the required circuit closure as the capillary outlet is not immersed in an electrolyte vessel, but protrudes in the ESI chamber [315,316]. The occurrence of two electrical circuits – one for CE separation and the other for hyphenation with MS – makes the situation even more intriguing, since one electrode is shared by both circuits [315,317]. Depending on the design of the mass spectrometer, the ground potential of the ESI-related circuit is situated either at the sprayer tip or at the front optics of the MS. This imposes different demands on the ESI interface. In so-called sheath liquid interfaces, electrical contact is provided by a conductive solution, the so-called sheath liquid (SL). The SL contains > 50% (v/v) of an organic solvent dissolved in water and a volatile acid for protein protonation [316]. The SL is applied by pressure via a coaxial SL interface. Whereas this sprayer is user-friendly with robust electrospray stability, dilution of analyte zones with the SL and competition for charges between analytes and SL constituents in the ESI process compromises the signal intensity in MS [316, 318]. Dovichi developed a low-flow version of the SL sprayer with the SL delivered electrokinetically [319] to minimize dilution effects. This sprayer was meanwhile commercialized by CMP Scientific under the product name EMASS-II.

Sheathless interfaces circumvent analyte dilution during the ESI process. Initial home-build designs were delicate to handle [316]. Meanwhile, commercial solutions are available. The CESI-sprayer of SCIEX provides electrical contact with the BGE via a porous section of the separation capillary and uses a stagnant conductive liquid - mostly sharing the composition with the BGE – surrounding the porous part to provide electrical contact. This avoids the application of a SL flow and leads to enhanced intensity of MS signals [320,321]. The commercial CESI sprayer is based on an interface prototype developed by Whitt and Moini [322]. A chip-based interface with a 22 cm separation channel was commercialized as ZipChip by 908 Devices/ThermoFisher Scientific and allows for fast protein analyses within a few minutes [323]. Fundamentals of CE-ESI-MS including further hyphenation strategies are reviewed elsewhere [315,316,324–326].

Recently, an online CZE-LIF-MS approach for the analysis of N-glycans was published employing an EMASS-II interface and a novel commercial non-reductive amination fluorescence dye, named TEAL™. LIF and MS were applied as orthogonal detection methods. MS allowed for the identification of the glycan structure, whereas LIF offered a wider dynamic range than MS and was appropriate for absolute quantification. In general, glycan labeling with fluorescence dyes is not only required for LIF detection, but may also improve the electrophoretic separation of glycans. Like the standard fluorescence dye in CGE-LIF, aminopyrene trisulfonic acid (APTS), TEAL™ adds three negative charges to glycans due to its sulfonic acid groups. The required excitation and emission wavelengths resemble APTS, which allows for a straightforward transfer of already existing workflows. The feasibility of the CZE-LIF-MS approach was shown for released glycans [327].

3.11.2.1. EPO. The glycosylation of rhEPO of the Ph. Eur. BRP-batches 2 and 3 was analyzed on the glycopeptide level after digest with trypsin, endoproteinase Glu-C, neuraminidase and a combination of the different enzymes. Resulting glycopeptides were separated in bfs capillaries with a combination of 50 mmol/L acetic acid and 50 mmol/L formic acid (pH 2.2). After ESI via a coaxial SL interface, glycopeptides were identified by means of TOF-MS. The major focus was on two glycopeptides carrying either an O- or an N-glycosylation site, i.e., O_{126} glycopeptide and N_{83} glycopeptide. In the O_{126} glycopeptide, acetylation and oxidation was localized on sialic acids, but not in other carbohydrate moieties. In addition, ~2% Neu5Gc content was revealed in the O_{126} glycopeptide, which carried two sialic acid residues. This non-human carbohydrate residue is expressed in CHO (see Section 2.2.2; Table 1) and the observed percentage corresponds with fractions typically produced by CHO lines. The ratio between Neu5Gc and Neu5Ac might offer a tool to distinguish endogenous and recombinant EPO. In case of the N_{83} glycopeptide, tetraantennary glycoforms with 1–3 N-acetyllactosamine units were most abundant. In addition, a sulfated sialoform was identified. The paper presented a comprehensive list of further identified glycopeptides [328].

3.11.2.2. PSA. Kammeijer et al. [329] identified glycopeptides of the prostate-specific antigen (PSA) by CZE-ESI-MS(-MS) after tryptic digest. Hyphenation via the porous CESI-interface prevented dilution and thus ensured increased signal intensity. When compared to nano-HPLC-ESI-MS, sheathless CE-ESI-MS offered a pronounced increase in sensitivity. CZE at pH 2.3 with in-capillary pre-concentration allowed for a separation of 75 different glycopeptides, comprising various non-sialylated, mono- and di-sialylated species. Remarkably, even isobaric sialic acid isomers, i.e., α(2,3)- or α(2,6)-sialylated glycopeptides, which cannot be distinguished by MS, were baseline resolved in CZE. α(2,3)- and α(2,6)-sialyllactose, for instance, differ by only $3.4{\cdot}10^{-2}$ units in their pK_a-values. The encountered ΔpK_a was assumed to cause the difference in μ_{eff}, whereas the influence on r_H seems to be only minute (see Eq. 1). An unidentified di-sialylated variant was assigned to an α(2,8)-linked species, but identity could not be confirmed by MALDI-TOF-MS. PSA concentration provides a limited diagnostic score in the evaluation of malignancy and staging of prostate cancer. However, PSA glycoprofiling is presumed more appropriate [329].

3.11.3. Comprehensive analysis of glycosylation on glycan, peptide and intact protein level with CE-MS

3.11.3.1. α-subunit of human chorionic gonadotropin. Thakur et al. [330] analyzed the commercial α-subunit of human chorionic gonadotropin (r-αhCG) expressed in a mouse cell line and compared this product to its CHO-derived pendant applying CE hyphenated to an LTQ-FT mass spectrometer. A PVA coated capillary reduced analyte interaction with the inner capillary surface and suppressed the EOF. r-αhCG possesses two N-glycosylation sites. Analyses were performed on the intact protein level, on tryptic glycopeptides and based on the released glycans. This increased the yielded information content by identifying the site-specific glyco-decoration. 60 different glycoforms containing up to 9 sialic acid residues were identified within an analysis time of 20 min. The r-αhCG glycosylation pattern of CHO cells was less complex in comparison to a murine host cell line. Glycovariants differed primarily in the sialic acid content: a maximum of five sialic acid residues was revealed for the CHO derived product contrary to nine sialic acids for the murine product. Glycopeptides of murine r-αhCG showed also immunogenic α-Gal (see Section 2.2.2). The different complexity of the products was also evident on the intact level as shown by total ion current (TIC) electropherograms. Results demonstrate that CE-ESI-MS is capable to distinguish between the glycosylation profiles of different host cells for the same protein thus proving its potential as an analysis tool in selecting the appropriate cell line for a desired PTM pattern [330].

3.12. CE-MS of intact recombinant proteins

3.12.1. Human IFN-β

The cytokine IFN-β possesses antiviral and immunoregulatory effects. Currently, two types of IFN-β are approved, namely aglycosylated rhIFN-β1b (expressed in *E. coli*) and glycosylated rhIFN-β1a (produced in CHO) [331]. IFN-β1a possesses one N-linked glycosylation site, and up to four sialic acid residues were assigned [332]. The glycosylated product has a size between 23 and 25 kDa [331]. It is applied in the treatment of multiple sclerosis to inhibit inflammation and to retard the damage of neuronal tissues thus reducing the risk for cognitive deterioration [333,334]. Its neuroprotective effect ameliorated glucose uptake in the hippocampus and the survival of neurons as shown in animal models and might therefore possess therapeutic potential in the

treatment of Alzheimer's disease [335].

Nine different glycoforms were distinguished for rhIFN-β1a with CZE-ESI-TOF-MS using a coaxial SL interface with a SL flow rate of 2 μL/min. BGE was 50 mmol/L acetic acid (pH 3.0). Due to the positive net charge of rhIFN-β1a under these conditions, a PB-DS-PB SMIL coated capillary was applied with a polycationic PB terminal layer [336]. In a refined setting, Haselberg et al. [320] analyzed rhIFN-β1a (Avonex®) with CZE-ESI-TOF-MS applying a commercial sheathless CESI sprayer. Separations were done in commercial capillaries coated with PAA. The durability of the coating was ~60–110 runs. rhIFN-β1a was separated in 50 mmol/L acetic acid (pH 3.0). The major species of rhIFN-β1a carried a fucosylated disialylated biantennary glycan structure. 18 different glycovariants were identified by mass differences, which corresponded to different sialic acid and hexose-N-acetylhexosamine (HexHexNAc) numbers, respectively. Together with coexisting deamidation, succinimide and oxidation variants, 80 rhIFN-β1a proteoforms were distinguished (Fig. 8) [320].

A commercial recombinant product of rhIFN-β1a (Avonex®) was analyzed with CZE-ESI-MS applying a CESI sprayer to hyphenate the CE instrument with an Orbitrap Elite mass spectrometer. rhIFN-β1a variants were separated in 3% acetic acid, pH 2.5, in commercial capillaries coated with cross-linked PEI. Under these conditions, the EOF is directed towards the MS, whereas the μ_{eff} of all protein variants was towards the capillary inlet. In total, 138 different proteoforms were distinguished, including non- and single deamidated variants, positional isomers with the third glycan antenna either attached to the α(1,3) or α(1,6)-arm, variants with succinimide, oxidation or a loss of the N-terminal methionine. For the first time, a sulfated glycovariant of rhIFN-β1a was identified. The resolved positional isomers showed differences of 0.9–2.5% in their r_H and were confirmed by an additional digest with sialidase and galactosidase. The N-terminal loss of methionine was revealed by a top-down approach with CE-MS^2 applying electron-transfer dissociation (ETD) and higher energy collisional dissociation (HCD) fragmentation. Moreover, for some PTMs relations in their occurrence were revealed, e.g., between methionine loss and deamidation as well as a negative correlation between the glycan size and the extent of deamidation [337].

3.12.1.1. rhGH. CZE-ESI-TOF-MS analysis of a CRS of rhGH was done in SMIL coated capillaries using a PB-PVS bilayer. BGE was 75 mmol/L ammonium formate (pH 8.5). Mass spectra showed two charge state distributions (CSDs) indicating the presence of two folding states. After thermal stressing of rhGH at 40 °C for 1d with subsequent storage for 1 year at − 18 °C, various PTMs, including oxidation, deamidation and the formation of sulfonic acid groups were detected. The latter occurred due to a cleavage of disulfide bonds [336].

Taichrib et al. [338] identified a non-deamidated species and two deamidation variants when analyzing stressed rhGH with CZE-ESI-TOF-MS in bfs capillaries with an alkaline BGE. For this protein size, a benchtop TOF instrument with 2 m flight path allowed for isotopic resolution at a mass resolution of 30,000 (full width at half maximum (FWHM)). The identity of deamidated rhGH variants was

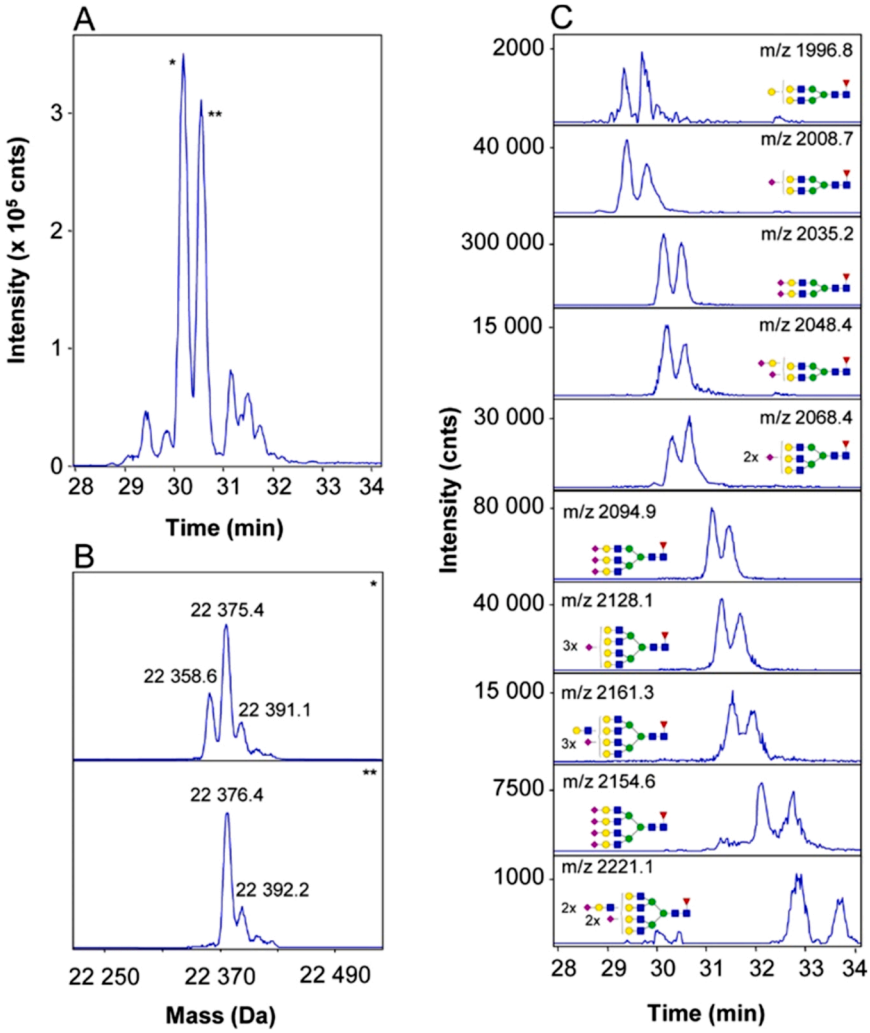

Fig. 8. (A) Base peak electropherogram obtained during sheathless CE–MS of rhIFN-β (45 μg/mL) employing a neutrally coated capillary. (B) Deconvoluted mass spectra obtained in the apexes of the peaks migrating at 30.1 min (*) and 30.5 min (**). (C) Extracted ion current electropherogram for 10 selected rhIFN-β glycoforms including their deamidated products at the indicated *m/z* value (± 0.3 Da; 11 + charge state); assigned glycan structures are shown as insets. Symbols: green circle/yellow circle, hexose (mannose/galactose); red triangle, fucose; blue square, *N*-acetylhexosamine; purple diamond, sialic acid. Conditions: BGE, 50 mM acetic acid (pH 3.0); CE voltage, 15 kV; tip-to-end plate distance, 1.0 mm. Copyright 2013 American Chemical Society.
Reprinted with permission from [320].

confirmed both by the isotopic pattern of individual peaks, which showed progressive mass shifts of 1 Da, and by the migration order observed in CZE [338].

3.12.1.2. rhGH-chelator conjugates for cancer therapy. Specific targeting of tumor cells is a hallmark in cancer diagnostic and therapy. This can be realized by addressing receptor molecules expressed either solely or at least to a major extent on the surface of cancer cells. Molecules binding to these receptors may either carry a label or can be modified to transport therapeutics selectively targeting cancer cells. In the current case, a bioconjugate composed of rhGH and a bifunctional chelator was synthesized and characterized by CZE-ESI-MS. The hexadentate chelator (specified as *p*-SCN-Bn-NOTA) forms a stable complex with Gallium(III) that is applied in radio-imaging, but also in cancer therapy. rhGH offers 9 potential binding sites, i.e., ε-amino groups of lysine, for the NOTA-chelator. Thus, the final reaction product with NOTA may contain various positional isomers and require characterization, since the occupational position influences the receptor binding. Besides RP-HPLC-ESI-MS with a C_4 column, CZE-ESI-MS was required for a comprehensive characterization. CZE separation was done in 75 mmol/L NH_4OH (pH 8.5) applying a SMIL capillary with a PB-PVS bilayer and a SL interface. Results were complemented by a bottom-up approach with trypsin or chymotrypsin and HPLC-ESI-MS^2 measurements revealing defined lysine residues as modification hotspots [339].

3.12.2. EPO

CZE-ESI-μTOF-MS with a SL interface was applied in the characterization and comparison of a BRP from Ph. Eur. and a commercial product of rhEPO [340] as well as for commercial pharmaceuticals of epoetin-α (Eprex®) and epoetin-β (NeoRecormon®) [172]. The separation capillary was coated with PB. 1 mol/L acetic acid with 20% methanol at pH 2.4 provided best resolution of the glycovariants. The observed differences in μ_{eff} were primarily related to diverse numbers in sialic acid residues. Different numbers of HexHexNAc blocks exerted only a minor influence on $\Delta\mu_{eff}$ and were addressed in extracted ion electropherograms (EIEs) via minute differences in their respective t_m, but could not be resolved electrophoretically due to their partial overlapping. HexHexNAc related shifts in μ_{eff} are not due to charge differences, but presumably caused by changes in r_H. In fact, the extent of the shift of μ_{eff} caused by four HexHexNAc units corresponded to that induced by one sialic acid. The influence different numbers of HexHexNAc blocks exerted on μ_{eff} seemed to be abandoned in the presence of urea, since previous separations missed this effect [172,340]. A further microheterogeneity was contributed by presumed O-acetylated subvariants. In total, 135 different glycoforms were distinguished in CZE-ESI-MS. A comparison of BRP from Ph. Eur. and the commercial rhEPO revealed differences in the HexHexNAc numbers, the acetylation and the oxidation profile [340]. For the comparison of Eprex® and NeoRecormon®, the epoetin-α product showed a considerably higher complexity in deconvoluted mass spectra. This is related to a higher number of acetylations [172]. Acetylation is known to increase the life-time of glycoproteins by enhancing their resistance against sialidases [341,342]. Both products differed in the sialic acid profile, with epoetin-β containing two additional variants with a lower sialic acid content [172]. Deamidations, reduction of disulfide bonds as well as different glycan linkages and isoform branching could not be addressed with the applied setting since mass resolution was not sufficient [340]. Depending on the protein size, the application of TOF mass spectrometers with higher flight paths can increase the mass resolution and thus allow for isotopic resolution. For the EPO BRP (from Ph. Eur.) with a molecular weight of 30 kDa an increased mass resolution of 40,000 (FWHM) was required for isotopic resolution. This was provided by a TOF instrument with a flight path of 5 m. The comparison of the experimentally determined and theoretical assumed isotopic pattern for deamidation showed a discrepancy. Thus, the observed isotope pattern revealed a more complex situation than initially assumed. In fact, the observed pattern was the result of two overlapping distributions caused by two co-migrating species. This excluded the presence of a deamidated variant, since an EPO species lacking deamidation and its single deamidated congener should differ in μ_{eff}. Instead, a co-migration of intact EPO and a reduced variant (with one of the two disulfide bonds cleaved) was proposed as an explanation model. However, for a confirmation of the concomitance of two different species, an electrophoretic separation would be required. The work demonstrated the refined information that can be derived by combining excellent electrophoretic separation with increased mass resolution and thus the outstanding potential of CE-ESI-MS [338].

Haselberg et al. [320] separated rhEPO variants in 2.0 mol/L acetic acid (pH 2.1) applying sheathless CZE-ESI-MS with a porous CESI sprayer. 74 glycoforms differing in the number of sialic acid and HexHexNAc residues were identified. Moreover, oxidized and acetylated variants were addressed. Individual glycoform concentrations between 0.35 nmol/L and 630 nmol/L were calculated. Differences in μ_{eff} were influenced by the number of sialic acids (~2 min per unit) and to a smaller extent by HexHexNAc (~0.5 min per unit) [320], as addressed elsewhere before [340].

3.12.3. Fibroblast growth factor 21-Fc fusion protein

Fibroblast growth factor 21-Fc fusion protein (Fc-FGF21) was analyzed by immunoaffinity off-line coupled to CE-MS for testing the stability and pharmacokinetics of the fusion protein in a mouse model [32]. FGF21 is a 19 kDa hormone that modulates glucose and lipid metabolism, thus representing a promising target for pharmaceuticals directed against type 2 diabetes and metabolic syndrome [32,343,344]. FGF21 was combined with the human Fc-fragment, leading to a fusion protein of 92 kDa. Beside the WT, i.e., Fc-FGF21 WT, an engineered mutant (Fc-FGF21 RG) was subjected to a pharmacokinetic study. The mutant carried two mutations compared to the WT. Both, WT and mutant were expressed in a bacterial host, extracted from inclusion bodies and then in parallel applied intravenously to two groups of mice. Extraction from murine serum was by immunoaffinity capture using biotinylated Neutravidin magnetic beads. After elution at pH 2.9, samples were directly analyzed with CZE-ESI-TOF-MS using LPA coated capillaries and an EMASS-II interface. Whereas FGF21 had a half-life < 2 h, both Fc-FGF21 fusion proteins showed a higher life-time, respectively. Based on CE-MS data, five truncated variants were identified in the mouse model for Fc-FGF21 WT within 96 h. The mutations in the Fc-FGF21 RG mutant apparently destroyed a proteolysis site of the WT, but created a novel one. This resulted in seven truncated variants, which differed from the WT. Data allowed for the construction of pharmacokinetic profiles [32].

3.12.4. Recombinant proteins of adeno-associated virus

Recombinant AAVs are frequently applied in gene therapy (trials) as transfer vehicles for single strand DNA encapsulated in a capsid of VPs. Individual AAV-serotypes differ in their feasibility to transfect defined target cells and organs [345]. The characterization of the AAV capsid including its PTMs is required to confirm the correct serotype and to guarantee quality and consistency of the virus particles [346]. Moreover, mutations in VPs may influence patient immune responses and the efficiency of transduction [347]. Zhang et al. [345] characterized the viral proteins 1–3 (VP1–3) of an rAAV-WT and a related mutant with three point mutations by means of a ZipChip CE ion source hyphenated to a Thermo Q Exactive HF mass spectrometer. Theoretical masses of the three VPs were between 59.9 and 81.8 kDa with their electrophoretic separation achieved in less than 4 min (Fig. 9). Mass errors for the VPs of the WT and the mutant were < 20 ppm and up to 60 ppm, respectively. Acetylation of VP1 and VP3 was revealed in either case. Both WT and mutant AAV could be distinguished by the different t_m of corresponding VPs, which proved the applicability of the method in revealing identity/heterogeneity of AAV and VPs in combination with fast throughput and minimal sample consumption (5 nL) [345].

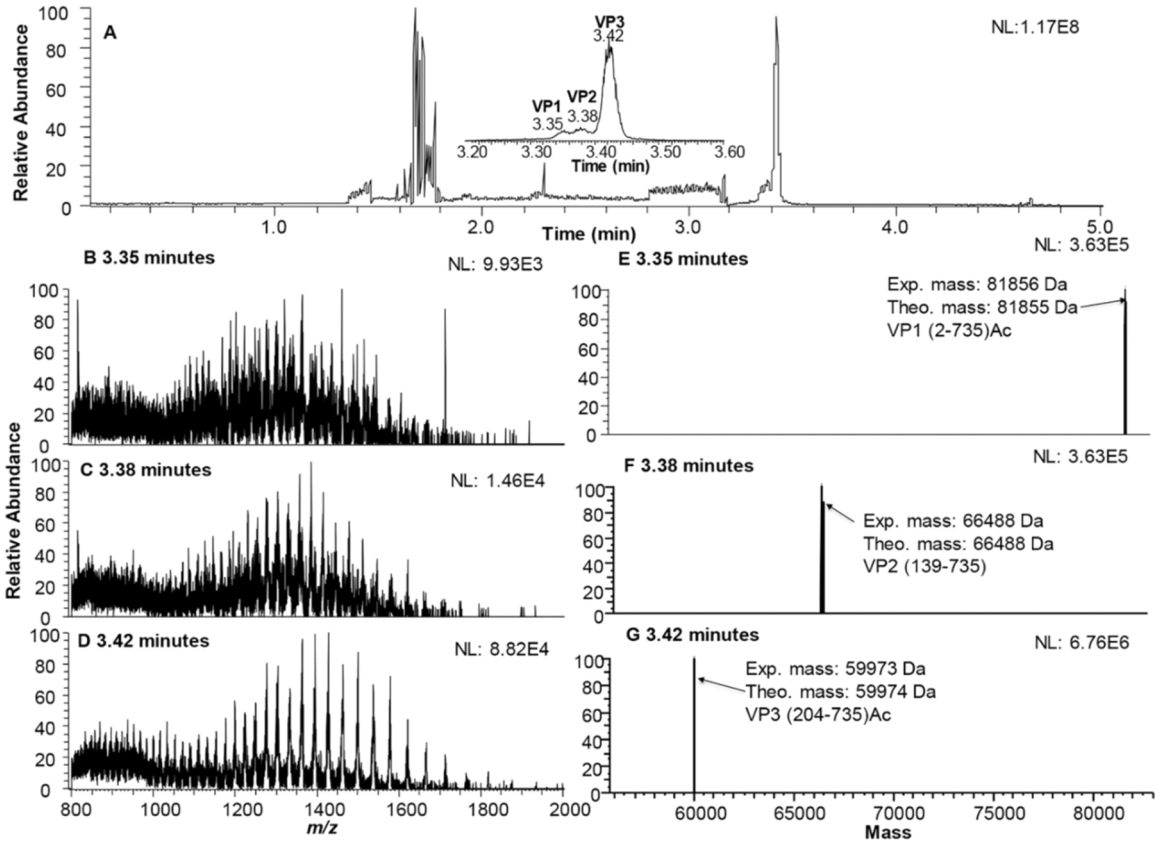

Fig. 9. (A) Total ion current electropherogram of AAV2 VPs with the migration time range from 0.1 min to 5.0 min; the migration time range from 3.20 min to 3.60 min is shown in the inset. Mass spectra of AAV2 VPs separated in (A): (B) peak at 3.35 min, (C) peak at 3.38 min, and (D) peak at 3.42 min. Deconvoluted mass spectra of AAV2 VPs separated in (A): (E) peak at 3.35 min, (F) peak at 3.38 min, and (G) peak at 3.42 min.
Reprinted from [345], with permission from Elsevier.

3.12.5. *Conformations of β2-M*

Native state and folding intermediate of recombinant WT-β2-M (see Sections 3.3.12 and 3.9.1) were characterized with different CZE-ESI-MS settings using a SL coaxial interface and a sheathless porous CESI sprayer, respectively. β2-M was dissolved either in water or 50% (v/v) ACN. ACN was applied to induce the folding intermediate of β2-M by partial denaturation. The applied BGE, i.e., 50 mmol/L ammonium bicarbonate (pH 7.4), provided native separation conditions. Both folding states (native, intermediate) were separated by CZE. With the SL sprayer, however, the CSDs for both conformations were identical showing up to 10 charges. This is due to the masking effect of propan-2-ol contained in the SL, which led to protein unfolding during the ESI process. In case, the length of the separation capillary was increased, higher charge states became more prominent. This was attributed to additional factors, like temperature, shear forces and interaction with the capillary surface. Without ACN, an additional deamidated variant was identified. With the porous sprayer, only two charge states (+6 and +7) were encountered. Their relative intensity differed between the two conformations [348]. As a future prospect, the separated conformations can be tested individually in the course of drug screening by ACE. This would provide species-resolved results under identical frame conditions, which improves the comparability of results.

3.12.6. *Allergens*

3.12.6.1. Nitrated allergen variants of Bet v 1a. Allergens can be nitrated by environmental pollutants, i.e., NO_2 and O_3, or by endogenous inflammation processes in allergic patients [349,350]. Compared to non-modified WTs, these modified allergens possess an increased allergenicity as shown for Bet 1a [351]. However, commercial standards for nitrated allergens are currently not available. These standards could be used as a specific diagnostic tool. Thus, recombinant Bet v 1a was in-house nitrated with peroxynitrite. The generated nitration variants were characterized by CZE-ESI-TOF-MS in bfs capillaries with 10 mmol/L ammonium bicarbonate (pH 7.50). Hyphenation was done by a commercial coaxial SL interface. The extent of nitration differed depending on the excess of the added nitration reagent. Besides the non-modified recombinant Bet v 1a species, between 9 and 12 nitration variants were separated in CZE and one- to six-fold nitrated species were identified with MS. Isobaric positional nitration isomers could not be distinguished by MS, but were resolved by CZE. This is due to slight differences in the pI, which are site specific, and possibly also by minute changes in the protein structure and thus r_H [352]. In an advanced approach, CE-hyphenation to a high-resolution mass spectrometer, i.e., LTQ-Orbitrap XL, was done by means of an in-lab designed SL interface. Nitrated recombinant Bet v 1a variants were identified using an integrated CE-MS strategy. For the first time, CE-ESI-MS data from intact proteins, bottom-up results after tryptic digest and top-down measurements were combined to a comprehensive approach for identification of PTM-variants. In top-down, in-source collision induced dissociation was combined with HCD. Since the same BGE could be applied to all CE-MS approaches, the rapid switch between the different strategies constitutes a major benefit. Defined hotspots for nitration were revealed by comparing quantification on intact and tryptic peptide level [353].

3.12.6.2. Temperature induced conformational changes of recombinant pollen allergen of mugwort – identification of the molecular mechanism. The pollen allergen of mugwort (*Artemisia vulgaris*) Art v 3 represents an important elicitor of allergies in the Mediterranean area [354]. In addition, patients develop allergic cross-reactivities to related proteins

contained in food, e.g., fruits and vegetables [355]. Treatment at increased temperatures induces conformational changes of the allergen. Depending on the prevailing pH, the thermal unfolding is either reversible (at pH 3.4) or irreversible (at pH 7.4). Some cross-reactive fruit allergens show a similar response [356]. Molecular fundamentals for explaining the irreversibility of this process are thus relevant to understand why thermally processed food (products) reduce or even abandon immune reactions of allergic patients against contained allergens. Recombinant Art v 3 was expressed in *E. coli* and heated to 90 °C at pH 3.4 and 7.4, respectively. Changes in the separation profiles were followed at defined time points over 120 min. CZE-UV was applied for profiling and quantitation of heat-induced Art v 3 variants, whereas CZE-ESI-TOF-MS with preceding in-capillary pre-concentration by transient capillary isotachophoresis identified allergen variants induced by thermal stress. First-order kinetics of temperature induced changes was revealed from CZE-UV data with the reaction constant 16-times faster at pH 7.4 [357]. Up to now, disulfide bond shuffling was postulated to explain conformational changes under the described conditions [356]. However, CZE-ESI-TOF-MS data revealed a cleavage of disulfide bonds with subsequent sulfur loss, formation of dehydroalanine and the final generation of thioether bonds, so-called lanthionines. Besides, trisulfide intermediates were revealed in the unfolding process. In addition, oxidated and deamidated variants as well as multiple combinations of all these modifications were addressed by CZE-ESI-TOF-MS. Deamidation contributed to conformational changes. Modifications were confirmed on the peptide level by HPLC-ESI-MS^2 after tryptic digest. In total, 25 variants of Art v 3 were identified by CZE-ESI-TOF-MS after thermal treatment. For the first time, thioether bond formation was elucidated as the molecular mechanism for heat-induced allergen "inactivation", this way destroying IgE-related epitopes [357]. Complementary methods confirmed the results on the protein-structure level as well as by immune reactions with patient sera [358].

3.13. Combination of different CE strategies in the characterization of recombinant proteins

3.13.1. rhCG

Camperi et al. [359] combined CGE-UV, CIEF-UV, CZE-UV and CZE-ESI-MS for characterizing intact rhCG drugs, i.e., Ovitrelle® and Pregnyl®. For CGE a commercial kit was used for analysis of rhCG that was partly reduced with β-mercaptoethanol. Besides different proteoforms of intact rhCG, also the β-subunit and two variants of the α-subunit were resolved. Moreover, signals > 80 kDa were attributed to rhCG aggregates. CIEF was done in hydroxypropyl cellulose coated capillaries under denaturing conditions in the presence of 6 mol/L urea. Focused zones were chemically mobilized with 350 mmol/L acetic acid. 15 isoforms of intact rhCG were resolved by CIEF with pI values between 3.49 and 4.78. In CZE-UV, a BGE composed of 800 mmol/L acetic acid, 800 mmol/L formic acid and 20% (v/v) MeOH (pH 2.2) allowed for the resolution of 8 variants. The optimized CZE-UV conditions were then applied in CZE-ESI-MS with a triple-quadrupole mass spectrometer with optimization of the SL. At least 12 rhCG variants were separated between 4.2 and 5.0 min. The comparison of an hCG drug extracted from urine with the rhCG drugs provided divergent profiles as revealed by the orthogonal CE-approaches. Mass spectra showed the presence of different CG isoforms for recombinant and urine-derived drugs. However, an identification of the isoforms was prevented by the restricted resolution of the applied mass spectrometer [359].

3.13.2. PEGylated rhG-CSF

rhG-CSF possesses five amines acting as possible PEGylation sites. rhG-CSF was modified either with 5 kDa or 20 kDa PEG. The resulting conjugates were analyzed with CZE-UV and CGE-UV after the respective mono-PEGylated variant was purified with SEC. CZE-UV profiles with 100 mmol/L phosphate buffer, pH 2.5, showed minor peaks for unmodified and di-PEGylated rhG-CSF in addition to the prominent single PEGylated species. The t_m increased with the PEGylation state, but also with the mass of the attached PEG due to the higher r_H. SDS-CGE was done by means of a commercial kit after sample heating to 100 °C in presence of 1% SDS. For a modification with the 20 kDa PEG, di-PEGylated rhG-CSF could only be detected within 40 min when the separation voltage was increased to 15.0 kV. Higher separation voltages were not applicable due to the pronounced Joule heating in the applied 100 μm i.d. capillary. Thus, for high-mass PEGylation the applied SDS-CGE method showed some limitations. Compared to SEC-UV, both CE methods provided better separations of the PEGylated species [360].

3.13.3. EPO

In an extension of a previous CZE-ESI-MS method [340] (see Section 3.12.2), different recombinant EPO products, i.e., BRP of Ph. Eur., epoetin-α (Eprex®) and epoetin-β (NeoRecorman®), were characterized with a refined CZE-ESI-TOF-MS method on intact protein and glycan level. For the analysis of intact EPO, capillaries were either shielded with PB or a commercial linear PAA coating (UltraTrol Dynamic Pre-Coat LN). Different BGEs were applied depending on the capillary coating. The linear PAA coating suppressed the EOF and resulted in a partial electrophoretic resolution of HexHexNAc variants (compare Section 3.12.2), contrary to the PB coating. In addition, glycans were released by digest with PNGase F and analyzed without derivatization. Most glycans were of tetra-antennary structure and carried four sialic acid residues. Furthermore, acetylation-, oxidation- and sulfation variants were separated on the glycan level and even deamidations could be addressed. Differences in the acetylation of glycans between the EPO products were revealed and related to different cell culture conditions. Since acetylation also governs the physicochemical and biological properties of recombinant proteins, its implementation in the product characterization is essential [361].

3.13.4. Fusion protein RC28-E

The fusion protein RC28-E (=eflimrufusp alfa) was expressed in CHO cells and combines receptor domains of the vascular endothelial growth factor (VEGFR1 and R2) and of a receptor for fibroblast growth factor (FGFR1) with a human IgG1-Fc domain. VEGF and FGF induce neovascularization, i.e., growth of blood vessels, and thus contribute to oncogenesis and angiogenesis-related diseases, such as age-related macula-degeneration. RC28-E acts as a dual trap for VEGF and FGF in combating neovascularization. The fusion protein was prepared in 50 mmol/L β-mercaptoethanol as well as in non-reductive buffer, both with 1% SDS, respectively, and was analyzed with SDS-CGE in uncoated capillaries with a commercial CGE-kit. In parallel, an iCIEF method with urea, CA pH 5–9 and 1% methylcellulose was applied. A purity > 99% was determined by CGE corresponding with SEC results. In iCIEF, 17 charge variants distributed over three peak clusters, which covered a pI range between 5.75 and 7.39, were resolved. Additional measurements with HPLC-MS^2 revealed C-terminal lysine variants and deamidations as reasons for charge variants [362].

3.14. Analysis of host cell proteins with CIEF-ESI-MS^2, CZE-ESI-MS^2 and RP-HPLC-CZE-ESI-MS^2

If HCPs escape the downstream processing of recombinant products, they might be co-purified in trace amounts with the target protein [363, 364]. The relevance of HCPs has been addressed previously (see Sections 2.2.2 and 2.7.2). This includes advantageous aspects as outlined for HCPs acting as autocrine growth factors [99], but mostly detrimental effects if HCPs affect the stability and potency of the recombinant product over time (as shown for proteases and peptidases) [57] or influence the product profile enzymatically, which would impair batch consistencies if not under control [97,98]. In the latter cases, HCPs impose clinical risks affecting the product quality and safety [363–365]. HCP-related hazards comprise immunogenicity and adjuvant-like effects [366]. In case of an unintended co-administration of HCPs, immune

responses resulting in influenza-like symptoms or - in the worst case - anaphylaxis may develop [367]. HCPs are traditionally addressed by ELISA, SDS-PAGE or 2DE with band excision and subsequent MS analysis. These methods either miss recognition of weak or non-immunogenic constituents, lack a distinction/identification of individual HCPs (ELISA) and quantitative information (SDS-PAGE) or are laborious, semi-quantitative and require manual handling steps (2DE) [364–367]. CE constitutes a promising alternative, which overcomes these limitations. Thus, CE cannot only be applied in the characterization and quantification of the recombinant target protein, but may also address unintentionally contained impurities. In comparison to RP-HPLC, CE offers accelerated analyses and carry-over effects are of less concern [365]. In order to address trace amounts of HCPs, the inherently limited injection volume of CE was remedied by in-capillary concentration techniques, such as field amplified sample stacking [363] or pH junction injection [365], which allow for the application of higher sample volumes without compromising the separation efficiency.

The group of Dovichi applied a bottom-up approach with CZE-ESI-MS^2 in the analysis of HCPs. Thereby, a sheathflow nanospray interface with electrokinetically driven SL (corresponding to the EMASS interface) was employed in hyphenating the CE system to an LTQ Orbitrap Velos instrument. All separations were done in LPA coated capillaries [363,365,366] either with 5% [365] or 1 mol/L acetic acid [366] or 0.1% formic acid [363,365]. The latter was used for pH junction pre-concentration with the sample prepared in 10 mmol/L NH_4HCO_3, pH 8.5. Besides *E. coli* lysates, a recombinant product that was spiked with 12 model proteins was analyzed. Proteins in either sample were denatured, reduced and alkylated prior to their tryptic digest. CZE-ESI-MS^2 results were compared to an UPLC-ESI-MS^2 approach using a C_{18} column. The separation windows were comparable for both strategies. However, CZE-ESI-MS^2 provided approximately five times higher intensities for base peak signals with smaller peak widths and identified thus more peptides than UPLC-ESI-MS^2 [365].

The same research group applied field amplified sample stacking to increase the injection volume. This required desalting of the samples after the tryptic digest of HCPs. The tested product was depleted from the recombinant protein prior to the digest. CZE separation was done in 0.1% formic acid. For a quantitation study, three HCPs from CHO cells were selected. Three tryptic peptides, which were specific for the individual HCP, respectively, were synthesized and isotopically labeled with ^{13}C and ^{15}N. These peptides were spiked to the digested samples. A 4-point calibration was done by plotting the peak area ratio of native and isotopically labeled peptide cognates against the peptide amount, respectively. Absolute amounts of the selected HCPs quantified in the recombinant product were between 6 and 25 pmol corresponding to 7–30 ppt [363]. Moreover, CZE-ESI-MS^2 and UPLC-ESI-MS^2 were compared for their respective capability in identifying HCPs in recombinant products produced in a CHO-K1 cell line after depletion of the therapeutic protein. Whereas the CZE-ESI-MS^2 approach addressed 220 protein groups and 976 peptides, only 34 protein groups and 53 peptides were revealed by UPLC-ESI-MS^2 when 50 ng of the depleted HCP digest was injected, respectively. With a 20-fold increase in the injected HCP mass, protein and peptide numbers identified with UPLC-ESI-MS^2 corresponded with CZE-ESI-MS^2 at 50 ng. Without a depletion of the therapeutic protein, the number of protein groups and peptides identified by CZE-ESI-MS^2 dropped to 185 and 709, respectively. Finally, an online cation exchange-CZE-ESI-MS^2 approach was tested for samples without preceding protein depletion. Thereby, a cation exchange hybrid monolith capillary was coupled to the actual CE separation capillary by means of a PEEK union. After sample loading and concentration, HCPs were eluted from the cation exchange capillary by stepwise pH increments from pH 3 to pH 8. After its elution, each fraction was separated by CZE before the next fraction was detached in a subsequent step. Under these conditions, 230 protein groups and 796 peptides were addressed [366].

Recently, Kumar et al. [367] applied a manual offline fractionation of 100 μg tryptic HCP digest with RP-HPLC followed by subsequent pooling to 16 fractions. The workflow was described in detail and referred to depleted supernatant of CHO cell cultures. Individual fractions were then analyzed by CZE-ESI-MS^2 using a porous CESI sprayer in order to reduce dilution effects. The tryptic digest was dissolved in 50 mmol/L ammonium acetate (pH 4) and separated in 10% acetic acid [367]. Their setting resembles an in-capillary pre-concentration strategy published previously by our group for intact proteins [147] based on a principle of Foret et al. [368]. Compared to individual RP-HPLC-MS^2 and CZE-ESI-MS^2 approaches, the offline hyphenation of RP-HPLC with CZE-ESI-MS^2 provided two- to three-fold higher numbers of identified HCPs, respectively. 225 HCPs were unique for the RP-HPLC-CZE-ESI-MS^2 strategy. This is related to the combination of two truly orthogonal separation methods, which improved the resolution prior to MS detection. Within the identified HCPs, peptidases constituted a major fraction. Besides, HCPs with N-acetylgalactosaminyltranferase and deglycase activity and disulfide isomerase enzymes were identified [367].

In addition, tryptic HCP digests were also separated by CIEF-ESI-MS^2. After depletion of the recombinant protein, HCPs were digested with trypsin immobilized on beads. CIEF focusing used wide pH range CAs (pH 3–10) in commercial LPA coated capillaries applying formic acid as anolyte and NH_4OH as catholyte. After the focusing step, the capillary outlet was inserted in an ESI interface. The applied SL, i.e., 0.05% formic acid/50% methanol in water, provided electrical contact, assisted the ESI process and initiated the chemical mobilization of focused peptide zones towards the mass spectrometer. Besides the analysis of three digested model proteins in the course of the method optimization, the final method was applied to a recombinant product. 53 peptides were distinguished, which led to the identification of 37 HCPs [364].

3.15. Validation of CE methods applied in the characterization of recombinant proteins

Validation of CE-based methods is mandatory in case they are intended for a characterization of recombinant proteins in industry. Method validation is primarily done according to the ICH-guideline Q2 (R1) [26]. This guideline refers to four major types of analytical procedures, including identification tests, quantification tests for impurities, limit tests for controlling impurities, and tests for quantifying the active moiety in drug samples or drug products. Key parameters in validation are specified, and recommendations for their analytical determination and calculation are provided. Recommended validation parameters comprise “accuracy”, precision (repeatability, intermediate precision), specificity, LOD and LOQ, linearity and range, complemented by robustness [26]. In this context, some essential aspects, which lead to frequent misconceptions, have to be outlined:

(1) The term “accuracy” as used in the ICH-guideline Q2(R1) is metrologically misleading. Metrologically, “trueness of measurement” is actually meant. According to the *International Vocabulary of Metrology (VIM),* trueness refers to the “…*closeness of agreement between the average of an infinite number of replicate measured quantity values and a reference quantity value*” [369]. Vitally important, the terms accuracy and trueness are not interchangeable [369] as this might be misunderstood from the ICH-guideline Q2(R1) [26] by the unexperienced reader. In addition, the trueness of a measurement is no quantitative parameter, but can be expressed quantitatively by means of the measurement bias, which is the (total) systematic measurement error [369].
(2) The second even more frequent misunderstanding refers to the precision of measurements, where the terms repeatability and reproducibility are erroneously mixed. In most cases, authors talk about "reproducibility" when stated measurement conditions prove in fact repeatability (conditions), since measurements were

done in the same lab, by the same operator, running the same measurement procedure on the same measurement system [369]. Thus, in this review the term "reproducibility" has been corrected whenever this was appropriate based on the information provided in the experimental section of the respective papers.

(3) The third misinterpretation is related to the coefficient of determination r^2 as a proof of linearity in calibration studies done in the majority of the validation reports. As outlined in several papers, this assumption constitutes a misconception [370,371]: r^2 addresses merely the correlation between an independent predictor (e.g., the analyte concentration) and one dependent variable (in terms of univariate regression, e.g., the detector signal for an analyte) or several dependent variables in multiple regression [372]. Even r^2 values close to 1.00, e.g., 0.995, are no ultimate proof for linearity since a different regression model, e.g., a quadratic regression, might provide a statistically significant improvement of r^2. Instead of r^2, graphical evaluations via residual plots [373] or statistical approaches, including the Mandel fitting test (see Section 3.7.2) [374] and the lack-of-fit test [373], can be consulted to evaluate the linearity of an applied regression model.

(4) Another relevant aspect refers to the general assumption that a calibration concentration misses an uncertainty and is thus considered a single value. Although commonly applied, one has to be aware that this does not truly reflect the analytical situation. Due to the preparation of calibration standards (weighing, volume adjustment, dilution, etc.) each calibration concentration possesses a combined standard uncertainty. Future approaches might consider this aspect and therefore replace or complement the currently used ordinal least square approach in regression by a more advanced strategy, e.g., orthogonal or Deming regression [375].

The majority of the CE methods addressed in this review included also a validation part. A detailed discussion of all the individual strategies and parameters would go beyond the scope of this review. Instead, relevant validation parameters of the individual methods have been compiled in Table 3 in a distinct column.

3.16. Suitability testing

System suitability tests target to check the performance of an analytical system regularly, e.g., daily or before testing novel batches. As appropriate test parameters, precision of t_m, lower LOQ and the chromatographic/electrophoretic separation have been proposed. Relevant parameters and related acceptance criteria are usually regarded already during the method validation. A precision $\leq$ 5% (for five replicates) may for instance be considered adequate [376].

Several CE methods for recombinant proteins included also related suitability tests. For rhIL-11, five injections of a BRS-rhIL-11 reference solution were done and the RSD for t_m, peak area, peak symmetry and peak width was evaluated and had to stay below 2%, respectively [165]. For rhPTH 1–34, suitability testing was done with a recombinant WHO reference product of the hormone. Repeatability was determined by five replicate injections using the optimized CZE-UV method. In case the RSD of t_m, peak area, peak symmetry and peak width was $<$ 2%, respectively, suitability of the system for the analysis was assumed [168]. For rhG-CSF, a related reference substance from the National Institute for Biological Standard and Control (NIBSC) was injected five times, and t_m, peak area and peak symmetry had to stay below 2% RSD [202]. Other authors used a multistep suitability testing in the analysis of recombinant adenovirus vaccines. First, the BGE and the performance of the capillary were evaluated by application of a defined voltage on the capillary filled with BGE, checking whether the related current stayed within defined limits. In a second step, blank injections tested for contaminations of the system. Finally, control samples were injected six times in order to evaluate whether the repeatability and the total error of the peak area of the analyte were $\leq$ 5% and $\leq$ 15%, respectively. Only in case all specifications of the suitability test were met, the measurement of samples was initiated. Finally, a calibrant, which acted as a control sample, was injected after every five samples and at the end of a sample sequence to check for the analyte concentration in this reference sample. Results were indicative for adsorption/coating problems and deviations of $\pm$ 10% were considered acceptable. In addition, control charts covering $>$ 500 analytical runs representing $>$ 18,000 samples, were provided [220].

4. Conclusion

Entering the (bio)analytical stage as a newcomer endowed with laurels in advance, CE became dropped soon by the biopharmaceutical industry for its initial failure in meeting exuberant expectations. After basic research built the fundament for overcoming most of the initial obstacles in the analysis of proteins, CE has regained terrain and reconquered its position as a highly versatile tool in the portfolio of bioanalytical techniques. The aspect that one CE instrument provides manifold separation modes is a major reason for resuming the track record. Due to its high separation efficiency, CE is capable to resolve closely related protein variants/proteoforms by minute differences in their charge, pI and/or size, including also folding variants, not accessible by other separation techniques. This is complemented by economic operation features, i.e., low consumption of sample and separation media, the option for full automation and short analysis times, which guarantee high throughput. The major restraint in the analysis of intact proteins by CE refers to their interaction with the surface of the separation capillary. Different strategies to combat this drawback have been developed and can be adjusted and allied to address analyte and sample specific challenges. Low injection volumes together with a small optical path length inherently result in an impaired concentration-related LOQ. This restriction has been remedied by in-capillary pre-concentration techniques and detection devices, such as LIF or advanced MS interfaces (CESI, EMASS and ZipChip sprayer), which offer an improved sensitivity. Established CE separation techniques, such CZE, CIEF and CGE, are successfully applied in the characterization of recombinant proteins and have been complemented by sophisticated approaches, e.g., ACE, μChipCE and iCIEF. Innovative CE techniques with in-capillary enzymatic reactions and Western blot were successfully applied in the screening of candidate drugs and therapeutic inhibitors. Moreover, CE-ESI-MS combines high separation efficiency with accurate mass determination allowing to distinguish recombinant protein variants of equivalent μ_{eff} by their mass differences and vice versa. This enables to reveal the microheterogeneity of recombinant proteins by numerous identified glycosylation variants. CE is not considered a game changer, tackling all analytical questions in the physicochemical characterization of recombinant proteins single-handedly, but constitutes a highly potent tool complementing the current analytical portfolio by providing both unique and orthogonal information. Besides a characterization of the recombinant drug substance, final product formulations were evaluated including batch consistency within and between manufacturers. This is indispensable for the quality control of commercial products and requires validated approaches according to related guidelines as shown for the majority of the CE methods discussed in this review. Objectives of CE analyses comprise the confirmation of the identity of the recombinant target protein, purity determination, identification and (ideally) quantification of individual subspecies, including isoforms, PTM- and truncation variants and degradation products, as well as stability testing. However, CE applications in biotechnology are not confined to the final product, but progressively prove their aptitude as a decisive tool for selecting appropriate host-cells as well as in the optimization of upstream and downstream processes, including cultivation conditions, upscaling, purification and polishing steps. This knowledge can later be exploited in the established manufacturing process for premature

prediction of product quality in early production stages thus allowing for intervention in best time in order to meet predefined product specifications. This includes also the analysis of process-related impurities, such as HCPs, where CE-based methods earned their merits as well.

CRediT authorship contribution statement

Hanno Stutz: Conceptualization, Writing – original draft, Writing – review & editing.

Declaration of Competing Interest

The author declares that he has no known competing financial interests or personal relationships that could have appeared to influence the work reported in this paper.

Data Availability

No data was used for the research described in the article.

Acknowledgement

Assoc. Prof. Dr. Peter Lackner from the University of Salzburg is gratefully acknowledged for providing the protein model used in Fig. 1 and in the Graphical Abstract.

References

[1] I.S. Johnson, Human insulin from recombinant DNA technology, Science 219 (4585) (1983) 632–637.
[2] G. Walsh, Biopharmaceutical benchmarks 2018, Nat. Biotechnol. 36 (12) (2018) 1136–1145.
[3] L. Bryan, M. Clynes, P. Meleady, The emerging role of cellular post-translational modifications in modulating growth and productivity of recombinant Chinese hamster ovary cells, Biotechnol. Adv. 49 (2021), 107757.
[4] R. O'Flaherty, A. Bergin, E. Flampouri, L.M. Mota, I. Obaidi, A. Quigley, Y. Xie, M. Butler, Mammalian cell culture for production of recombinant proteins: A review of the critical steps in their biomanufacturing, Biotechnol. Adv. 43 (2020), 107552.
[5] T.K. Ha, D. Kim, C.L. Kim, L.M. Grav, G.M. Lee, Factors affecting the quality of therapeutic proteins in recombinant Chinese hamster ovary cell culture, Biotechnol. Adv. 54 (2022), 107831.
[6] F.R. Schmidt, Optimization and scale up of industrial fermentation processes, Appl. Microbiol. Biotechnol. 68 (4) (2005) 425–435.
[7] C. Li, X. Teng, H. Peng, X. Yi, Y. Zhuang, S. Zhang, J. Xia, Novel scale-up strategy based on three-dimensional shear space for animal cell culture, Chem. Eng. Sci. 212 (2020), 115329.
[8] A.A. Shukla, L.S. Wolfe, S.S. Mostafa, C. Norman, Evolving trends in mAb production processes, Bioeng. Transl. Med. 2 (1) (2017) 58–69.
[9] Y.-H. Kao, D.P. Hewitt, M. Trexler-Schmidt, M.W. Laird, Mechanism of antibody reduction in cell culture production processes, Biotechnol. Bioeng. 107 (4) (2010) 622–632.
[10] ICH, ICH-guideline Q6B: Specifications: test procedures and acceptance criteria for biotechnological/biological products, ICH Steer. Comm. (1999) 1–16.
[11] ICH, ICH guideline Q11: Development and manufacture of drug substances (chemical entities and biotechnological/biological entities), ICH Steer. Comm. (2012) 1–26.
[12] ICH, ICH Guideline Q5E: Comparability of biotechnological/biological products subject to changes in their manufacturing process, ICH Steer. Comm. (2004) 1–12.
[13] M. Khraishi, D. Stead, M. Lukas, F. Scotte, H. Schmid, Biosimilars: a multidisciplinary perspective, Clin. Ther. 38 (5) (2016) 1238–1249.
[14] R. Ratih, M. Asmari, A.M. Abdel-Megied, F. Elbarbry, S. El Deeb, Biosimilars: review of regulatory, manufacturing, analytical aspects and beyond, Microchem. J. 165 (2021), 106143.
[15] A.S. Rathore, Follow-on protein products: scientific issues, developments and challenges, Trends Biotechnol. 27 (12) (2009) 698–705.
[16] A.M. Alsamil, T.J. Giezen, T.C. Egberts, H.G. Leufkens, A.G. Vulto, M.R. van der Plas, H. Gardarsdottir, Reporting of quality attributes in scientific publications presenting biosimilarity assessments of (intended) biosimilars: a systematic literature review, Eur. J. Pharm. Sci. 154 (2020), 105501.
[17] S.A. Berkowitz, J.R. Engen, J.R. Mazzeo, G.B. Jones, Analytical tools for characterizing biopharmaceuticals and the implications for biosimilars, Nat. Rev. Drug Discov. 11 (7) (2012) 527–540.
[18] N.M. Ritter, 3.40 - Characterization of biotechnological/biological/biosimilar products, in: M. Moo-Young (Ed.), Comprehensive Biotechnology, Second edition.,, Academic Press, Burlington, 2011, pp. 459–466.
[19] C.M. Ouimet, C.I. D'amico, R.T. Kennedy, Advances in capillary electrophoresis and the implications for drug discovery, Expert Opin. Drug Discov. 12 (2) (2017) 213–224.
[20] P.G. Righetti, R. Sebastiano, A. Citterio, Capillary electrophoresis and isoelectric focusing in peptide and protein analysis, Proteomics 13 (2) (2013) 325–340.
[21] S. Štěpánová, V. Kašička, Recent applications of capillary electromigration methods to separation and analysis of proteins, Anal. Chim. Acta 933 (2016) 23–42.
[22] M. Dawod, N.E. Arvin, R.T. Kennedy, Recent advances in protein analysis by capillary and microchip electrophoresis, Analyst 142 (11) (2017) 1847–1866.
[23] S. Štěpánová, V. Kašička, Applications of capillary electromigration methods for separation and analysis of proteins (2017–mid 2021) – A review, Anal. Chim. Acta 1209 (2022), 339447.
[24] ICH, ICH Guideline Q4B Annex 11: Evaluation and recommendation of pharmacopoeial texts for use in the ICH regions on capillary electrophoresis general chapter, ICH Steer. Comm. (2010) 1–2.
[25] <1053>Biotechnology-Derived Articles - Capillary Electrophoresis, in: U.S. Pharmacopeia (Ed.) August 2020, pp. 1–8.
[26] ICH, ICH Guideline Q2(R1): Validation of analytical procedures: text and methodology, ICH Steer. Comm. (2005) 1–13.
[27] P. Buckel, Recombinant proteins for therapy, Trends Pharmacol. Sci. 17 (12) (1996) 450–456.
[28] J.K.C. Ma, P.M.W. Drake, P. Christou, The production of recombinant pharmaceutical proteins in plants, Nat. Rev. Genet. 4 (10) (2003) 794–805.
[29] P. Rudge, Z. Jaunmuktane, P. Adlard, N. Bjurstrom, D. Caine, J. Lowe, P. Norsworthy, H. Hummerich, R. Druyeh, J.D.F. Wadsworth, S. Brandner, H. Hyare, S. Mead, J. Collinge, Iatrogenic CJD due to pituitary-derived growth hormone with genetically determined incubation times of up to 40 years, Brain 138 (11) (2015) 3386–3399.
[30] X. Yang, M.G. Bartlett, Glycan analysis for protein therapeutics, J. Chromatogr. B 1120 (2019) 29–40.
[31] G. Wu, C. Yu, W. Wang, R. Zhang, M. Li, L. Wang, A platform method for charge heterogeneity characterization of fusion proteins by icIEF, Anal. Biochem. 638 (2022), 114505.
[32] M. Han, J.T. Pearson, Y. Wang, D. Winters, M. Soto, D.A. Rock, B.M. Rock, Immunoaffinity capture coupled with capillary electrophoresis - mass spectrometry to study therapeutic protein stability in vivo, Anal. Biochem. 539 (2017) 118–126.
[33] J.M. Harris, R.B. Chess, Effect of pegylation on pharmaceuticals, Nat. Rev. Drug Discov. 2 (3) (2003) 214–221.
[34] T.A. de Oliveira, Wd Silva, N. da Rocha Torres, J.V. Badaró de Moraes, R.L. Senra, T.A. de Oliveira Mendes, A.S. Júnior, G.C. Bressan, J.L.R. Fietto, Application of the LEXSY Leishmania tarentolae system as a recombinant protein expression platform: A review, Process Biochem. 87 (2019) 164–173.
[35] J.R. Brady, J.C. Love, Alternative hosts as the missing link for equitable therapeutic protein production, Nat. Biotechnol. 39 (4) (2021) 404–407.
[36] J. Staudacher, C. Rebnegger, T. Dohnal, N. Landes, D. Mattanovich, B. Gasser, Going beyond the limit: Increasing global translation activity leads to increased productivity of recombinant secreted proteins in *Pichia pastoris*, Metab. Eng. 70 (2022) 181–195.
[37] B. Tolner, L. Smith, R.H.J. Begent, K.A. Chester, Production of recombinant protein in *Pichia pastoris* by fermentation, Nat. Protoc. 1 (2) (2006) 1006–1021.
[38] P.J. Punt, N. van Biezen, A. Conesa, A. Albers, J. Mangnus, C. van den Hondel, Filamentous fungi as cell factories for heterologous protein production, Trends Biotechnol. 20 (5) (2002) 200–206.
[39] O.P. Ward, Production of recombinant proteins by filamentous fungi, Biotechnol. Adv. 30 (5) (2012) 1119–1139.
[40] S. Hellwig, J. Drossard, R.M. Twyman, R. Fischer, Plant cell cultures for the production of recombinant proteins, Nat. Biotechnol. 22 (11) (2004) 1415–1422.
[41] E.A. McKenzie, W.M. Abbott, Expression of recombinant proteins in insect and mammalian cells, Methods 147 (2018) 40–49.
[42] M.C.M. Mellado, C. Franco, A. Coelho, P.M. Alves, A.L. Simplício, Sodium dodecyl sulfate-capillary gel electrophoresis analysis of rotavirus-like particles, J. Chromatogr. A 1192 (1) (2008) 166–172.
[43] C. Geisler, D.L. Jarvis, Adventitious viruses in insect cell lines used for recombinant protein expression, Protein Expr. Purif. 144 (2018) 25–32.
[44] M. Zang, H. Trautmann, C. Gandor, F. Messi, F. Asselbergs, C. Leist, A. Fiechter, J. Reiser, Production of recombinant proteins in chinese hamster ovary cells using a protein-free cell culture medium, Nat. Biotechnol. 13 (4) (1995) 389–392.
[45] B. Tihanyi, L. Nyitray, Recent advances in CHO cell line development for recombinant protein production, Drug Discov. Today.: Technol. 38 (2020) 25–34.
[46] F.M. Wurm, Production of recombinant protein therapeutics in cultivated mammalian cells, Nat. Biotechnol. 22 (11) (2004) 1393–1398.
[47] D. Ghaderi, M. Zhang, N. Hurtado-Ziola, A. Varki, Production platforms for biotherapeutic glycoproteins. Occurrence, impact, and challenges of non-human sialylation, Biotechnol. Genet. Eng. Rev. 28 (1) (2012) 147–176.
[48] T. Ouellette, S. Destrau, T. Ouellette, J. Zhu, J.M. Roach, J.D. Coffman, T. Hecht, J.E. Lynch, S.L. Giardina, Production and purification of refolded recombinant human IL-7 from inclusion bodies, Protein Expr. Purif. 30 (2) (2003) 156–166.
[49] S.M. West, A.D. Guise, J.B. Chaudhuri, A comparison of the denaturants urea and guanidine hydrochloride on protein refolding, Food Bioprod. Process. 75 (1) (1997) 50–56.
[50] I. Palmer, P.T. Wingfield, Preparation and extraction of insoluble (Inclusion-Body) Proteins from *Escherichia coli*, Curr. Protoc. Protein Sci. 38 (1) (2004) 6.3.1–6.3.18.

[51] Y.Y. Siew, W. Zhang, Downstream processing of recombinant human insulin and its analogues production from *E. coli* inclusion bodies, Bioresour. Bioprocess. 8 (1) (2021) 65.
[52] Z.S.-L. Heng, J.Y. Yeo, D.W.-S. Koh, S.K.-E. Gan, W.-L. Ling, Augmenting recombinant antibody production in HEK293E cells: optimizing transfection and culture parameters, Antib. Ther. 5 (1) (2022) 30–41.
[53] M.-E. Lalonde, Y. Durocher, Therapeutic glycoprotein production in mammalian cells, J. Biotechnol. 251 (2017) 128–140.
[54] O.W. Merten, Virus contaminations of cell cultures - a biotechnological view, Cytotechnology 39 (2) (2002) 91–116.
[55] J.P. Oza, H.R. Aerni, N.L. Pirman, K.W. Barber, C.M. ter Haar, S. Rogulina, M. B. Amrofell, F.J. Isaacs, J. Rinehart, M.C. Jewett, Robust production of recombinant phosphoproteins using cell-free protein synthesis, Nat. Commun. 6 (1) (2015) 8168.
[56] V.M. Cardoso, G. Campani, M.P. Santos, G.G. Silva, M.C. Pires, V.M. Gonçalves, R. de, C. Giordano, C.R. Sargo, A.C.L. Horta, T.C. Zangirolami, Cost analysis based on bioreactor cultivation conditions: Production of a soluble recombinant protein using *Escherichia coli* BL21(DE3), Biotechnol. Rep. 26 (2020), e00441.
[57] H. Dahodwala, K.H. Lee, The fickle CHO: a review of the causes, implications, and potential alleviation of the CHO cell line instability problem, Curr. Opin. Biotechnol. 60 (2019) 128–137.
[58] D. Ghaderi, R.E. Taylor, V. Padler-Karavani, S. Diaz, A. Varki, Implications of the presence of N-glycolylneuraminic acid in recombinant therapeutic glycoproteins, Nat. Biotechnol. 28 (8) (2010) 863–867.
[59] J. Dumont, D. Euwart, B. Mei, S. Estes, R. Kshirsagar, Human cell lines for biopharmaceutical manufacturing: history, status, and future perspectives, Crit. Rev. Biotechnol. 36 (6) (2016) 1110–1122.
[60] C. Doucet, I. Ernou, Y. Zhang, J.-R. Llense, L. Begot, X. Holy, J.-J. Lataillade, Platelet lysates promote mesenchymal stem cell expansion: A safety substitute for animal serum in cell-based therapy applications, J. Cell. Physiol. 205 (2) (2005) 228–236.
[61] M. Vanderlaan, J. Zhu-Shimoni, S. Lin, F. Gunawan, T. Waerner, K.E. Van Cott, Experience with host cell protein impurities in biopharmaceuticals, Biotechnol. Prog. 34 (4) (2018) 828–837.
[62] Z.X. Chong, S.K. Yeap, W.Y. Ho, Transfection types, methods and strategies: a technical review, PeerJ 9 (2021) e11165-e11165.
[63] T.K. Kim, J.H. Eberwine, Mammalian cell transfection: the present and the future, Anal. Bioanal. Chem. 397 (8) (2010) 3173–3178.
[64] M.F. Naso, B. Tomkowicz, W.L. Perry, W.R. Strohl, Adeno-associated virus (AAV) as a vector for gene therapy, BioDrugs 31 (4) (2017) 317–334.
[65] R. Fischer, J.F. Buyel, Molecular farming – the slope of enlightenment, Biotechnol. Adv. 40 (2020), 107519.
[66] A. Spök, R.M. Twyman, R. Fischer, J.K.C. Ma, P.A.C. Sparrow, Evolution of a regulatory framework for pharmaceuticals derived from genetically modified plants, Trends Biotechnol. 26 (9) (2008) 506–517.
[67] S.M. Noh, S. Shin, G.M. Lee, Comprehensive characterization of glutamine synthetase-mediated selection for the establishment of recombinant CHO cells producing monoclonal antibodies, Sci. Rep. 8 (1) (2018) 5361.
[68] M. Jordan, A. Schallhorn, F.M. Wurm, Transfecting mammalian cells: optimization of critical parameters affecting calcium-phosphate precipitate formation, Nucleic Acids Res. 24 (4) (1996) 596–601.
[69] T. Sun, W.C. Kwok, K.J. Chua, T.-M. Lo, J. Potter, W.S. Yew, J.D. Chesnut, I. Y. Hwang, M.W. Chang, Development of a proline-based selection system for reliable genetic engineering in chinese hamster ovary cells, ACS Synth. Biol. 9 (7) (2020) 1864–1872.
[70] A.A. Stepanenko, H.H. Heng, Transient and stable vector transfection: pitfalls, off-target effects, artifacts, Mutat. Res. /Rev. Mutat. Res. 773 (2017) 91–103.
[71] H. Tanaka, S.J. Tapscott, B.J. Trask, M.-C. Yao, Short inverted repeats initiate gene amplification through the formation of a large DNA palindrome in mammalian cells, Proc. Natl. Acad. Sci. 99 (13) (2002) 8772–8777.
[72] V. Mutskov, G. Felsenfeld, Silencing of transgene transcription precedes methylation of promoter DNA and histone H3 lysine 9, EMBO J. 23 (1) (2004) 138–149.
[73] O. Karnieli, O.M. Friedner, J.G. Allickson, N. Zhang, S. Jung, D. Fiorentini, E. Abraham, S.S. Eaker, T.K. Yong, A. Chan, S. Griffiths, A.K. Wehn, S. Oh, O. Karnieli, A consensus introduction to serum replacements and serum-free media for cellular therapies, Cytotherapy 19 (2) (2017) 155–169.
[74] K. Subbiahanadar Chelladurai, J.D. Selvan Christyraj, K. Rajagopalan, B. V. Yesudhason, S. Venkatachalam, M. Mohan, N. Chellathurai Vasantha, J.R. S. Selvan, Christyraj, Alternative to FBS in animal cell culture - An overview and future perspective, Heliyon 7 (8) (2021), e07686.
[75] Y. Vojgani, A. Shirazi, S. Zarei, O. Yeganeh, M. Jeddi-Tehrani, Comparison of efficacies of fetal bovine sera from different suppliers in cell culture experiments, Comp. Clin. Pathol. 27 (2) (2018) 519–527.
[76] X. Zheng, H. Baker, W.S. Hancock, F. Fawaz, M. McCaman, E. Pungor Jr., Proteomic analysis for the assessment of different lots of fetal bovine serum as a raw material for cell culture. Part IV. Application of proteomics to the manufacture of biological drugs, Biotechnol. Prog. 22 (5) (2006) 1294–1300.
[77] J. v.d. Valk, Fetal bovine serum - a cell culture dilemma, Science 375 (6577) (2022) 143–144.
[78] G. Gstraunthaler, T. Lindl, J. van der Valk, A plea to reduce or replace fetal bovine serum in cell culture media, Cytotechnology 65 (5) (2013) 791–793.
[79] W. Xu, S. Mann, G. Curone, Á. Kenéz, Heat treatment of bovine colostrum: effects on colostrum metabolome and serum metabolome of calves, Animal 15 (4) (2021), 100180.
[80] S. Mann, G. Curone, T.L. Chandler, A. Sipka, J. Cha, R. Bhawal, S. Zhang, Heat treatment of bovine colostrum: II. Effects on calf serum immunoglobulin, insulin, and IGF-I concentrations, and the serum proteome, J. Dairy Sci. 103 (10) (2020) 9384–9406.
[81] N.L. Anderson, M. Polanski, R. Pieper, T. Gatlin, R.S. Tirumalai, T.P. Conrads, T. D. Veenstra, J.N. Adkins, J.G. Pounds, R. Fagan, A. Lobley, The human plasma proteome: a nonredundant list developed by combination of four separate sources, Mol. Cell. Proteom. 3 (4) (2004) 311–326.
[82] J.P. Pilili, N.V. González, G. Molinari, M.A. Reigosa, S. Soloneski, M. L. Larramendy, Testing genotoxicity and cytotoxicity strategies for the evaluation of commercial radiosterilized fetal calf sera, Biologicals 38 (1) (2010) 135–143.
[83] M.S. Even, C.B. Sandusky, N.D. Barnard, Serum-free hybridoma culture: ethical, scientific and safety considerations, Trends Biotechnol. 24 (3) (2006) 105–108.
[84] OECD, Guidance Document on Good In Vitro Method Practices (GIVIMP), 2018.
[85] EMA, Guideline on the use of bovine serum in the manufacture of human biological medicinal products, CHMP/BWP/457920/2012 rev 1, 2013, p. 8.
[86] C. Saury, A. Lardenois, C. Schleder, I. Leroux, B. Lieubeau, L. David, M. Charrier, L. Guével, S. Viau, B. Delorme, K. Rouger, Human serum and platelet lysate are appropriate xeno-free alternatives for clinical-grade production of human MuStem cell batches, Stem Cell Res. Ther. 9 (1) (2018) 128.
[87] J.-M. Bielser, M. Wolf, J. Souquet, H. Broly, M. Morbidelli, Perfusion mammalian cell culture for recombinant protein manufacturing – a critical review, Biotechnol. Adv. 36 (4) (2018) 1328–1340.
[88] S. Kern, O. Platas-Barradas, R. Pörtner, B. Frahm, Model-based strategy for cell culture seed train layout verified at lab scale, Cytotechnology 68 (4) (2016) 1019–1032.
[89] C. He, P. Ye, H. Wang, X. Liu, F. Li, A systematic mass-transfer modeling approach for mammalian cell culture bioreactor scale-up, Biochem. Eng. J. 141 (2019) 173–181.
[90] A.K. Srivastava, S. Gupta, 2.38 - fed-batch fermentation – design strategies, in: M. Moo-Young (Ed.), Comprehensive Biotechnology, second ed., Academic Press, Burlington, 2011, pp. 515–526.
[91] D.J. Karst, F. Steinebach, M. Morbidelli, Continuous integrated manufacturing of therapeutic proteins, Curr. Opin. Biotechnol. 53 (2018) 76–84.
[92] N. Alt, T.Y. Zhang, P. Motchnik, R. Taticek, V. Quarmby, T. Schlothauer, H. Beck, T. Emrich, R.J. Harris, Determination of critical quality attributes for monoclonal antibodies using quality by design principles, Biologicals 44 (5) (2016) 291–305.
[93] O. Kwon, J. Joung, Y. Park, C.W. Kim, S.H. Hong, Considerations of critical quality attributes in the analytical comparability assessment of biosimilar products, Biologicals 48 (Supplement C) (2017) 101–108.
[94] J.-M. Bielser, L. Chappuis, Y. Xiao, J. Souquet, H. Broly, M. Morbidelli, Perfusion cell culture for the production of conjugated recombinant fusion proteins reduces clipping and quality heterogeneity compared to batch-mode processes, J. Biotechnol. 302 (2019) 26–31.
[95] D.A.M. Pais, M.J.T. Carrondo, P.M. Alves, A.P. Teixeira, Towards real-time monitoring of therapeutic protein quality in mammalian cell processes, Curr. Opin. Biotechnol. 30 (2014) 161–167.
[96] J. Štor, D.E. Ruckerbauer, D. Széliová, J. Zanghellini, N. Borth, Towards rational glyco-engineering in CHO: from data to predictive models, Curr. Opin. Biotechnol. 71 (2021) 9–17.
[97] J.H. Park, J.H. Jin, M.S. Lim, H.J. An, J.W. Kim, G.M. Lee, Proteomic analysis of host cell protein dynamics in the culture supernatants of antibody-producing CHO cells, Sci. Rep. 7 (1) (2017) 44246.
[98] J.H. Park, J.H. Jin, I.J. Ji, H.J. An, J.W. Kim, G.M. Lee, Proteomic analysis of host cell protein dynamics in the supernatant of Fc-fusion protein-producing CHO DG44 and DUKX-B11 cell lines in batch and fed-batch cultures, Biotechnol. Bioeng. 114 (10) (2017) 2267–2278.
[99] U.M. Lim, M.G.S. Yap, Y.P. Lim, L.-T. Goh, S.K. Ng, Identification of autocrine growth factors secreted by CHO cells for applications in single-cell cloning media, J. Proteome Res. 12 (7) (2013) 3496–3510.
[100] B. Yang, W. Li, H. Zhao, A. Wang, Y. Lei, Q. Xie, S. Xiong, Discovery and characterization of CHO host cell protease-induced fragmentation of a recombinant monoclonal antibody during production process development, J. Chromatogr. B 1112 (2019) 1–10.
[101] K. Yasuno, E. Hamamura-Yasuno, D. Nishimiya, M. Soma, M. Imaoka, K. Kai, K. Mori, Host cell proteins induce inflammation and immunogenicity as adjuvants in an integrated analysis of in vivo and in vitro assay systems, J. Pharmacol. Toxicol. Methods 103 (2020), 106694.
[102] S. Louie, J. Lakkyreddy, B.M. Castellano, B. Haley, A. Nguyen Dang, C. Lam, D. Tang, S. Lang, B. Snedecor, S. Misaghi, Insulin degrading enzyme (IDE) expressed by Chinese hamster ovary (CHO) cells is responsible for degradation of insulin in culture media, J. Biotechnol. 320 (2020) 44–49.
[103] <1132> Residual Host Cell Protein Measurement in Biopharmaceuticals, in: U.S. Pharmacopeia (Ed.) USP 39, 2016, pp. 1416–1432.
[104] EMA, CPMP Position Statement on DNA and Host Cell Proteins (HCP) Impurities, Routine Testing Versus Validation Studies, CPMP/BWP/382/97, 1997, pp. 1–2.
[105] P.T. Wingfield, Overview of the purification of recombinant proteins, Curr. Protoc. Protein Sci. 80 (2015) 6.1.1–6.1.35.
[106] N.K. Tripathi, A. Shrivastava, Recent developments in bioprocessing of recombinant: proteins: expression hosts and process development, Front. Bioeng. Biotechnol. 7 (2019) 1–35.
[107] R. Kuhn, S. Hofstetter-Kuhn, Capillary Electrophoresis: Principles and Practice, Springer-Verlag, Heidelberg, Berlin. New York, 1993.
[108] A. Jouyban, E. Kenndler, Theoretical and empirical approaches to express the mobility of small ions in capillary electrophoresis, Electrophoresis 27 (5–6) (2006) 992–1005.

[109] F. Kálmán, S. Ma, R.O. Fox, C. Horváth, Capillary electrophoresis of S. nuclease mutants, J. Chromatogr. A 705 (1) (1995) 135–154.
[110] V.J. Hilser, E. Freire, Quantitative analysis of conformational equilibrium using capillary electrophoresis: applications to protein folding, Anal. Biochem. 224 (2) (1995) 465–485.
[111] J.H. Knox, I.H. Grant, Miniaturisation in pressure and electroendosmotically driven liquid chromatography: Some theoretical considerations, Chromatographia 24 (1) (1987) 135–143.
[112] T.L. Huang, P. Tsai, C.T. Wu, C.S. Lee, Mechanistic studies of electroosmotic control at the capillary-solution interface, Anal. Chem. 65 (20) (1993) 2887–2893.
[113] T.S. Stevens, H.J. Cortes, Electroosmotic propulsion of eluent through silica-based chromatographic media, Anal. Chem. 55 (8) (1983) 1365–1370.
[114] C.L.A. Berli, M.V. Piaggio, J.A. Deiber, Modeling the zeta potential of silica capillaries in relation to the background electrolyte composition, Electrophoresis 24 (10) (2003) 1587–1595.
[115] S. Ghosal, Fluid mechanics of electroosmotic flow and its effect on band broadening in capillary electrophoresis, Electrophoresis 25 (2) (2004) 214–228.
[116] B.J. Kirby, E.F. Hasselbrink Jr., Zeta potential of microfluidic substrates: 1. Theory, experimental techniques, and effects on separations, Electrophoresis 25 (2) (2004) 187–202.
[117] M.O. Fatehah, H.A. Aziz, S. Stoll, Nanoparticle properties, behavior, fate in aquatic systems and characterization methods, J. Colloid Sci. Biotechnol. 3 (2) (2014) 111–140.
[118] M.R. Schure, A.M. Lenhoff, Consequences of wall adsorption in capillary electrophoresis: theory and simulation, Anal. Chem. 65 (21) (1993) 3024–3037.
[119] S.A. Swedberg, Characterization of protein behavior in high-performance capillary electrophoresis using a novel capillary system, Anal. Biochem. 185 (1) (1990) 51–56.
[120] J.S. Green, J.W. Jorgenson, Minimizing adsorption of proteins on fused silica in capillary zone electrophoresis by the addition of alkali metal salts to the buffers, J. Chromatogr. A 478 (1989) 63–70.
[121] J.K. Towns, F.E. Regnier, Impact of polycation adsorption on efficiency and electroosmotically driven transport in capillary electrophoresis, Anal. Chem. 64 (21) (1992) 2473–2478.
[122] M. Rabiller-Baudry, B. Chaufer, Specific adsorption of phosphate ions on proteins evidenced by capillary electrophoresis and reversed-phase high-performance liquid chromatography, J. Chromatogr. B: Biomed. Sci. Appl. 753 (1) (2001) 67–77.
[123] B. Verzola, C. Gelfi, P.G. Righetti, Protein adsorption to the bare silica wall in capillary electrophoresis: quantitative study on the chemical composition of the background electrolyte for minimising the phenomenon, J. Chromatogr. A 868 (1) (2000) 85–99.
[124] A. Kondo, J. Mihara, Comparison of adsorption and conformation of hemoglobin and myoglobin on various inorganic ultrafine particles, J. Colloid Interface Sci. 177 (1) (1996) 214–221.
[125] G.A. Parks, The isoelectric points of solid oxides, solid hydroxides, and aqueous hydroxo complex systems, Chem. Rev. 65 (2) (1965) 177–198.
[126] M. Zhu, R. Rodriguez, D. Hansen, T. Wehr, Capillary electrophoresis of proteins under alkaline conditions, J. Chromatogr. A 516 (1) (1990) 123–131.
[127] I. Hamrníková, I. Mikšík, Z. Deyl, V. Kašicka, Binding of proline- and hydroxyproline-containing peptides and proteins to the capillary wall, J. Chromatogr. A 838 (1) (1999) 167–177.
[128] F.-T.A. Chen, Rapid protein analysis by capillary electrophoresis, J. Chromatogr. A 559 (1) (1991) 445–453.
[129] T. Wehr, R. Rodriguez-Díaz, M. Zhu, Capillary Electrophoresis of Proteins, Marcel Dekker, New York, Basel, Hong Kong, 1999.
[130] H. Stutz, G. Bordin, A.R. Rodriguez, Separation of selected metal-binding proteins with capillary zone electrophoresis, Anal. Chim. Acta 477 (1) (2003) 1–19.
[131] Y. Alahmad, M. Taverna, H. Mobdi, J. Duboeuf, A. Grégoire, I. Rancé, N.T. Tran, A validated capillary electrophoresis method to check for batch-to-batch consistency during recombinant human glycosylated interleukin-7 production campaigns, J. Pharm. Biomed. Anal. 51 (4) (2010) 882–888.
[132] A. Amini, Separation of somatropin charge variants by multiple-injection CZE with Polybrene/chondroitin sulfate A double-coated capillaries, J. Sep. Sci. 36 (16) (2013) 2686–2690.
[133] H. Stutz, Protein attachment onto silica surfaces – a survey of molecular fundamentals, resulting effects and novel preventive strategies in CE, Electrophoresis 30 (12) (2009) 2032–2061.
[134] C.A. Lucy, A.M. MacDonald, M.D. Gulcev, Non-covalent capillary coatings for protein separations in capillary electrophoresis, J. Chromatogr. A 1184 (1–2) (2008) 81–105.
[135] L. Leclercq, C. Renard, M. Martin, H. Cottet, Quantification of adsorption and optimization of separation of proteins in capillary electrophoresis, Anal. Chem. 92 (15) (2020) 10743–10750.
[136] M.E. Bohlin, L.G. Blomberg, N.H.H. Heegaard, Utilizing the pH hysteresis effect for versatile and simple electrophoretic analysis of proteins in bare fused-silica capillaries, Electrophoresis 26 (21) (2005) 4043–4049.
[137] W.J. Lambert, D.L. Middleton, pH hysteresis effect with silica capillaries in capillary zone electrophoresis, Anal. Chem. 62 (15) (1990) 1585–1587.
[138] C.J. van Oss, A. Docoslis, R.F. Giese, Free energies of protein adsorption onto mineral particles — from the initial encounter to the onset of hysteresis, Colloids Surf. B: Biointerfaces 22 (4) (2001) 285–300.
[139] M. Graf, R.G. García, H. Wätzig, Protein adsorption in fused-silica and polyacrylamide-coated capillaries, Electrophoresis 26 (12) (2005) 2409–2417.
[140] D.K. Lloyd, H. Wätzig, Sodium dodecyl sulfate solution is an effective between-run rinse for capillary electrophoresis of samples in biological matrices, J. Chromatogr. B: Biomed. Sci. Appl. 663 (2) (1995) 400–405.
[141] R. Kurrat, J.E. Prenosil, J.J. Ramsden, Kinetics of human and bovine serum albumin adsorption at silica-titania surfaces, J. Colloid Interface Sci. 185 (1) (1997) 1–8.
[142] R.M. McCormick, Capillary zone electrophoretic separation of peptides and proteins using low pH buffers in modified silica capillaries, Anal. Chem. 60 (21) (1988) 2322–2328.
[143] B.M. Mitsyuk, Mechanism of the reaction of silica with phosphoric acid in aqueous soluions, Russ. J. Inorg. Chem. 17 (4) (1972) 471–473.
[144] A.D. Tran, S. Park, P.J. Lisi, O.T. Huynh, R.R. Ryall, P.A. Lane, Separation of carbohydrate-mediated microheterogeneity of recombinant human erythropoietin by free solution capillary electrophoresis: effects of pH, buffer type and organic additives, J. Chromatogr. A 542 (0) (1991) 459–471.
[145] R. Gilmanshin, R.B. Dyer, R.H. Callender, Structural heterogeneity of the various forms of apomyoglobin; implications for protein folding, Protein Sci. 6 (10) (1997) 2134–2142.
[146] M. Jamin, S.-R. Yeh, D.L. Rousseau, R.L. Baldwin, Submillisecond unfolding kinetics of apomyoglobin and its pH 4 intermediate, J. Mol. Biol. 292 (3) (1999) 731–740.
[147] H. Stutz, G. Bordin, A.R. Rodriguez, Capillary zone electrophoresis of metal-binding proteins in formic acid with UV- and mass spectrometric detection using cationic transient capillary isotachophoresis for preconcentration, Electrophoresis 25 (7–8) (2004) 1071–1089.
[148] X. Xuan, D. Li, Analytical study of Joule heating effects on electrokinetic transportation in capillary electrophoresis, J. Chromatogr. A 1064 (2) (2005) 227–237.
[149] L. Hajba, A. Guttman, Recent advances in column coatings for capillary electrophoresis of proteins, TrAC Trends Anal. Chem. 90 (2017) 38–44.
[150] R. Barberi, J.J. Bonvent, R. Bartolino, J. Roeraade, L. Capelli, P.G. Righetti, Probing soft polymeric coatings of a capillary by atomic force microscopy, J. Chromatogr. B: Biomed. Sci. Appl. 683 (1) (1996) 3–13.
[151] A. Cifuentes, J.C. Díez-Masa, J. Fritz, D. Anselmetti, A.E. Bruno, Polyacrylamide-coated capillaries probed by atomic force microscopy: correlation between surface topography and electrophoretic performance, Anal. Chem. 70 (16) (1998) 3458–3462.
[152] M. Leitner, L.G. Stock, L. Traxler, L. Leclercq, K. Bonazza, G. Friedbacher, H. Cottet, H. Stutz, A. Ebner, Mapping molecular adhesion sites inside SMIL coated capillaries using atomic force microscopy recognition imaging, Anal. Chim. Acta 930 (2016) 39–48.
[153] L.G. Stock, M. Leitner, L. Traxler, K. Bonazza, L. Leclercq, H. Cottet, G. Friedbacher, A. Ebner, H. Stutz, Advanced portrayal of SMIL coating by allying CZE performance with in-capillary topographic and charge-related surface characterization, Anal. Chim. Acta 951 (2017) 1–15.
[154] H. Katayama, Y. Ishihama, N. Asakawa, Stable capillary coating with successive multiple ionic polymer layers, Anal. Chem. 70 (11) (1998) 2254–2260.
[155] H. Katayama, Y. Ishihama, N. Asakawa, Stable cationic capillary coating with successive multiple ionic polymer layers for capillary electrophoresis, Anal. Chem. 70 (24) (1998) 5272–5277.
[156] S. Roca, L. Dhellemmes, L. Leclercq, H. Cottet, Polyelectrolyte multilayers in capillary electrophoresis, ChemPlusChem 87 (4) (2022), e202200028.
[157] M. Weinbauer, H. Stutz, Successive multiple ionic polymer layer coated capillaries in the separation of proteins – recombinant allergen variants as a case study, Electrophoresis 31 (11) (2010) 1805–1812.
[158] L.A. Kartsova, A.V. Kravchenko, E.A. Kolobova, Covalent coatings of quartz capillaries for the electrophoretic determination of biologically active analytes, J. Anal. Chem. 74 (8) (2019) 729–737.
[159] Y. Alahmad, N. Thuy Tran, J. Duboeuf, A. Grégoire, I. Rancé, M. Taverna, CZE for glycoform profiling and quality assessment of recombinant human interleukin-7, Electrophoresis 30 (13) (2009) 2347–2354.
[160] M. Rabiller-Baudry, B. Chaufer, Small molecular ion adsorption on proteins and DNAs revealed by separation techniques, J. Chromatogr. B 797 (1–2) (2003) 331–345.
[161] D. Corradini, E. Cogliandro, L. D'Alessandro, I. Nicoletti, Influence of electrolyte composition on the electroosmotic flow and electrophoretic mobility of proteins and peptides, J. Chromatogr. A 1013 (1) (2003) 221–232.
[162] S. Hoffstetter-Kuhn, A. Paulus, E. Gassmann, H.M. Widmer, Influence of borate complexation on the electrophoretic behavior of carbohydrates in capillary electrophoresis, Anal. Chem. 63 (15) (1991) 1541–1547.
[163] Z. Liu, Y. Wang, J. Yan, J. Liu, B. Chen, L. Zhang, L. Cheng, Efficacy and safety of recombinant human interleukin-11 in the treatment of acute leukaemia patients with chemotherapy-induced thrombocytopenia: a systematic review and meta-analysis, J. Eval. Clin. Pract. 26 (1) (2020) 262–271.
[164] Y. Su, Y. Zheng, S. Wang, S. Zhang, R. Yu, C. Zhang, Facile production of tag-free recombinant human interleukin-11 by transforming into soluble expression in *Escherichia coli*, Protein Expr. Purif. 197 (2022), 106107.
[165] R.B. Souto, F.P. Stamm, J.B. Schumacher, C.D.A. Cardoso, G.W. de Freitas, R. F. Perobelli, S.L. Dalmora, Stability-indicating capillary zone electrophoresis method for the assessment of recombinant human interleukin-11 and its correlation with reversed-phase liquid chromatography and biossay, Talanta 123 (2014) 179–185.
[166] J. How, G. Hobbs, Use of interferon alfa in the treatment of myeloproliferative neoplasms: perspectives and review of the literature, Cancers 12 (7) (2020) 1954.

[167] J.R. Catai, H.A. Tervahauta, G.J. de Jong, G.W. Somsen, Noncovalently bilayer-coated capillaries for efficient and reproducible analysis of proteins by capillary electrophoresis, J. Chromatogr. A 1083 (1–2) (2005) 185–192.
[168] F.P.S. Maldaner, R.F. Perobelli, B. Xavier, G.L. Remuzzi, M.E. Walter, S. L. Dalmora, Evaluation of recombinant human parathyroid hormone by CZE method and its correlation with in vitro bioassay and LC methods, Talanta 162 (2017) 567–573.
[169] G. Tuli, R. Buganza, D. Tessaris, S. Einaudi, P. Matarazzo, L. de Sanctis, Teriparatide (rhPTH 1–34) treatment in the pediatric age: long-term efficacy and safety data in a cohort with genetic hypoparathyroidism, Endocrine 67 (2) (2020) 457–465.
[170] L. Zhang, K. Lawson, B. Yeung, J. Wypych, Capillary zone electrophoresis method for a highly glycosylated and sialylated recombinant protein: development, characterization and application for process development, Anal. Chem. 87 (1) (2015) 470–476.
[171] S.A. Berkowitz, H. Zhong, M. Berardino, Z. Sosic, J. Siemiatkoski, I.S. Krull, R. Mhatre, Rapid quantitative capillary zone electrophoresis method for monitoring the micro-heterogeneity of an intact recombinant glycoprotein, J. Chromatogr. A 1079 (1) (2005) 254–265.
[172] E. Balaguer, C. Neusüß, Intact glycoform characterization of erythropoietin-α and erythropoietin-β by CZE-ESI-TOF-MS, Chromatographia 64 (5) (2006) 351–357.
[173] S.T. Provatopoulou, P.N. Ziroyiannis, Clinical use of erythropoietin in chronic kidney disease: outcomes and future prospects, Hippokratia 15 (2) (2011) 109–115.
[174] D.P. Steensma, C.L. Loprinzi, Erythropoietin use in cancer patients: a matter of life and death? J. Clin. Oncol. 23 (25) (2005) 5865–5868.
[175] Y. Cao, Erythropoietin in cancer: a dilemma in risk therapy, Trends Endocrinol. Metab. 24 (4) (2013) 190–199.
[176] N. Debeljak, P. Solár, A.J. Sytkowski, Erythropoietin and cancer: the unintended consequences of anemia correction, Front. Immunol. 5 (583) (2014) 1–14.
[177] F. Lasne, J. Thioulouse, L. Martin, J. de Ceaurriz, Detection of recombinant human erythropoietin in urine for doping analysis: interpretation of isoelectric profiles by discriminant analysis, Electrophoresis 28 (12) (2007) 1875–1881.
[178] V. Brinks, A. Hawe, A.H. Basmeleh, L. Joachin-Rodriguez, R. Haselberg, G. Somsen, W. Jiskoot, H. Schellekens, Quality of original and biosimilar epoetin products, Pharm. Res 28 (2) (2011) 386–393.
[179] M. de Frutos, A. Cifuentes, J.C. Diez-Masa, Differences in capillary electrophoresis profiles of urinary and recombinant erythropoietin, Electrophoresis 24 (4) (2003) 678–680.
[180] V. Sanz-Nebot, F. Benavente, E. Giménez, J. Barbosa, Capillary electrophoresis and matrix-assisted laser desorption/ionization-time of flight-mass spectrometry for analysis of the novel erythropoiesis-stimulating protein (NESP), Electrophoresis 26 (7–8) (2005) 1451–1456.
[181] P. Lara-Quintanar, I. Lacunza, J. Sanz, J.C. Diez-Masa, M. de Frutos, Immunochromatographic removal of albumin in erythropoietin biopharmaceutical formulations for its analysis by capillary electrophoresis, J. Chromatogr. A 1153 (1) (2007) 227–234.
[182] Y. Jia, J. Cao, J. Zhou, P. Zhou, Methyl chitosan coating for glycoform analysis of glycoproteins by capillary electrophoresis, Electrophoresis 41 (9) (2020) 729–734.
[183] T. Gao, X. Li, Z. Jia, F. Hendrickx, J.B. Falmagne, H.X. Chen, Rapid capillary zone electrophoresis of recombinant erythropoietin by the use of dynamic double layer coating, Anal. Lett. 53 (16) (2020) 2596–2606.
[184] P. Hermentin, I-Number assay and erythropoietin potency: retrospective capillary zone electrophoresis data analysis of the biological reference preparations of erythropoietin, J. Chromatogr. Sep. Tech. (2017) S1.
[185] P.D. Hermentin, Ibio-number assay: a physicochemical assay that predicts the bioactivity of erythropoietin with high precision and accuracy and may replace the mouse bioassay in the quality control of EPO batch release, Pharm. Anal. Acta 8 (2017) 1–9.
[186] P. Hermentin, Isoform number I - a new tool to evaluate the quality of erythropoietin, Pharmeuropa Sci. Notes 2006 (1) (2006) 37–40.
[187] M. Ghezlou, F. Mokhtari, A. Kalbasi, G. Riazi, H. Kaghazian, R. Emadi, A.R. Aref, Aggregate forms of recombinant human erythropoietin with different charge profile substantially impact biological activities, J. Pharm. Sci. 109 (1) (2020) 277–283.
[188] J. Tani, Y. Ito, S. Tatemichi, M. Yamakami, T. Fukui, Y. Hatano, S. Kakimoto, A. Kotani, A. Sugimura, K. Mihara, R. Yamamoto, N. Tanaka, K. Minami, K. Takahashi, T. Hirato, Physicochemical and biological evaluation of JR-131 as a biosimilar to a long-acting erythropoiesis-stimulating agent darbepoetin alfa, PLOS ONE 15 (4) (2020), e0231830.
[189] I. Lacunza, P. Lara-Quintanar, G. Moya, J. Sanz, J.C. Diez-Masa, M. de Frutos, Selection of migration parameters for a highly reliable assignment of bands of isoforms of erythropoietin separated by capillary electrophoresis, Electrophoresis 25 (10–11) (2004) 1569–1579.
[190] S. Boucher, A. Kane, M. Girard, Qualitative and quantitative assessment of marketed erythropoiesis-stimulating agents by capillary electrophoresis, J. Pharm. Biomed. Anal. 71 (0) (2012) 207–213.
[191] H.P. Bietlot, M. Girard, Analysis of recombinant human erythropoietin in drug formulations by high-performance capillary electrophoresis, J. Chromatogr. A 759 (1) (1997) 177–184.
[192] T. Fournier, Human chorionic gonadotropin: different glycoforms and biological activity depending on its source of production, Ann. D. 'Endocrinol. 77 (2) (2016) 75–81.
[193] L.A. Cole, Biological functions of hCG and hCG-related molecules, Reprod. Biol. Endocrinol. 8 (1) (2010) 102.
[194] L.A. Cole, New discoveries on the biology and detection of human chorionic gonadotropin, Reprod. Biol. Endocrinol. 7 (1) (2009) 8.
[195] M. Lenhard, A. Tsvilina, L. Schumacher, M. Kupka, N. Ditsch, D. Mayr, K. Friese, U. Jeschke, Human chorionic gonadotropin and its relation to grade, stage and patient survival in ovarian cancer, BMC Cancer 12 (2) (2012) 1–8.
[196] Rd.B.F. Leão, S.C. Esteves, Gonadotropin therapy in assisted reproduction: an evolutionary perspective from biologics to biotech, Clinics 69 (4) (2014) 279–293.
[197] L. Boeri, P. Capogrosso, A. Salonia, Gonadotropin treatment for the male hypogonadotropic hypogonadism, Curr. Pharm. Des. 27 (24) (2021) 2775–2783.
[198] T. Kuuranne, L. Ahola, C. Pussinen, A. Leinonen, Analysis of human chorionic gonadotropin (hCG): application of routine immunological methods for initial testing and confirmation analysis in doping control, Drug Test. Anal. 5 (8) (2013) 614–618.
[199] A. Durgaryan, T. Rundlöf, M. Lavén, A. Amini, Identification of human chorionic gonadotropin hormone in illegally distributed products by MALDI-TOF mass spectrometry and double-injection capillary zone electrophoresis, Anal. Methods 8 (21) (2016) 4188–4196.
[200] A. Amini, H. Lodén, C. Pettersson, T. Arvidsson, Principles for different modes of multiple-injection CZE, Electrophoresis 29 (19) (2008) 3952–3958.
[201] P. Laidler, D.A. Cowan, R.C. Hider, A.T. Kicman, Characterization of human chorionic gonadotropin microheterogeneity by capillary electrophoresis: potential application for quality control in the pharmaceutical industry, Pharm. Pharmacol. Commun. 3 (10) (1997) 487–491.
[202] S.L. Dalmora, F.B. D'Avila, L.Md Silva, A.C. Bergamo, E.S. Zimmermann, Development and validation of a capillary zone electrophoresis method for assessment of recombinant human granulocyte colony-stimulating factor in pharmaceutical formulations and its correlation with liquid chromatography methods and bioassay, J. Chromatogr. B 877 (24) (2009) 2471–2476.
[203] N. Iki, E.S. Yeung, Non-bonded poly(ethylene oxide) polymer-coated column for protein separation by capillary electrophoresis, J. Chromatogr. A 731 (1) (1996) 273–282.
[204] M.C.M. Mellado, J.A. Mena, A. Lopes, O.T. Ramírez, M.J.T. Carrondo, L. A. Palomares, P.M. Alves, Impact of physicochemical parameters on in vitro assembly and disassembly kinetics of recombinant triple-layered rotavirus-like particles, Biotechnol. Bioeng. 104 (4) (2009) 674–686.
[205] R.M. Castro-Acosta, A.L. Revilla, O.T. Ramírez, L.A. Palomares, Separation and quantification of double- and triple-layered rotavirus-like particles by CZE, Electrophoresis 31 (8) (2010) 1376–1381.
[206] X. Huang, X. Wang, J. Zhang, N. Xia, Q. Zhao, *Escherichia coli*-derived virus-like particles in vaccine development, npj Vaccin. 2 (1) (2017) 3.
[207] S. Nooraei, H. Bahrulolum, Z.S. Hoseini, C. Katalani, A. Hajizade, A.J. Easton, G. Ahmadian, Virus-like particles: preparation, immunogenicity and their roles as nanovaccines and drug nanocarriers, J. Nanobiotechnol. 19 (1) (2021), 59-59.
[208] M.K. Estes, J. Cohen, Rotavirus gene structure and function, Microbiol Rev. 53 (4) (1989) 410–449.
[209] P.K. Mathis, M. Ciarlet, K.M. Campbell, S. Wang, K.E. Owen, T.S. Ranheim, Separation of rotavirus double-layered particles and triple-layered particles by capillary zone electrophoresis, J. Virol. Methods 169 (1) (2010) 13–21.
[210] C.-M. Zhou, Characterization of human papillomavirus by capillary isoelectric focusing with whole-column imaging detection, Electrophoresis 34 (20–21) (2013) 3046–3053.
[211] F.T. Cutts, S. Franceschi, S. Goldie, X. Castellsague, S. de Sanjose, G. Garnett, W. J. Edmunds, P. Claeys, K.L. Goldenthal, D.M. Harper, L. Markowitz, Human papillomavirus and HPV vaccines: a review, Bull. World Health Organ 85 (9) (2007) 719–726.
[212] J.T. Schiller, M. Müller, Next generation prophylactic human papillomavirus vaccines, Lancet Oncol. 16 (5) (2015) e217–e225.
[213] V. Bettonville, J.T.J. Nicol, T. Furst, N. Thelen, G. Piel, M. Thiry, M. Fillet, N. Jacobs, A.C. Servais, Quantitation and biospecific identification of virus-like particles of human papillomavirus by capillary electrophoresis, Talanta 175 (2017) 325–330.
[214] V. Bettonville, J.T.J. Nicol, N. Thelen, M. Thiry, M. Fillet, N. Jacobs, A.-C. Servais, Study of intact virus-like particles of human papillomavirus by capillary electrophoresis, Electrophoresis 37 (4) (2016) 579–586.
[215] B. Mann, J.A. Traina, C. Soderblom, P.K. Murakami, E. Lehmberg, D. Lee, J. Irving, E. Nestaas, E. Pungor, Capillary zone electrophoresis of a recombinant adenovirus, J. Chromatogr. A 895 (1) (2000) 329–337.
[216] G.B. Gordon, P.T. Richard, H.A.S. Martins, A. New, High-sensitivity capillary electrophoresis detector cell and advanced manufacturing paradigm, Hewlett-Packard J. 46 (3) (1995) 62–70.
[217] H. Engelhardt, W. Beck, T. Schmitt, Capillary Electrophoresis - Methods and Potentials, Friedr, Vieweg & Sohn Verlagsgesellschaft mbH,, Braunschweig, Wiesbaden, 1996.
[218] H. Stutz, H. Malissa Jr, Determination of regularly distributed plant protectants in raw and drinking waters, using a multiresidue method with cyclodextrin-modified micellar electrokinetic chromatography, J. AOAC Int. 82 (6) (1999) 1510–1522.
[219] E. van Tricht, L. Geurink, H. Backus, M. Germano, G.W. Somsen, C.E. Sänger–van de Griend, One single, fast and robust capillary electrophoresis method for the direct quantification of intact adenovirus particles in upstream and downstream processing samples, Talanta 166 (2017) 8–14.
[220] E. van Tricht, L. Geurink, F. Galindo Garre, M. Schenning, H. Backus, M. Germano, G.W. Somsen, C.E. Sänger– van de Griend, Implementation of at-line capillary zone electrophoresis for fast and reliable determination of adenovirus concentrations in vaccine manufacturing, Electrophoresis 40 (18–19) (2019) 2277–2284.

[221] A.E. Merrick, E.J. Ilett, A.A. Melcher, JX-594, a targeted oncolytic poxvirus for the treatment of cancer, Curr. Opin. Investig. Drugs 10 (12) (2009) 1372–1382.
[222] D.H. Kirn, S.H. Thorne, Targeted and armed oncolytic poxviruses: a novel multi-mechanistic therapeutic class for cancer, Nat. Rev. Cancer 9 (1) (2009) 64–71.
[223] G.G. Mironov, A.V. Chechik, R. Ozer, J.C. Bell, M.V. Berezovski, Viral quantitative capillary electrophoresis for counting intact viruses, Anal. Chem. 83 (13) (2011) 5431–5435.
[224] S.D. Khare, K.C. Wilcox, P. Gong, N.V. Dokholyan, Sequence and structural determinants of Cu, Zn superoxide dismutase aggregation, Protein.: Struct., Funct., Bioinforma. 61 (3) (2005) 617–632.
[225] E. Herczenik, M.F.B.G. Gebbink, Molecular and cellular aspects of protein misfolding and disease, FASEB J. 22 (7) (2008) 2115–2133.
[226] G. Esposito, R. Michelutti, G. Verdone, P. Viglino, H.H. Ández, C.V. Robinson, A. Amoresano, F.D. Piaz, M. Monti, P. Pucci, P. Mangione, M. Stoppini, G. Merlini, G. Ferri, V. Bellotti, Removal of the N-terminal hexapeptide from human β2-microglobulin facilitates protein aggregation and fibril formation, Protein Sci. 9 (5) (2000) 831–845.
[227] N.H.H. Heegaard, E. De Lorenzi, Interactions of charged ligands with β_2-microglobulin conformers in affinity capillary electrophoresis, Biochim. et Biophys. Acta (BBA) - Proteins Proteom. 1753 (1) (2005) 131–140.
[228] R. Scarpioni, M. Ricardi, V. Albertazzi, S. De Amicis, F. Rastelli, L. Zerbini, Dialysis-related amyloidosis: challenges and solutions, Int J. Nephrol. Renov. Dis. 9 (2016) 319–328.
[229] S. Giorgetti, A. Rossi, P. Mangione, S. Raimondi, S. Marini, M. Stoppini, A. Corazza, P. Viglino, G. Esposito, G. Cetta, G. Merlini, V. Bellotti, β2-Microglobulin isoforms display an heterogeneous affinity for type I collagen, Protein Sci. 14 (3) (2005) 696–702.
[230] L. Bertoletti, F. Bisceglia, R. Colombo, S. Giorgetti, S. Raimondi, P.P. Mangione, E. De Lorenzi, Capillary electrophoresis analysis of different variants of the amyloidogenic protein β2-microglobulin as a simple tool for misfolding and stability studies, Electrophoresis 36 (19) (2015) 2465–2472.
[231] S. Tresch, D. Holzmann, S. Baumann, K. Blaser, B. Wüthrich, R. Crameri, P. Schmid-Grendelmeier, In vitro and in vivo allergenicity of recombinant Bet v 1 compared to the reactivity of natural birch pollen extract, Clin. Exp. Allergy 33 (8) (2003) 1153–1158.
[232] M.D. Chapman, A.M. Smith, L.D. Vailes, L.K. Arruda, V. Dhanaraj, A. Pomés, Recombinant allergens for diagnosis and therapy of allergic disease, J. Allergy Clin. Immunol. 106 (3) (2000) 409–418.
[233] P. Moingeon, Sublingual immunotherapy: from biological extracts to recombinant allergens, Allergy 61 (S81) (2006) 15–19.
[234] G.W. Canonica, L. Cox, R. Pawankar, C.E. Baena-Cagnani, M. Blaiss, S. Bonini, J. Bousquet, M. Calderón, E. Compalati, S.R. Durham, R.G. van Wijk, D. Larenas-Linnemann, H. Nelson, G. Passalacqua, O. Pfaar, N. Rosário, D. Ryan, L. Rosenwasser, P. Schmid-Grendelmeier, G. Senna, E. Valovirta, H. Van Bever, P. Vichyanond, U. Wahn, O. Yusuf, Sublingual immunotherapy: World Allergy Organization position paper 2013 update, World Allergy Organ J. 7 (1) (2014), 6-6.
[235] M. Jutel, I. Agache, S. Bonini, A.W. Burks, M. Calderon, W. Canonica, L. Cox, P. Demoly, A.J. Frew, R. O'Hehir, J. Kleine-Tebbe, A. Muraro, G. Lack, D. Larenas, M. Levin, H. Nelson, R. Pawankar, O. Pfaar, R. van Ree, H. Sampson, A.F. Santos, G. Du Toit, T. Werfel, R. Gerth van Wijk, L. Zhang, C.A. Akdis, International consensus on allergy immunotherapy, J. Allergy Clin. Immunol. 136 (3) (2015) 556–568.
[236] R. Valenta, R. Campana, M. Focke-Tejkl, V. Niederberger, Vaccine development for allergen-specific immunotherapy based on recombinant allergens and synthetic allergen peptides: lessons from the past and novel mechanisms of action for the future, J. Allergy Clin. Immunol. 137 (2) (2016) 351–357.
[237] K. Marth, M. Focke-Tejkl, C. Lupinek, R. Valenta, V. Niederberger, Allergen peptides, recombinant allergens and hypoallergens for allergen-specific immunotherapy, Curr. Treat. Options Allergy 1 (1) (2014) 91–106.
[238] S. Vieths, S. Scheurer, J. Reindl, D. Lüttkopf, A. Wangorsch, M. Kästner, T. Haase, D. Haustein, Optimized allergen extracts and recombinant allergens in diagnostic applications, Allergy 56 (Suppl 67) (2001) 78–82.
[239] R. Valenta, V. Niederberger, Recombinant allergens for immunotherapy, J. Allergy Clin. Immunol. 119 (4) (2007) 826–830.
[240] F.C. Arntzen, T.W. Wilhelmsen, H. Løwenstein, B. Gjesing, H.J. Maasch, R. Strömberg, R. Einarsson, A. Backman, S. Mäkinen-Kiljunen, A. Ford, The international collaborative study on the first international standard of birch (Betula verrucosa)-pollen extract, J. Allergy Clin. Immunol. 83 (1) (1989) 66–82.
[241] O. Cromwell, R. Suck, H. Kahlert, A. Nandy, B. Weber, H. Fiebig, Transition of recombinant allergens from bench to clinical application, Methods 32 (3) (2004) 300–312.
[242] S. Roland, C. Oliver, Quality control of recombinant pollen allergens, Curr. Pharm. Anal. 2 (3) (2006) 249–257.
[243] Allergen immunotherapy: therapeutic vaccines for allergic diseases. Geneva: January 27–29 1997, Allergy 53(44 Suppl) (1998) 1–42.
[244] R. Movérare, L. Elfman, E. Vesterinen, T. Metso, T. Haahtela, Development of new IgE specificities to allergenic components in birch pollen extract during specific immunotherapy studied with immunoblotting and Pharmacia CAP system™, Allergy 57 (5) (2002) 423–430.
[245] EMA, Guideline on the the clinical development of products for specific immunotherapy for the treatment of allergic diseases, CHMP/EWP/18504/2006, 2008, p. 13.
[246] M. Punzet, F. Ferreira, P. Briza, R. van Ree, H. Malissa Jr., H. Stutz, Profiling preparations of recombinant birch pollen allergen Bet v 1a with capillary zone electrophoresis in pentamine modified fused-silica capillaries, J. Chromatogr. B 839 (1–2) (2006) 19–29.
[247] M.-F. Lin, C. Williams, M.V. Murray, G. Conn, P.A. Ropp, Ion chromatographic quantification of cyanate in urea solutions: estimation of the efficiency of cyanate scavengers for use in recombinant protein manufacturing, J. Chromatogr. B 803 (2) (2004) 353–362.
[248] L. Kollipara, R.P. Zahedi, Protein carbamylation: in vivo modification or in vitro artefact? Proteomics 13 (6) (2013) 941–944.
[249] Y. Ma, M. Tonelli, L.D. Unsworth, Effect of carbamylation on protein structure and adsorption to self-assembled monolayer surfaces, Colloids and Surfaces B: Biointerfaces 203 (2021), 111719.
[250] K.C. Mun, T.A. Golper, Impaired biological activity of erythropoietin by cyanate carbamylation, Blood Purif. 18 (1) (2000) 13–17.
[251] B. Kronsteiner, H. Malissa, H. Stutz, Profiling recombinant major birch pollen allergen Bet v 1a and carbamylated variants with CZE and CIEF, Electrophoresis 28 (13) (2007) 2241–2251.
[252] C. Grégoire, M. Chapman, Recombinant allergens, Clin. Rev. Allergy Immunol. 21 (3) (2007) 215–227.
[253] T. Thalhamer, H. Dobias, T. Stepanoska, M. Pröll, H. Stutz, O. Dissertori, P. Lackner, F. Ferreira, M. Wallner, J. Thalhamer, A. Hartl, Designing hypoallergenic derivatives for allergy treatment by means of in silico mutation and screening, J. Allergy Clin. Immunol. 125 (4) (2010) 926–934.
[254] R. Vassar, The beta-secretase, BACE: a prime drug target for Alzheimer's disease, J. Mol. Neurosci. MN (2001) 157–170.
[255] C.M. Dobson, Principles of protein folding, misfolding and aggregation, Semin. Cell Dev. Biol. 15 (1) (2004) 3–16.
[256] Q. Zheng, Z. Guo, Y. Chen, Capillary array electrophoresis imaging of biochemicals in tissue sections, Talanta 240 (2022), 123183.
[257] R. Řemínek, L. Slezáčková, J. Schejbal, Z. Glatz, Development and comprehensive comparison of two on-line capillary electrophoretic methods for β-secretase inhibitor screening, J. Chromatogr. A 1518 (2017) 89–96.
[258] Z. Zhu, J.J. Lu, S. Liu, Protein separation by capillary gel electrophoresis: a review, Anal. Chim. Acta 709 (2012) 21–31.
[259] S.F. Santos, D. Zanette, H. Fischer, R. Itri, A systematic study of bovine serum albumin (BSA) and sodium dodecyl sulfate (SDS) interactions by surface tension and small angle X-ray scattering, J. Colloid Interface Sci. 262 (2) (2003) 400–408.
[260] A. Demelenne, A. Napp, F. Bouillenne, J. Crommen, A.C. Servais, M. Fillet, Insulin aggregation assessment by capillary gel electrophoresis without sodium dodecyl sulfate: Comparison with size-exclusion chromatography, Talanta 199 (2019) 457–463.
[261] A. Shala-Lawrence, S. Beheshti, E. Newman, M. Tang, S.M. Krylova, M. Leach, B. Carpick, S.N. Krylov, High-precision quantitation of a tuberculosis vaccine antigen with capillary-gel electrophoresis using an injection standard, Talanta 175 (2017) 273–279.
[262] B.X. Mayer, How to increase precision in capillary electrophoresis, J. Chromatogr. A 907 (1) (2001) 21–37.
[263] D.H. Na, E.J. Park, Y.S. Youn, B.W. Moon, Y.W. Jo, S.H. Lee, W.-B. Kim, Y. Sohn, K.C. Lee, Sodium dodecyl sulfate-capillary gel electrophoresis of polyethylene glycolylated interferon alpha, Electrophoresis 25 (3) (2004) 476–479.
[264] D.H. Na, E.J. Park, Y.W. Jo, K.C. Lee, Capillary electrophoretic separation of high-molecular-weight poly(ethylene glycol)-modified proteins, Anal. Biochem. 373 (2) (2008) 207–212.
[265] R. Dec, W. Dzwolak, A tale of two tails: Self-assembling properties of A- and B-chain parts of insulin's highly amyloidogenic H-fragment, Int. J. Biol. Macromol. 186 (2021) 510–518.
[266] E. Pryor, J.A. Kotarek, M.A. Moss, C.N. Hestekin, Monitoring insulin aggregation via capillary electrophoresis, Int. J. Mol. Sci. 12 (12) (2011) 9369–9388.
[267] L. Heinemann, K. Braune, A. Carter, A. Zayani, L.A. Krämer, Insulin storage: a critical reappraisal, J. Diabetes Sci. Technol. 15 (1) (2020) 147–159.
[268] Y. Shikama, J.-i Kitazawa, N. Yagihashi, O. Uehara, Y. Murata, N. Yajima, R. Wada, S. Yagihashi, Localized amyloidosis at the site of repeated insulin injection in a diabetic patient, Intern. Med. 49 (5) (2010) 397–401.
[269] C. Samlaska, S. Reber, T. Murry, Insulin-derived amyloidosis: the insulin ball, amyloidoma, JAAD Case Rep. 6 (4) (2020) 351–353.
[270] M.N. Albarghouthi, B.A. Buchholz, P.J. Huiberts, T.M. Stein, A.E. Barron, Poly-N-hydroxyethylacrylamide (polyDuramide™): a novel, hydrophilic, self-coating polymer matrix for DNA sequencing by capillary electrophoresis, Electrophoresis 23 (10) (2002) 1429–1440.
[271] E.J. Park, K.S. Lee, K.C. Lee, D.H. Na, Application of microchip CGE for the analysis of PEG-modified recombinant human granulocyte-colony stimulating factors, Electrophoresis 31 (22) (2010) 3771–3774.
[272] B.K. Seyfried, M. Marchetti-Deschmann, J. Siekmann, M.J. Bossard, F. Scheiflinger, P.L. Turecek, G. Allmaier, Microchip capillary gel electrophoresis of multiply PEGylated high-molecular-mass glycoproteins, Biotechnol. J. 7 (5) (2012) 635–641.
[273] C.L. Naydenov, E.P. Kirazov, L.P. Kirazov, T.T. Genadiev, New approach to calculating and predicting the ionic strength generated during carrier ampholyte isoelectric focusing, J. Chromatogr. A 1121 (1) (2006) 129–139.
[274] P.G. Righetti, The Alpher, Bethe, Gamow of isoelectric focusing, the alpha-Centaury of electrokinetic methodologies. Part I, Electrophoresis 27 (5–6) (2006) 923–938.
[275] P.G. Righetti, C. Simó, R. Sebastiano, A. Citterio, Carrier ampholytes for IEF, on their fortieth anniversary (1967–2007), brought to trial in court: The verdict, Electrophoresis 28 (21) (2007) 3799–3810.
[276] A.B. Chen, C.A. Rickel, A. Flanigan, G. Hunt, K.G. Moorhouse, Comparison of ampholytes used for slab gel and capillary isoelectric focusing of recombinant

tissue-type plasminogen activator glycoforms, J. Chromatogr. A 744 (1–2) (1996) 279–284.
[277] O. Vesterberg, H. Svensson, Isoelectric fractionation, analysis, and characterization of ampholytes in natural pH gradients. IV. Further studies on the resolving power in connection with separation of myoglobins, Acta Chem. Scand. 20 (1966) 820–834.
[278] H. Rilbe, Historical and theoretical aspects of isoelectric focusing, Ann. N. Y. Acad. Sci. 209 (1) (1973) 11–22.
[279] M. Conti, M. Galassi, A. Bossi, P.G. Righetti, Capillary isoelectric focusing: the problem of protein solubility, J. Chromatogr. A 757 (1–2) (1997) 237–245.
[280] M. Zhu, R. Rodriguez, T. Wehr, Optimizing separation parameters in capillary isoelectric focusing, J. Chromatogr. A 559 (1–2) (1991) 479–488.
[281] W. Thormann, T. Huang, J. Pawliszyn, R.A. Mosher, High-resolution computer simulation of the dynamics of isoelectric focusing of proteins, Electrophoresis 25 (2) (2004) 324–337.
[282] R. Rodriguez-Diaz, M. Zhu, T. Wehr, Strategies to improve performance of capillary isoelectric focusing, J. Chromatogr. A 772 (1–2) (1997) 145–160.
[283] T. Kristl, H. Stutz, Comparison of different mobilization strategies for capillary isoelectric focusing of ovalbumin variants, J. Sep. Sci. 38 (1) (2015) 148–156.
[284] S. Mack, I. Cruzado-Park, J. Chapman, C. Ratnayake, G. Vigh, A systematic study in CIEF: defining and optimizing experimental parameters critical to method reproducibility and robustness, Electrophoresis 30 (23) (2009) 4049–4058.
[285] R.A. Mosher, W. Thormann, High-resolution computer simulation of the dynamics of isoelectric focusing: in quest of more realistic input parameters for carrier ampholytes, Electrophoresis 29 (5) (2008) 1036–1047.
[286] Q. Mao, J. Pawliszyn, Capillary isoelectric focusing with whole column imaging detection for analysis of proteins and peptides, J. Biochem. Biophys. Methods 39 (1) (1999) 93–110.
[287] E. Gianazza, Isoelectric focusing as a tool for the investigation of post-translational processing and chemical modifications of proteins, J. Chromatogr. A 705 (1) (1995) 67–87.
[288] L.H.H. Silvertand, J.S. Toraño, W.P. van Bennekom, G.J. de Jong, Recent developments in capillary isoelectric focusing, J. Chromatogr. A 1204 (2) (2008) 157–170.
[289] T. Kristl, H. Stutz, C. Wenz, G. Rozing, Principles and applications of capillary isoelectric focusing - primer, Agilent Technologies (2014) 1–36.
[290] P. Lopez-Soto-Yarritu, J.C. Díez-Masa, A. Cifuentes, M. de Frutos, Improved capillary isoelectric focusing method for recombinant erythropoietin analysis, J. Chromatogr. A 968 (1–2) (2002) 221–228.
[291] A. Cifuentes, M.A.V. Moreno-Arribas, M. de Frutos, J.C. Díez-Masa, Capillary isoelectric focusing of erythropoietin glycoforms and its comparison with flat-bed isoelectric focusing and capillary zone electrophoresis, J. Chromatogr. A 830 (2) (1999) 453–463.
[292] B. Kronsteiner, V. Dullnig, H. Stutz, Validation of capillary zone electrophoresis and capillary isoelectric focusing separations optimized for the characterization of two recombinant products of the birch pollen allergen Bet v 1a, Electrophoresis 29 (12) (2008) 2539–2549.
[293] M. Horká, O. Kubíček, A. Kubesoví, Z. Kubíčková, K. Rosenbergová, K. Šlais, Testing of the influenza virus purification by CIEF, Electrophoresis 31 (2) (2010) 331–338.
[294] J. Wu, W. McElroy, J. Pawliszyn, C.D. Heger, Imaged capillary isoelectric focusing: applications in the pharmaceutical industry and recent innovations of the technology, TrAC Trends Anal. Chem. 150 (2022), 116567.
[295] B. Cowper, X. Li, L. Yu, Y. Zhou, W.H. Fan, C.M. Rao, Comprehensive glycan analysis of twelve recombinant human erythropoietin preparations from manufacturers in China and Japan, J. Pharm. Biomed. Anal. 153 (2018) 214–220.
[296] X. Li, L. Yu, X. Shi, C. Rao, Y. Zhou, Capillary isoelectric focusing with UV fluorescence imaging detection enables direct charge heterogeneity characterization of erythropoietin drug products, J. Chromatogr. A 2021 (1643), 462043.
[297] M. Siedler, Implementation of a platform approach for early biologics, Dev., Am. Pharm. Rev. 14 (2011).
[298] J. Schmailzl, M.W. Vorage, H. Stutz, Intact and middle-down CIEF of commercial therapeutic monoclonal antibody products under non-denaturing conditions, Electrophoresis 41 (12) (2020) 1109–1117.
[299] L. Regazzoni, R. Colombo, L. Bertoletti, G. Vistoli, G. Aldini, M. Serra, M. Carini, R.M. Facino, S. Giorgetti, M. Stoppini, G. Caccialanza, E. De Lorenzi, Screening of fibrillogenesis inhibitors of β2-microglobulin: integrated strategies by mass spectrometry capillary electrophoresis and in silico simulations, Anal. Chim. Acta 685 (2) (2011) 153–161.
[300] V. Dullnig, R. Weiss, S. Amon, A. Rizzi, H. Stutz, Confirmation of immuno-reactivity of the recombinant major birch pollen allergen Bet v 1a by affinity-CIEF, Electrophoresis 30 (13) (2009) 2337–2346.
[301] V.M. Okun, B. Ronacher, D. Blaas, E. Kenndler, Affinity capillary electrophoresis for the assessment of complex formation between viruses and monoclonal antibodies, Anal. Chem. 72 (19) (2000) 4634–4639.
[302] V. Okun, B. Ronacher, D. Blaas, E. Kenndler, Capillary electrophoresis with postcolumn infectivity assay for the analysis of different serotypes of human rhinovirus (Common Cold Virus), Anal. Chem. 72 (11) (2000) 2553–2558.
[303] D. Xu, K. Marchionni, Y. Hu, W. Zhang, Z. Sosic, Quantitative analysis of a biopharmaceutical protein in cell culture samples using automated capillary electrophoresis (CE) western blot, J. Pharm. Biomed. Anal. 145 (2017) 10–15.
[304] R.R. Rustandi, J.W. Loughney, M. Hamm, C. Hamm, C. Lancaster, A. Mach, S. Ha, Qualitative and quantitative evaluation of Simon™, a new CE-based automated Western blot system as applied to vaccine development, Electrophoresis 33 (17) (2012) 2790–2797.
[305] D. Xu, S. Mane, Z. Sosic, Characterization of a biopharmaceutical protein and evaluation of its purification process using automated capillary Western blot, Electrophoresis 36 (2) (2015) 363–370.
[306] A. Koller, H. Wätzig, Precision and variance components in quantitative gel electrophoresis, Electrophoresis 26 (12) (2005) 2470–2475.
[307] G.J. Anderson, C.M. Cipolla, R.T. Kennedy, Western blotting using capillary electrophoresis, Anal. Chem. 83 (4) (2011) 1350–1355.
[308] S. Jin, M.D. Furtaw, H. Chen, D.T. Lamb, S.A. Ferguson, N.E. Arvin, M. Dawod, R. T. Kennedy, Multiplexed western blotting using microchip electrophoresis, Anal. Chem. 88 (13) (2016) 6703–6710.
[309] WHO Expert Committee on Biological Standardization, WHO Technical Report Series 941, WHO, Geneva, 2007, p. 340.
[310] J.W. Loughney, C. Lancaster, S. Ha, R.R. Rustandi, Residual bovine serum albumin (BSA) quantitation in vaccines using automated Capillary Western technology, Anal. Biochem. 461 (2014) 49–56.
[311] J. Wang, A. Valdez, Y. Chen, Evaluation of automated Wes system as an analytical and characterization tool to support monoclonal antibody drug product development, J. Pharm. Biomed. Anal. 139 (2017) 263–268.
[312] M. Kinoshita, K. Yamada, Recent advances and trends in sample preparation and chemical modification for glycan analysis, J. Pharm. Biomed. Anal. 207 (2022), 114424.
[313] S. Ijiri, K. Todoroki, H. Yoshida, T. Yoshitake, H. Nohta, M. Yamaguchi, Highly sensitive capillary electrophoresis analysis of N-linked oligosaccharides in glycoproteins following fluorescence derivatization with rhodamine 110 and laser-induced fluorescence detection, Electrophoresis 32 (24) (2011) 3499–3509.
[314] C.G. Huber, A. Premstaller, G. Kleindienst, Evaluation of volatile eluents and electrolytes for high-performance liquid chromatography–electrospray ionization mass spectrometry and capillary electrophoresis–electrospray ionization mass spectrometry of proteins: II. Capillary electrophoresis, J. Chromatogr. A 849 (1) (1999) 175–189.
[315] M. Moini, Capillary electrophoresis mass spectrometry and its application to the analysis of biological mixtures, Anal. Bioanal. Chem. 373 (6) (2002) 466–480.
[316] H. Stutz, Advances in the analysis of proteins and peptides by capillary electrophoresis with matrix-assisted laser desorption/ionization and electrospray-mass spectrometry detection, Electrophoresis 26 (7–8) (2005) 1254–1290.
[317] A.D. Smith, M. Moini, Control of electrochemical reactions at the capillary electrophoresis outlet/electrospray emitter electrode under CE/ESI-MS through the application of redox buffers, Anal. Chem. 73 (2) (2001) 240–246.
[318] E. Barceló-Barrachina, E. Moyano, M.T. Galceran, State-of-the-art of the hyphenation of capillary electrochromatography with mass spectrometry, Electrophoresis 25 (13) (2004) 1927–1948.
[319] R. Wojcik, O.O. Dada, M. Sadilek, N.J. Dovichi, Simplified capillary electrophoresis nanospray sheath-flow interface for high efficiency and sensitive peptide analysis, Rapid Commun. Mass Spectrom. 24 (17) (2010) 2554–2560.
[320] R. Haselberg, G.J. de Jong, G.W. Somsen, Low-flow sheathless capillary electrophoresis–mass spectrometry for sensitive glycoform profiling of intact pharmaceutical proteins, Anal. Chem. 85 (4) (2013) 2289–2296.
[321] M. Moini, Simplifying CE−MS operation. 2. Interfacing low-flow separation techniques to mass spectrometry using a porous tip, Anal. Chem. 79 (11) (2007) 4241–4246.
[322] J.T. Whitt, M. Moini, Capillary electrophoresis to mass spectrometry interface using a porous junction, Anal. Chem. 75 (9) (2003) 2188–2191.
[323] S. Carillo, C. Jakes, J. Bones, In-depth analysis of monoclonal antibodies using microfluidic capillary electrophoresis and native mass spectrometry, J. Pharm. Biomed. Anal. 185 (2020), 113218.
[324] R. Haselberg, G.J. de Jong, G.W. Somsen, CE-MS for the analysis of intact proteins 2010–2012, Electrophoresis 34 (1) (2013) 99–112.
[325] I. Mikšík, Coupling of CE-MS for protein and peptide analysis, J. Sep. Sci. 42 (1) (2019) 385–397.
[326] A. Stolz, K. Jooß, O. Höcker, J. Römer, J. Schlecht, C. Neusüß, Recent advances in capillary electrophoresis-mass spectrometry: Instrumentation, methodology and applications, Electrophoresis 40 (1) (2019) 79–112.
[327] S. Khan, J. Liu, Z. Szabo, B. Kunnummal, X. Han, Y. Ouyang, R.J. Linhardt, Q. Xia, On-line capillary electrophoresis/laser-induced fluorescence/mass spectrometry analysis of glycans labeled with Teal™ fluorescent dye using an electrokinetic sheath liquid pump-based nanospray ion source, Rapid Commun. Mass Spectrom. 32 (11) (2018) 882–888.
[328] E. Giménez, R. Ramos-Hernan, F. Benavente, J. Barbosa, V. Sanz-Nebot, Analysis of recombinant human erythropoietin glycopeptides by capillary electrophoresis electrospray–time of flight-mass spectrometry, Anal. Chim. Acta 709 (2012) 81–90.
[329] G.S.M. Kammeijer, B.C. Jansen, I. Kohler, A.A.M. Heemskerk, O.A. Mayboroda, P. J. Hensbergen, J. Schappler, M. Wuhrer, Sialic acid linkage differentiation of glycopeptides using capillary electrophoresis – electrospray ionization – mass spectrometry, Sci. Rep. 7 (1) (2017) 3733.
[330] D. Thakur, T. Rejtar, B.L. Karger, N.J. Washburn, C.J. Bosques, N.S. Gunay, Z. Shriver, G. Venkataraman, Profiling the glycoforms of the intact α subunit of recombinant human chorionic gonadotropin by high-resolution capillary electrophoresis−mass spectrometry, Anal. Chem. 81 (21) (2009) 8900–8907.
[331] M. Spearman, J. Rodriguez, N. Huzel, M. Butler, Production and glycosylation of recombinant beta-interferon in suspension and cytopore microcarrier cultures of CHO cells, Biotechnol. Prog. 21 (1) (2005) 31–39.
[332] R. Mastrangeli, M. Rossi, M. Mascia, W. Palinsky, A. Datola, M. Terlizzese, H. Bierau, In vitro biological characterization of IFN-β-1a major glycoforms, Glycobiology 25 (1) (2014) 21–29.

[333] C.E. Markowitz, Interferon-beta - mechanism of action and dosing issues, Neurology 68 (24 suppl 4) (2007) S8–S11.
[334] N. Mokhber, A. Azarpazhooh, E. Orouji, S.M. Rao, B. Khorram, M.A. Sahraian, M. Foroghipoor, M.M. Gharavi, S. Kakhi, K. Nikkhah, M.R. Azarpazhooh, Cognitive dysfunction in patients with multiple sclerosis treated with different types of interferon beta: a randomized clinical trial, J. Neurol. Sci. 342 (1) (2014) 16–20.
[335] F. Azarafrouz, M. Farhangian, S. Chavoshinezhad, S. Dargahi, M. Nassiri-Asl, L. Dargahi, Interferon beta attenuates recognition memory impairment and improves brain glucose uptake in a rat model of Alzheimer's disease: involvement of mitochondrial biogenesis and PI3K pathway, Neuropeptides 95 (2022), 102262.
[336] R. Haselberg, V. Brinks, A. Hawe, G.J. de Jong, G.W. Somsen, Capillary electrophoresis-mass spectrometry using noncovalently coated capillaries for the analysis of biopharmaceuticals, Anal. Bioanal. Chem. 400 (1) (2011) 295–303.
[337] D.R. Bush, L. Zang, A.M. Belov, A.R. Ivanov, B.L. Karger, High resolution CZE-MS quantitative characterization of intact biopharmaceutical proteins: proteoforms of interferon-β1, Anal. Chem. 88 (2) (2016) 1138–1146.
[338] A. Taichrib, M. Pelzing, C. Pellegrino, M. Rossi, C. Neusüß, High resolution TOF MS coupled to CE for the analysis of isotopically resolved intact proteins, J. Proteom. 74 (7) (2011) 958–966.
[339] N. Bracke, E. Wynendaele, M. D'Hondt, R. Haselberg, G.W. Somsen, E. Pauwels, C. Van de Wiele, B. De Spiegeleer, Analytical characterization of NOTA-modified somatropins, J. Pharm. Biomed. Anal. 96 (2014) 1–9.
[340] C. Neusüß, U. Demelbauer, M. Pelzing, Glycoform characterization of intact erythropoietin by capillary electrophoresis-electrospray-time of flight-mass spectrometry, Electrophoresis 26 (7–8) (2005) 1442–1450.
[341] A.P. Corfield, M. Sander-Wewer, R.W. Veh, M. Wember, R. Schauer, The action of sialidases on substrates containing O-acetylsialic acids, Biol. Chem. Hoppe Seyler 367 (1) (1986) 433–440.
[342] A. Ylönen, N. Kalkkinen, J. Saarinen, J. Bøgwald, J. Helin, Glycosylation analysis of two cysteine proteinase inhibitors from Atlantic salmon skin: di-O-acetylated sialic acids are the major sialic acid species on N-glycans, Glycobiology 11 (7) (2001) 523–531.
[343] S. Stanislaus, R. Hecht, J. Yie, T. Hager, M. Hall, C. Spahr, W. Wang, J. Weiszmann, Y. Li, L. Deng, D. Winters, S. Smith, L. Zhou, Y. Li, M.M. Véniant, J. Xu, A. Novel, Fc-FGF21 with improved resistance to proteolysis, increased affinity toward β-klotho, and enhanced efficacy in mice and cynomolgus monkeys, Endocrinology 158 (5) (2017) 1314–1327.
[344] T. Xie, P.S. Leung, Fibroblast growth factor 21: a regulator of metabolic disease and health span, Am. J. Physiol. Endocrinol. Metab. 313 (3) (2017) E292–E302.
[345] Y. Zhang, Y. Wang, Z. Sosic, L. Zang, S. Bergelson, W. Zhang, Identification of adeno-associated virus capsid proteins using ZipChip CE/MS, Anal. Biochem. 555 (2018) 22–25.
[346] X. Jin, L. Liu, S. Nass, C. O'Riordan, E. Pastor, X.K. Zhang, Direct liquid chromatography/mass spectrometry analysis for complete characterization of recombinant adeno-associated virus capsid proteins, Hum. Gene Ther. Methods 28 (5) (2017) 255–267.
[347] C. Li, N. Diprimio, D.E. Bowles, M.L. Hirsch, P.E. Monahan, A. Asokan, J. Rabinowitz, M. Agbandje-McKenna, R.J. Samulski, Single amino acid modification of adeno-associated virus capsid changes transduction and humoral immune profiles, J. Virol. 86 (15) (2012) 7752–7759.
[348] L. Bertoletti, J. Schappler, R. Colombo, S. Rudaz, R. Haselberg, E. Domínguez-Vega, S. Raimondi, G.W. Somsen, E. De Lorenzi, Evaluation of capillary electrophoresis-mass spectrometry for the analysis of the conformational heterogeneity of intact proteins using beta2-microglobulin as model compound, Anal. Chim. Acta 945 (2016) 102–109.
[349] T. Franze, M.G. Weller, R. Niessner, U. Pöschl, Protein nitration by polluted air, Environ. Sci. Technol. 39 (6) (2005) 1673–1678.
[350] D. Salvemini, T.M. Doyle, S. Cuzzocrea, Superoxide, peroxynitrite and oxidative/nitrative stress in inflammation, Biochem. Soc. Trans. 34 (5) (2006) 965–970.
[351] A.C. Karle, G.J. Oostingh, S. Mutschlechner, F. Ferreira, P. Lackner, B. Bohle, G. F. Fischer, A.B. Vogt, A. Duschl, Nitration of the pollen allergen bet v 1.0101 enhances the presentation of bet v 1-derived peptides by HLA-DR on human dendritic cells, PLoS ONE 7 (2) (2012), e31483.
[352] S. Gusenkov, C. Ackaert, H. Stutz, Separation and characterization of nitrated variants of the major birch pollen allergen by CZE-ESI-μTOF MS, Electrophoresis 34 (18) (2013) 2695–2704.
[353] S. Gusenkov, H. Stutz, Top-down and bottom-up characterization of nitrated birch pollen allergen Bet v 1a with CZE hyphenated to an Orbitrap mass spectrometer, Electrophoresis 39 (9–10) (2018) 1190–1200.
[354] M. Lombardero, F.J. García-Sellés, F. Polo, L. Jimeno, M.J. Chamorro, G. García-Casado, R. Sánchez-Monge, A. Díaz-Perales, G. Salcedo, D. Barber, Prevalence of sensitization to Artemisia allergens Art v 1, Art v 3 and Art v 60 kDa. Cross-reactivity among Art v 3 and other relevant lipid-transfer protein allergens, Clin. Exp. Allergy 34 (9) (2004) 1415–1421.
[355] S. Vieths, Allergenic cross-reactivity, food allergy and pollen, Environ. Toxicol. Pharmacol. 4 (1) (1997) 61–70.
[356] S. Gaier, J. Marsh, C. Oberhuber, N.M. Rigby, A. Lovegrove, S. Alessandri, P. Briza, C. Radauer, L. Zuidmeer, R. van Ree, W. Hemmer, A.I. Sancho, C. Mills, K. Hoffmann-Sommergruber, P.R. Shewry, Purification and structural stability of the peach allergens Pru p 1 and Pru p 3, Mol. Nutr. Food Res. 52 (S2) (2008) S220–S229.
[357] L.G. Stock, S. Wildner, C. Regl, G. Gadermaier, C.G. Huber, H. Stutz, Monitoring of deamidation and lanthionine formation in recombinant mugwort allergen by capillary zone electrophoresis (CZE)-UV and transient capillary isotachophoresis-CZE-electrospray ionization-TOF-MS, Anal. Chem. 90 (20) (2018) 11933–11940.
[358] S. Wildner, I. Griessner, T. Stemeseder, C. Regl, W.T. Soh, L.G. Stock, T. Völker, C. Alessandri, A. Mari, C.G. Huber, H. Stutz, H. Brandstetter, G. Gadermaier, Boiling down the cysteine-stabilized LTP fold - loss of structural and immunological integrity of allergenic Art v 3 and Pru p 3 as a consequence of irreversible lanthionine formation, Mol. Immunol. 116 (2019) 140–150.
[359] J. Camperi, B. De Cock, V. Pichon, A. Combes, J. Guibourdenche, T. Fournier, Y. Vander Heyden, D. Mangelings, N. Delaunay, First characterizations by capillary electrophoresis of human Chorionic Gonadotropin at the intact level, Talanta 193 (2019) 77–86.
[360] K.S. Lee, D.H. Na, Capillary electrophoretic separation of poly(ethylene glycol)-modified granulocyte-colony stimulating factor, Arch. Pharm. Res. 33 (3) (2010) 491–495.
[361] E. Balaguer, U. Demelbauer, M. Pelzing, V. Sanz-Nebot, J. Barbosa, C. Neusüß, Glycoform characterization of erythropoietin combining glycan and intact protein analysis by capillary electrophoresis – electrospray – time-of-flight mass spectrometry, Electrophoresis 27 (13) (2006) 2638–2650.
[362] X. Yao, G. Qi, Y. Qu, S. Yun, W. Sun, C. Liang, M. Du, Z. Li, Structural characterization of RC28-E, a recombinant fusion protein with dual targets on VEGF and FGF2, Nat. Prod. Commun. 17 (3) (2022) 1–11.
[363] G. Zhu, L. Sun, T. Linkous, D. Kernaghan, J.B. McGivney IV, N.J. Dovichi, Absolute quantitation of host cell proteins in recombinant human monoclonal antibodies with an automated CZE-ESI-MS/MS system, Electrophoresis 35 (10) (2014) 1448–1452.
[364] G. Zhu, L. Sun, R. Wojcik, D. Kernaghan, J.B. McGivney, N.J. Dovichi, A rapid cIEF–ESI–MS/MS method for host cell protein analysis of a recombinant human monoclonal antibody, Talanta 98 (2012) 253–256.
[365] G. Zhu, L. Sun, J. Heidbrink-Thompson, S. Kuntumalla, H.-Y. Lin, C.J. Larkin, J. B. McGivney IV, N.J. Dovichi, Capillary zone electrophoresis tandem mass spectrometry detects low concentration host cell impurities in monoclonal antibodies, Electrophoresis 37 (4) (2016) 616–622.
[366] Z. Zhang, T. Albanetti, T. Linkous, C.J. Larkin, R. Schoner, J.B. McGivney IV, N. J. Dovichi, Comprehensive analysis of host cell impurities in monoclonal antibodies with improved sensitivity by capillary zone electrophoresis mass spectrometry, Electrophoresis 38 (3–4) (2017) 401–407.
[367] R. Kumar, R.L. Shah, S. Ahmad, A.S. Rathore, Harnessing the power of electrophoresis and chromatography: Offline coupling of reverse phase liquid chromatography-capillary zone electrophoresis-tandem mass spectrometry for analysis of host cell proteins in monoclonal antibody producing CHO cell line, Electrophoresis 42 (6) (2021) 735–741.
[368] F. Foret, E. Szökő, B.L. Karger, Trace analysis of proteins by capillary zone electrophoresis with on-column transient isotachophoretic preconcentration, Electrophoresis 14 (1) (1993) 417–428.
[369] Joint Committee for Guides in Metrology, International vocabulary of metrology - Basic and general concepts and associated terms (VIM), 2012, pp. 1–90.
[370] M. Thompson, S.L.R. Ellison, R. Wood, Harmonized guidelines for single-laboratory validation of methods of analysis (IUPAC Technical Report), Pure Appl. Chem. 74 (5) (2002) 835–855.
[371] S.V.C. de Souza, R.G. Junqueira, A procedure to assess linearity by ordinary least squares method, Anal. Chim. Acta 552 (1) (2005) 25–35.
[372] F. Raposo, Evaluation of analytical calibration based on least-squares linear regression for instrumental techniques: a tutorial review, TrAC Trends Anal. Chem. 77 (2016) 167–185.
[373] J. Van Loco, M. Elskens, C. Croux, H. Beernaert, Linearity of calibration curves: use and misuse of the correlation coefficient, Accred Qual. Assur 7 (7) (2002) 281–285.
[374] J.M. Andrade, M.P. Gomez-Carracedo, Notes on the use of Mandel's test to check for nonlinearity in laboratory calibrations, Anal. Methods 5 (5) (2013) 1145–1149.
[375] M. Tod, A. Aouimer, O. Petitjean, Estimation of pharmacokinetic parameters by orthogonal regression: comparison of four algorithms, Comput. Methods Prog. Biomed. 67 (1) (2002) 13–26.
[376] F. Garofolo, Bioanalytical Method Validation, in: C.C. Chan, Y.C. Lee, H. Lam, X.-M. Zhang (Eds.), Analytical Method Validation and Instrument Performance Verification, John Wiley & Sons, Inc, Hoboken, New Jersey, 2004, pp. 105–138.
[377] L. Garcia, E. Viaplana, A. Urniza, Comparison of BHK-21 cell growth on microcarriers vs in suspension at 2L scale both in conventional bioreactor and single-use bioreactor (Univessel® SU), BMC Proc. 7 (6) (2013) P40.
[378] X. Teng, C. Li, X. Yi, Y. Zhuang, A novel scale-up strategy for cultivation of BHK-21 cells based on similar hydrodynamic environments in the bioreactors, Bioresour. Bioprocess. 8 (1) (2021) 74.
[379] V. Dill, B. Hoffmann, A. Zimmer, M. Beer, M. Eschbaumer, Influence of cell type and cell culture media on the propagation of foot-and-mouth disease virus with regard to vaccine quality, Virol. J. 15 (1) (2018) 46.
[380] K. Tachibana, T. Uchida, K. Ogawa, N. Yamashita, K. Tamura, Induction of cell-membrane porosity by ultrasound, Lancet 353 (9162) (1999) 1409.
[381] M. Du, Y. Li, Z. Chen, Sonoporation-mediated gene transfection: a novel direction for cell reprogramming in vivo, Front. Bioeng. Biotechnol. 9 (2022).